Secoisolariciresinol (SECO) Analogues: Oxidative Metabolism, Cytochrome P450 Inhibition and Implications for Toxicity

A Thesis Submitted to the College of

Graduate Studies and Research

in Partial Fulfillment of the Requirements

for the Degree of Master of Science

in the Toxicology Graduate Program

University of Saskatchewan

Saskatoon, Saskatchewan

Canada

By

Leah McGurn

PERMISSION TO USE

In presenting this thesis/dissertation in partial fulfillment of the requirements for a Postgraduate degree from the University of Saskatchewan, I agree that the Libraries of this University may make it freely available for inspection. I further agree that permission for copying of this thesis/dissertation in any manner, in whole or in part, for scholarly purposes may be granted by the professor or professors who supervised my thesis/dissertation work or, in their absence, by the Head of the Department or the Dean of the College in which my thesis work was done. It is understood that any copying or publication or use of this thesis/dissertation or parts thereof for financial gain shall not be allowed without my written permission. It is also understood that due recognition shall be given to me and to the University of Saskatchewan in any scholarly use which may be made of any material in my thesis/dissertation.

Dean

College of Graduate Studies and Research
University of Saskatchewan
107 Administration Place
Saskatoon, Saskatchewan
S7N 5A2
Canada

ABSTRACT

Secoisolariciresinol (SECO) is the major lignan present in flaxseed,[1-3] but unlike the structurally related lignan nordihydroguaiaretic acid, it is not associated with toxicity.[3-5] The major phase I metabolite of SECO is lariciresinol, likely formed as a result of *para*-quinone methide (p-QM) formation followed by an intramolecular cyclization, thereby minimizing any toxicity associated with the p-QM.[2] Four analogues of SECO were used to investigate substituent effects on lignan metabolism and formation of reactive quinones.

HPLC methods were developed for analysis of SECO analogues and their metabolites. The stability of SECO analogues (1 mM) in a 50 mM Na_2HPO_4 buffer at pH 6.0 and 7.4 were quantified. Enzymatic oxidation experiments using mushroom tyrosinase and microsomes harvested from male Sprague-Dawley rats were performed with and without a GSH trapping system. Mass spectrometry and LC-MS were used to identify metabolites. Life Technologies was contracted to perform IC_{50} inhibition assays on SECO and the SECO analogues against CYP3A4, CYP3A5, CYP2C9 and CYP2C19 cytochrome P450 isoforms.

All SECO analogues were stable at pH 6.0. SECO-2 was stable at pH 7.4 but SECO-1, -3 and -4 were unstable at pH 7.4. Autoxidation of SECO -1, -3 and -4 were 1st order reactions with $t_{1/2}$ of 9.0 h, 1.7 h and 7.0 h respectively. Mushroom tyrosinase oxidations were performed to generate *ortho*-quinone standards. SECO-1 -3 and -4 were oxidized by mushroom tyrosinase but SECO-2 was not. Trapping with GSH produces aromatic ring conjugates for SECO-1, -3, -4. Results from microsomal oxidations for SECO-1, -3 and -4 are consistent with these standards. SECO-2 was metabolized by a microsomal system to produce a benzyl GSH adduct. Dealkylation products were also observed. All SECO analogues formed quinones but interestingly, GSH conjugation was competitive with intramolecular cyclization. All cytochrome P450 isoforms were inhibited by every analogue tested to varying degrees, a potential cause of toxicity concerns.

Quinones are known to cause toxicity *in vivo*, including cytotoxicity, immunotoxicity, and carcinogenesis. Our results suggest that since the phenol and catechol lignans form GSH adducts

in addition to intramolecular cyclization products, this class of lignans have the potential to cause toxicity.

ACKNOWLEDGEMENTS

I would first like to recognize and extend heartfelt thanks to my supervisor Dr. Ed Krol for his continued patience, support and guidance throughout my research and whilst writing this thesis. I have grown so much in my two-and-a-half years in his lab and I could not have asked for a better mentor for my M.Sc. studies.

I would also like to thank the members of my committee: Dr. Lynn Weber and Dr. Paul Jones. for their perspectives, insightful comments, constructive criticism and encouragement.

My sincere gratitude to the NSERC CREATE HERA and iTraP programs for their support and allowing me the opportunity to expand my horizons.

I thank all of my lab mates: Kholud Algabbass, Ahmed Almousa, Yunyun Di, Kevin Allen and Isaac Asiamah for all of their help and stimulating discussions. I would like to send a special thank you and acknowledgement to Kevin Allen and Isaac Asiamah for synthesizing all of the SECO analogues, Isaac Asiamah for the development of the MS method and Deb Michel for all of her invaluable help in particular with the mass spectrometer.

This research would not have been possible without the financial support of the Toxicology Graduate Program, the University of Saskatchewan, The Canadian Foundation for Innovation and NSERC CREATE.

Lastly I want to thank my friends, family and most especially my sisters, Michaela and Tess for their support and keeping me sane, well, mostly.

DEDICATION

This thesis is dedicated to …

… My Parents
Stephen McGurn and Karen Morris-McGurn
Without whose support
This study would not have been possible

… And my Grandmother
Anne Morris
Who passed away during my course of study
She will always be an inspiration

TABLE OF CONTENTS

LIST OF FIGURES

LIST OF TABLES

LIST OF ABBREVIATIONS

ABC – ATP-Binding Cassette

ADME – Absorption, Distribution, Metabolism and Elimination

DIN-HM – Homeopathic Medicine Number

DMSO – Dimethyl Sulfoxide

DNA – Deoxyribonucleic Acid

ED – Enterodiol

EL – Enterolactone

ESI – Electro Spray Ionization

GRAS – Generally Recognized As Safe

GSH – Glutathione

HPLC – High Performance Liquid Chromatography

IC_{50} – Half maximal inhibitory concentration

IDR – Idiosyncratic drug reactions

LC-MS – Liquid Chromatography – Mass Spectrometry

MS – Mass Spectrometry

NADPH – Reduced Nicotinamide Adenine Dinucleotide Phosphate

NDGA – Nordihydroguaiaretic Acid

NHPs – Natural Health Products

NHPD – Natural Health Products Directorate

NL – Neutral Loss

NMNH – Nicotinamide Mononucleotide

NNHPD – Natural and Non-prescription Health Product Directorates

NPN – Natural Product Number

o-Q – *ortho*-quinone

p-QM – *para*-quinone methide

P450 – Cytochrome P450

ROS – Reactive Oxygen Species

RT – Retention time

SDG – Secoisolariciresinol Diglucoside

SECO – Secoisolariciresinol

SLC – Solute Carrier

SPP – Sodium pyrophosphate

1.0 Introduction

Many Canadians are turning to natural products as alternatives to pharmaceutical drugs, and believe that natural products are safer than chemical products or pharmaceutical drugs according to a recent study.[1] This belief remains, despite the lack of scientific data on their toxicity and the absence of strict regulations present for pharmaceuticals.[2] At the same time the number of North Americans taking multiple medications at the same time is on the rise, increasing the chances of drug-drug interactions, which can lead to the occurrence of dangerous toxicological effects.[3]

The toxicity of many chemicals is linked to their metabolism. Metabolism can lead to the formation of reactive intermediates, which can either react covalently with cellular macromolecules or generate reactive oxygen species (ROS) causing oxidative stress. Metabolic drug-drug interactions can cause changes on the scale of an order of magnitude or more in blood and tissue concentrations of a drug or metabolite. This can in turn affect the extent to which toxic or active metabolites are formed. Large changes in drug or active metabolite exposure can alter its safety and efficacy profile. Changes in exposure are always a concern but are especially significant when a drug has a narrow therapeutic range.[4]

Flax (*Linum usitatisimum* L)[5] has been farmed since 7000 BC but today a great deal of interest in flax stems from its potential health benefits and the increased presence of flaxseed in the human diet.[6] Flaxseed's potential health benefits may be due to natural products called lignans,[7] as flaxseed is one of the richest known sources of lignans. Interest in lignans and their use as a natural product, arose from associated beneficial changes in blood lipid profiles, antioxidative effects and estrogenic, antiviral, antiestrogenic and anticarcinogenic activities.[6,8-12] Secoisolarisiresinol diglucoside (SDG) is the major lignan in flaxseed, where it is found in levels greater than 100 times those in other food sources, such as bramble, soy beans, garlic and tea.[13] SDG is hydrolyzed to secoisolarisiresinol (SECO), in the mammalian gastrointestinal tract.[2-4]

Some putative health benefits of SECO include reduction in serum cholesterol levels, delaying the onset of type II diabetes, the treatment/prevention of cardiovascular diseases and decreased formation of breast, prostate and colon cancers.[9,10] SECO has also been found to be an anti-

oxidative phenolic lignan, efficient at protecting cells *in vitro* from oxidative damage, which increases SECOs value as a therapeutic agent.[10] SECO undergoes oxidative metabolism to a *para*-quinone methide (p-QM) in both rat and human hepatic microsomes.[3] The major metabolite of SECO from hepatic microsomal studies is lariciresinol, which is likely formed as a result of p-QM formation followed by an intramolecular cyclization thereby minimizing any toxicity associated with formation of the p-QM.[3] Therefore SECO, unlike the structurally related nordihydroguaiaretic acid (NDGA), is not associated with toxicity.[1,4,5]

Quinones can have various toxicological effects *in vivo*, including cytotoxicity, immunotoxicity, and carcinogenesis.[14] Quinones are highly reactive compounds as they are both oxidants and electrophiles.[15] Covalent binding can cause cytotoxicity if the electrophilic quinones react with nucleophilic groups on cellular macromolecules like thiol and amine groups in proteins and DNA. Quinones are also potent redox active compounds, which can undergo redox cycling with their semi-quinone radicals, generating reactive oxygen species (ROS) and leading to oxidative stress through the formation of oxidized cellular macromolecules, including: lipids, proteins and DNA.[14,16]

Several analogues of SECO (SECO-1,2,3,4) with altered functional groups were previously synthesized and will be used to investigate substituent effects on: lignan metabolism and formation of reactive quinones and to probe the effect of structure on the pharmacological and toxicological properties of SECO.

2.0 Literature Review

2.1 Natural Health Products

Natural health products (NHPs) are naturally occurring substances used to restore or maintain good health.[17] NHPs are often made from plants, but can also be made from other sources including animals and microorganisms.[18] NHPs include: vitamins and minerals, herbal remedies, homeopathic medicines, traditional medicines like traditional Chinese and Ayurvedic (East Indian) medicines, probiotics and other products like amino acids and essential fatty acids.[19]

NHPs are sold in a wide variety of forms including: tablets, capsules, tinctures, solutions, creams, ointments and drops.[19] NHPs are marketed for an assortment of different health concerns such as: the prevention or treatment of an illness or condition, reduction of health risks and the maintenance of overall optimal health.[19] Canadians that consume NHPs do so for a variety of reasons but according to a 2010 survey the top reasons are health maintenance (85%), illness prevention and strengthening one's immune system (79%) and general concern about one's health (76%).[1]

2.1.2 Canadian use of NHPs

Many Canadians (73%) have used natural health products and a large proportion of Canadians (71%) indicate they believe NHPs are better for them than chemical products or pharmaceutical drugs,[1] however just because a product is natural does not mean that it is safe.[2,17,20] There is a general perception among Canadians that products derived from natural sources are safe to use. Encouragingly, consumer awareness of the possible dangers is growing; the percentage of Canadians who indicated natural products are safe decreased from 52% in 2005 to 42% in 2010.[1] Of the Canadians who use NHPs, 15% reported adverse reactions to Health Canada and 41% of individuals who experienced an adverse reaction reported it;[1,19] meaning the percentage of Canadians who experience adverse reactions from NHPS is closer to 24%. This percentage of voluntary reports is unusually high for a voluntary reporting system. It is well documented in the literature that under reporting of adverse events or adverse drug events occurs in voluntary reporting systems with only about 5% of incidences reported.[21-24] Unlike pharmaceuticals, which must have their physicochemical properties fully characterized before clinical development or marketing, NHPs are not subject to the same scrutiny and regulations.[2,17] This less stringent regulatory requirement is an issue, as many Canadians do not scrutinize NHPs the way they do pharmaceuticals. The inherent toxicity of NHPs, contamination, adulteration, misidentification and interactions with other natural products or pharmaceutical drugs can contribute to the potential harm of natural products.[20] Regulations on the safety of these products rely both on the assessment of reported cases of adverse reactions and on published toxicity information. Unfortunately, there is a lack of scientific information on the toxicity of natural products and their constituents including metabolites.[20]

2.1.3 Natural and Non-prescription Health Products Directorate (NNHPD)

NHPs are regulated under the Natural and Non-prescriptive Health Products Directorates (NNHPD) formerly the Natural Health Products Directorate (NHPD) under the Natural Health Products Regulations which came into effect in 2004 under the Food and Drugs Act.[18] All NHPs must have a product license to be legally sold in Canada.[18] If a product has been licensed it will have either a Natural Product Number (NPN) or a Homeopathic Medicine Number (DIN-HM) on the label. Canadian sites that manufacture, package, label and import NHPs must also have a license.[18] Health Canada has issued over 70,000 NHP product licenses and over 2,000 site licenses since 2004 when these regulations came into effect.[18] One caveat to these regulations is that they only pertain to Canadian stores and websites. Non-Canadian websites are not covered under these regulations. When a google search was conducted on November 12, 2015 for "Echinacea, purchase", 9 out of the first 10 hits were non-Canadian sites.

2.2 Flaxseed

2.2.1 A brief history of flax

Flax (*Linum usitatisimum* L)[5] has been farmed since 7000 BC and has been used in bread since 1000 BC, but today interest in flaxseed stems from its potential health benefits and its increased presence in the human diet.[6] Flax is an oilseed crop predominantly grown in the cooler regions of the world[25] and was first brought to Canada in 1617 by Louis Hébert.[26] Canada is now the world's largest producer and exporter of flax with Saskatchewan growing approximately 85% of Canada's flax.

2.2.2 Canadian flaxseed

Flaxseed is an oilseed whose seed mass is 32-45% oil with α-linolenic acid (an essential omega-3 fatty acid) comprising approximately 51-55% of the oil.[27] In 2014, Canadian farmers seeded

628,000 hectares of land with flax yielding approximately 1,400 kg/hectare or a total of 846,000 metric tonnes.[28] The 2014 harvest had an average oil content of 45.6% and an average protein content of 21.1%. The main cause of the fluctuation in protein and oil content as well as oil composition within a variety are environmental factors related to growing conditions.[28] Long-term harvest samples collected by the Canadian Grain Research Laboratory show that crops grown in Canada also contains high levels of dietary fiber.[28]

2.3 Lignans

Though lignans are found in most fiber rich plants and legumes, flaxseed is one of the richest known sources of lignan.[5,6] Lignans are an important class of secondary plant metabolites that consist of two phenylpropanoid units (Figure 2.1) formed by the coupling of two coniferyl alcohol residues present in the plant cell wall and are widely distributed in the plant kingdom.[5]

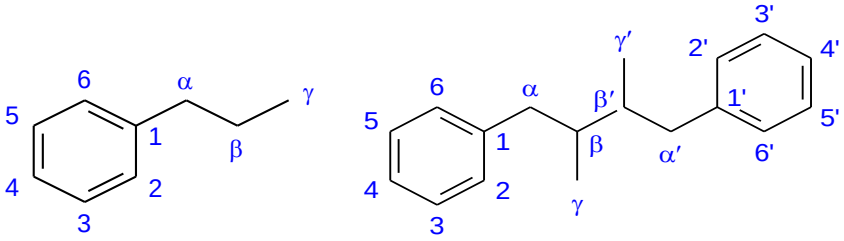

Figure 2.1 Structures for C_6C_3 phenylpropane subunit (left) and basic lignan skeleton (right)

As lignans present an enormous diversity in structure they have been classified into different families.[7,8] The difference between plant and mammalian lignans (Figure 2.2) is that mammalian lignans have hydroxyl groups at the 3' position while plant lignans have oxygenated substituents at the 3' and 4' positions.[5]

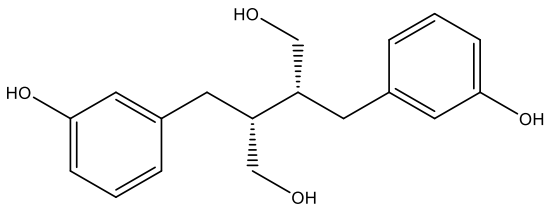

Enterodiol

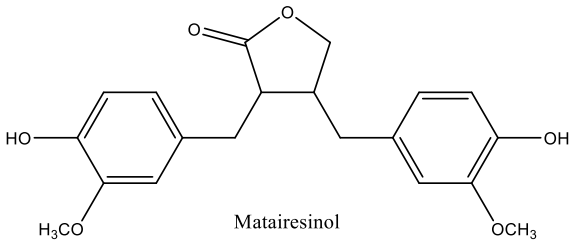

Matairesinol

Figure 2.2 Structures of an example of a mammalian lignan, enterodiol (ED; left) and plant lignan, matairesinol (right)

Interest in lignans and their use as natural products, arose from numerous studies indicating their putative beneficial changes in blood lipid profiles, antioxidative effects and estrogenic, antiviral, antiestrogenic and anticarcinogenic activities.[6,8-12]

2.3.1 Secoisolariciresinol diglucoside

Secoisolariciresinol diglucoside (SDG), whose structure is shown in Figure 2.3, is the major lignan component in flaxseed.

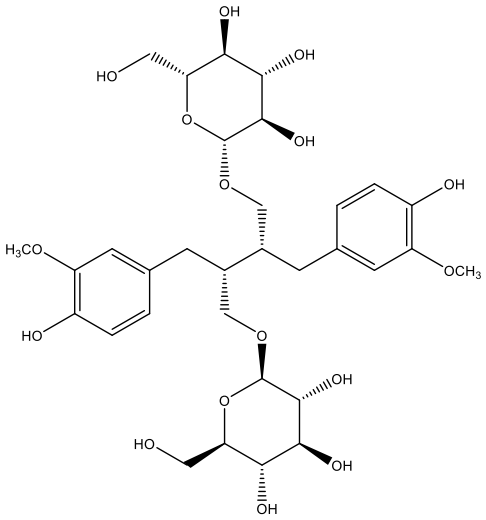

Figure 2.3 Structure of Secoisolariciresinol diglucoside (SDG)

The SDG content of whole flaxseed is between 6.1 – 13.3 mg/g of whole flaxseed.[29] Flaxseed contains greater than 100 times the levels of SDG as other food sources, such as bramble, soybeans, garlic and tea.[13] Importantly, the majority of the plant lignans are located in the

aleuronic layer of the seed coat, thus milled flaxseed often has a low lignan content,[13] and ingestion may not provide all the benefits associated with flaxseed use.

2.4 Secoisolariciresinol

2.4.1 Physical properties of SECO

SDG undergoes acid catalyzed and β-glycosidase-mediated hydrolysis to its aglycone form, secoisolariciresinol ([2R*,3R*]-2,3-Bis[4-hydroxy-3-methoxybenzyl]-1,4-butanediol; SECO; Figure 2.4) in the mammalian gastrointestinal tract. [6,9-12]

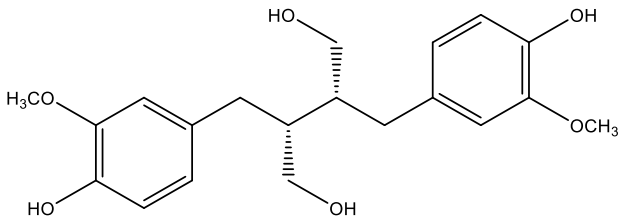

Figure 2.4 Structure of secoisolariciresinol

SECO is a solid at room temperature with a molecular formula $C_{20}H_{26}O_6$ and has a molecular weight of 362.42 g/mol.[30] SECO is classified as a dibenzylbutane lignan and is an antioxidant.[31] Benzylic hydrogen abstraction at the 3-methoxy-4-hydroxyl substituents and potential resonance stabilization is thought to be the source of SECO's antioxidant activity. [7,32]

2.4.2 Pharmacokinetic parameters of SECO

SECO can be further metabolized to enterodiol (ED) and enterolactone (EL) (Figure 2.5) in the intestine or absorbed through the intestinal epithelia.[10]

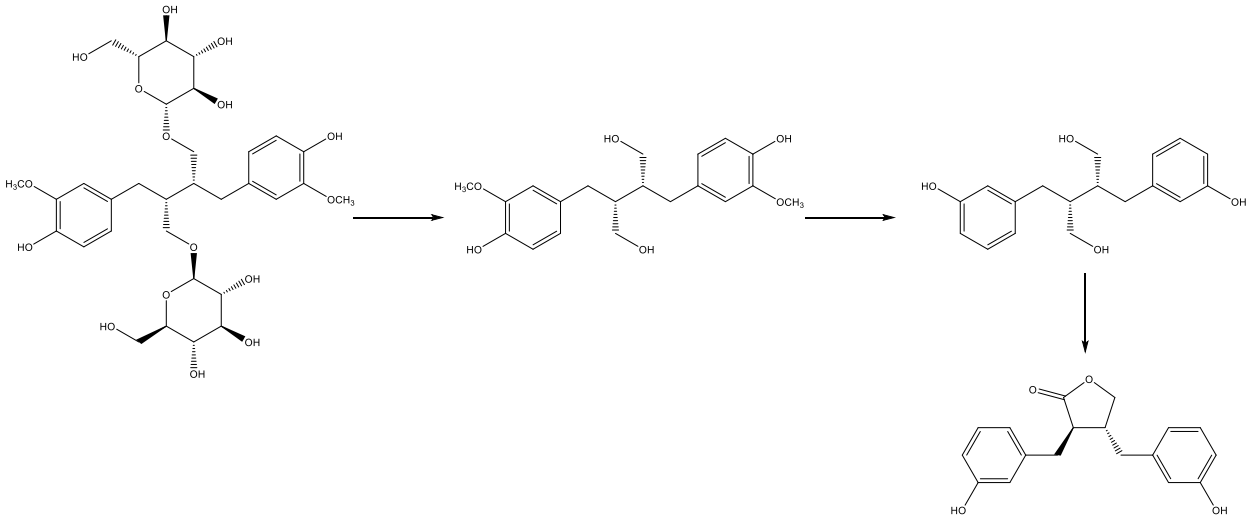

Figure 2.5 From left to right the structures of secoisolariciresinol diglucoside, secoisolariciresinol, enterodiol and enterolactone as a result of human intestinal metabolism.

In male Wistar rats the oral bioavailability of SECO is 26% and SECO was present in the systemic circulation for at least 21 h with evidence of enterohepatic recirculation.[33] SECO is a reversible inhibitor of the drug metabolizing enzyme family CYP3A (concentration-dependent but not time-dependent manner) and induces the activity of the drug metabolizing family CYP2B.[2]

SECO undergoes phase I oxidative metabolism in both rat and human hepatic microsomes and SECO may be oxidized to a *para*-quinone methide (p-QM; Figure 2.6).[10] The major metabolite of SECO from hepatic microsomal studies is lariciresinol, which is likely formed as a result of p-QM formation followed by an intramolecular cyclization, thereby minimizing any toxicity associated with formation of the p-QM (Figure 2.6).[10]

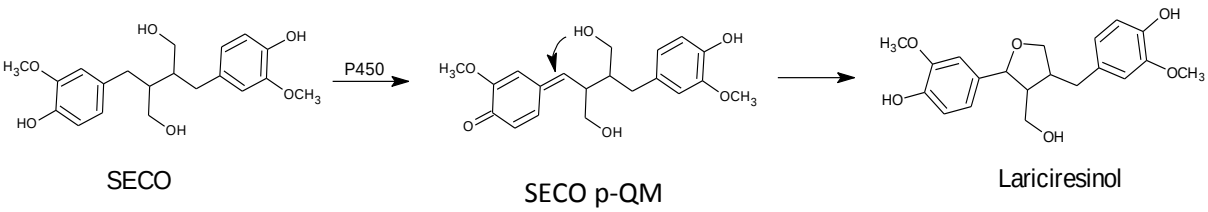

Figure 2.6 SECO oxidation and intramolecular cyclization to lariciresinol.

2.4.3 Pharmacological properties of SECO

Some putative health benefits of SECO include a reduction in serum LDL and total cholesterol levels, delaying the onset of type II diabetes, the treatment/prevention of cardiovascular diseases and decreased formation of breast, prostate and colon cancers.[9,10] Of particular interest is the use of SECO as a protective agent against hormone dependent cancers, especially breast and prostate cancers.[9] One in nine (1/9) Canadian women will be diagnosed with breast cancer in her lifetime and one in twenty nine (1/29) will die from it. Prostate cancer represents 24.5% of all new male cancer cases and everyday 11 Canadian men die from prostate cancer.[34] SECO has been found to demonstrate antioxidant activity, and is efficient at protecting cells *in vitro* from oxidative damage, which increases SECO's potential value as a therapeutic agent.[9,10]

2.5 Nordihydroguaiaretic acid (NDGA)

Nordihydroguaiaretic acid (NDGA; Figure 2.7) is closely related structurally to SECO. However, unlike SECO, NDGA is associated with toxicity.[7,8,35]

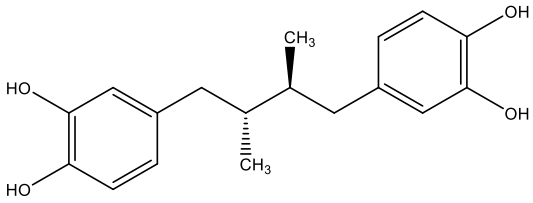

Figure 2.7 Structure of nordihydroguaiaretic acid.

2.5.1 Traditional uses of NDGA

NDGA is found in the leaves of the creosote bush (*Larrea tridentata)* also known as chaparral or greasewood in the United States and as gobernadora or hediondilla in Mexico.[36] The creosote bush can be found in the southwestern United States and the desert areas of Mexico.[37] Chaparral tea made from resinous extracts of the creosote bush, containing NDGA, has been used for centuries by Native North Americans to treat a wide verity of illnesses, including: chicken pox, skin sores, diabetes, kidney and gallbladder stones, venereal disease, tuberculosis, colds, and rheumatism.[36,37] NDGA has promising applications in the treatment of multiple diseases including the inhibition of tumors in historical reports as well as *in vitro* and animal studies.[36]

2.5.2 NDGA: Chemical properties

NDGA is unstable in aqueous media at physiological pH (pH 7.4; $t_{1/2}$ = 3.1 h). In the presence of O_2, NDGA undergoes an autoxidation reaction and forms an *ortho*-quinone,[35] which can be trapped as a glutathione (GSH) conjugate and is consistent with the observed increase in oxidative stress. In the absence of a trapping agent an intramolecular cyclization can occur to form a dibenzocyclooctadiene lignan (Figure 2.8)[35] that may be responsible for some of the biological effects of NDGA, although the half-life of the dibenzocyclooctadiene (41 h) is comparable to the parent compound.[38]

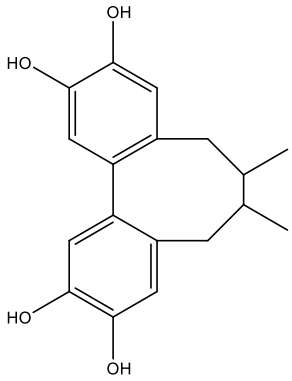

Figure 2.8 Structure of NDGA dibenzocyclooctadiene (cyclicNDGA).

Curiously, NDGA does not appear to form the expected p-QM in the process of forming the dibenzocyclooctadiene lignan.[39] It seems that spontaneous intramolecular cyclization to a dibenzocyclooctadiene requires a di-catechol lignan, which opens the possibility that this process may not be dependent on quinone formation.[39]

2.5.3 Pharmacological properties of NDGA

Numerous different pharmacological applications of NDGA have been studied, notably its anti-inflammatory and anti-cancer properties, which have been reviewed by Lambert, J. et al. 2004, Arteaga, S. et al. 2005 and Lu, JM et al. 2010.[40-42] NDGA is a strong antioxidant and a potent *in vitro* scavenger of reactive oxygen species (ROS).[37] It has been demonstrated that NDGA has benefits in areas of cancer chemoprevention, cancer therapy, antimicrobial, fertility and

hypoglycaemic effects in *in vitro* and *in vivo* studies as well as human clinical trials.[41] In 1992 Actinex® (Chemex Pharmaceuticals, Denver CO), a topical formulation of NDGA, was approved by the FDA for treatment of actinic keratosis,[43] however Actinex® was voluntarily withdrawn from the U.S. market in 1996 due to reports of skin hypersensitivity.[44,45] NDGA is an inhibitor of CYP1A2[37] and a potent inhibitor of lipoxygenase,[44,46] HPV,[42] HSV and HIV.[41,44] The use of NDGA in a clinical setting however, is limited due to reports of its toxicity.

2.5.4 NDGA toxicity

Chronic exposure (260 – 3800 mg/day over several months)[47] to chaparral is known to cause liver damage. Chronic consumption of chaparral tea is associated with drug-induced hepatitis[46] and cystic renal disease.[48] There is one reported case of total liver failure[46,49] and several cases of cirrhosis of the liver.[46] When the use of Chaparral was discontinued the symptoms of hepatotoxicity were reversed.[42,46,49,50] In humans, high doses of NDGA (for example 160 mg/d for 2 months) are associated with dermatitis, nephrotoxicity, biliary toxicity and hepatotoxicity including fulminant liver failure, and renal cell carcinoma.[37]

The Meat Inspection Division of the US War Food Administration initially approved NDGA for commercial use in 1943 as a food antioxidant to preserve fats and butter.[37] In 1968, NDGA was shown to induce cystic nephrotoxicity by the Canadian Food and Drug Directorate.[51] Due to this finding, the use of NDGA as a food preservative was banned in Canada. Subsequently the U.S. Food and Drug Administration removed NDGA from its "Generally Recognized As Safe" (GRAS) list in 1970.[37,41,51] There is also evidence that NDGA acts as a pro-oxidant in rat hepatocyte cultures at higher concentrations leading to oxidative stress, oxidative cell injury and cytotoxicity.[48] Contrarily, at lower concentrations NDGA has displayed beneficial antioxidant effects.[48]

2.6 Drug-Drug Interactions

Polypharmacy, the use of multiple medications, is common in North America especially among the elderly (65+), of which, over 50% take five or more prescription drugs at one time.[52,53] Drug interactions occur when a drug, pollutant or dietary constituent alters the pharmacokinetic or pharmacodynamic properties of a co-administered drug.[3] The effects can be antagonistic, additive, synergistic or idiosyncratic and can result in treatment failure, increased pharmacological effects or toxicity.[3] Pharmacodynamic interactions occur when the effects of a drug are either exaggerated or diminished without affecting its disposition or metabolism.[3,52] Pharmacokinetic interactions occur when one drug affects one or several of absorption, distribution, metabolism, and elimination (ADME) processes of another drug. This often occurs because one drug inhibits or induces the metabolism of the co-administered drug.[3] The effects of a drug, desirable or undesirable, are related to its concentration at its site(s) of action.[4]

Drug interactions may occur based on a combination of mechanisms.[4,54,55] For example a drug could both induce and inhibit an enzyme, or it could inhibit an enzyme and a transporter.[4] The prediction of *in vivo* interactions based on extrapolation from *in vitro* results is exceedingly challenging when there are multiple factors that affect clearance and multiple mechanisms of interaction.[4,56,57]

2.6.1 Enzyme inhibition and induction

Enzyme induction is the increased activity of an enzyme after exposure to an environmental factor, i.e. drug, toxicant or dietary constituent. If the environmental factor is no longer present, the activity of the enzyme will slowly return to baseline levels.[58] Increased metabolic activity can occur through a variety of mechanisms such as: increasing the amount of enzyme produced, stabilizing the enzyme, which allows for more efficient catalysis or by preventing the degradation of the enzyme. Enzyme inhibition is the reduction of enzyme activity after exposure to an environmental factor.[57] Inhibition can occur through many different mechanisms,

including: decreased enzyme production, inhibition of catalytic activity and increased degradation.[58] This is an important problem in the pharmaceutical and health sectors. While many drug-drug interactions have been identified and reported to health-care practitioners and patients, this has not been the case for most drug-natural product interactions. Since many natural products are self-medicated, the potential for serious drug-natural product interactions is a concern.[59]

2.6.2 Drug-drug interaction warning labels

Information on a drug-drug interaction could lead to a decision to alter the dose or dosage regimen or avoidance of the drug-drug interaction altogether.[4] However, warnings on drug labels may have limited effectiveness as there are numerous examples, such as astemizole, requiring withdrawal from the market because warning labels did not adequately manage the risk of drug interactions.[60]

2.6.3 Metabolism-based drug-drug interactions

Many different metabolic routes of elimination can be affected by concomitant drug treatment.[4] Metabolic drug-drug interactions can cause changes on the scale of an order of magnitude or more in blood and tissue concentrations of a drug or metabolite. This can in turn affect the extent to which toxic or active metabolites are formed. Large changes in drug or active metabolite exposure can alter its safety and efficacy profile. Changes in exposure are always a concern but are especially significant when a drug has a narrow therapeutic range.[4]

Drug-drug interactions can differ among individuals based on genetic variation of a polymorphic enzyme.[4] An example of a human polymorphic metabolic enzyme is CYP2D6, a drug metabolizing enzyme. An individual who has an enzyme phenotype that is less active than the general population, or the most common phenotype, is considered a poor metabolizer of CYP2D6. Conversely an individual with a phenotype that is more active than average is

considered an extensive metabolizer. It is important to study the effect of drug-drug interactions in people with different and varied genotypes or phenotypes.[4]

2.6.4 Transporter-based drug-drug interactions

Transporters govern the transport of solutes, including drugs and other xenobiotics, into and out of cells.[4] Transporters are present in all body tissues and play important roles in drug distribution, tissue-specific drug targeting, drug absorption, and elimination.[4,54,57] Most identified transporters belong to either the ATP-Binding Cassette (ABC) superfamily or the Solute Carrier (SLC) superfamily.[4]

The pharmacokinetics of a drug may be altered if a co-administered drug is an inhibitor or an inducer of its transporter.[4,54] Various drugs (e.g. verapamil) have been documented as increasing plasma levels of digoxin by inhibiting the efflux transporter, P-gylocoprotein (P-gp), at the intestinal level.[54] The schisandrins, which are present in a number of traditional Chinese medicines, are also known to inhibit P-gp, so caution must be exercised in their use with narrow range therapeutics like digoxin.[61] It should be noted that drug-drug interactions can have beneficial effects as well. Cidofovir, an antiviral drug, causes nephrotoxicity, while probenecid inhibits organic anion transport in the kidney. If cidofovir and probenecid are co-administered, prebenecid prevents the uptake of cidofovir into the kidney reducing toxicity.[4]

2.7 Adverse Reactions

Adverse reactions are defined by Health Canada as undesirable effects of health products.[60] Drugs (prescription and non-prescription pharmaceuticals, vaccines etc.), medical devices and natural health products fall under the umbrella of health products. In Canada, the Food and Drug Act and the Food and Drug Regulations, regulate health products after they are approved for use. The Food and Drug Regulations define an adverse drug reaction as a "noxious and unintended response to a drug which occurs at doses normally used or tested for the diagnosis, treatment or prevention of a disease or the modification of an organic function".[60] Reactions may occur

almost immediately, within minutes, or may not be evident until years after exposure.[60] The severity of reactions can range from minor (skin rash) to life threatening (heart attack).

2.7.1 Monitoring of adverse reactions

Most of the monitoring of adverse reactions after a product is marketed is done through voluntary reporting by both health officials and consumers.[60] Clinical trials testing the safety and efficacy of a pharmaceutical drug are performed prior to releasing a product to market. Unfortunately, most initial clinical trials only detect adverse reactions that occur commonly or frequently among the population. Adverse reactions, which typically take a longer timeframe to develop, are less likely to be observed in the number of patients involved in a clinical trial. In addition, the controlled setting and exclusion criteria of a clinical trial may not be reflective of the drug's use once marketed. Voluntary reports of adverse reaction may illuminate previously unknown adverse reactions.[60] Health Canada estimates that 41% of adverse reactions due to NHPs are reported[19] but this is unusually high compared to other voluntary reporting systems. The literature has established significant under reporting of adverse reactions in voluntary reporting systems for pharmaceutical products with only about 5% of incidences reported.[21-24]

2.7.2 Idiosyncratic drug reactions

Idiosyncratic drug reactions (IDRs) are considered a subclass of adverse reactions that do not occur in most patients and do not involve the therapeutic effect of the drug.[62] IDRs are unpredictable and often life threatening. There is evidence to suggest that most IDRs are immune mediated and caused by reactive chemical species. This means that even if a dug has the chemical characteristics to cause an IDR it is the patient-specific factors that determine susceptibility. IDRs represent a major problem for drug development and a large area of uncertainty for pharmaceutical companies because IDRs are not normally detected during clinical trials. Serious IDRs have led to the withdrawal of drugs from the market. The unpredictable nature of IDRs and the multiple mechanisms by which they can occur make developing mechanistic studies in humans difficult, and there are presently few valid animal

models.[62] Processes that are believed to contribute to IDRs (reactive intermediates, free radical formation, reactive oxygen species and oxidative stress) are outlined in the following sections. It should be noted that these processes can also have direct toxicological consequences.

2.7.3 Reactive intermediates

The toxicity of many chemicals is linked to their metabolism, a concept discovered in the 1950s[58,63] well before many of the underlying metabolic systems were understood. Metabolism can lead to the formation of reactive intermediates, which can cause toxicity by covalently modifying biochemically important macromolecules such as proteins and deoxyribonucleic acid (DNA) or through inhibition of detoxification pathways. These adverse reactions are deemed bioactivation reactions (also called metabolic activation).[64] Chemically, a reactive intermediate is a short-lived, high-energy, highly reactive molecule. Reactive intermediates are generally electrophiles such as quinones, epoxides, carbonium ions, and nitrenium ions.[63] Reactive intermediates play an important role as toxicity mediators, therefore, it is important to consider the structural features and metabolic processes that lead to biological activity.[65]

2.7.4 Free radicals

Free radicals are a type of reactive intermediate that may result from bioactivation. There are many different sources of free radicals including: pollutants, drugs, metal ions, radiation, the consumption of high levels of polyunsaturated fatty acids, mitochondrial dysfunction and smoking.[5] Uncontrolled free radical formation may contribute to a number of deleterious biological conditions including: cancer, diabetes, premature aging, and neurological, lung, vascular, autoimmune, and ocular diseases.[5]

2.7.5 Reactive oxygen species

Reactive oxygen species (ROS) is a term encompassing numerous compounds such as singlet oxygen, superoxide, peroxide, nitric oxide, peroxynitrite, peroxyl radical and hydroxyl radical

which can be formed through a variety of processes including metabolic bioactivation.[64] ROS can cause cellular damage directly by oxidizing or reducing cellular macromolecules. The cell damage that occurs as a result of ROS is called oxidative stress. ROS can oxidize DNA leading to mutations, oxidize proteins and oxidize lipids to form lipid peroxides. Lipid peroxides are thought to play an important role in the promotion and progression stages of chemical carcinogenesis. Lipid peroxidation generates a complex array of reactive electrophilic products and free radicals that react with proteins and DNA.[66] ROS can also cause damage indirectly by generating more ROS through propagation reactions.[64]

2.7.6 Oxidative stress

Oxidative stress is a term used to describe an imbalance between oxidants (ROS) and antioxidants in a system.[64,67] Oxidative stress may result from the overproduction of ROS and/or a decreased ability to deactivate them. Antioxidants are defined as "any substance that, when present at low concentrations compared with that of an oxidizable substrate, significantly delays or inhibits oxidation of that substrate".[67] This definition includes both enzymes and non-enzymatic substances. An increasing number of chemicals, have been shown to function as antioxidants including glutathione, vitamin C, vitamin A, and vitamin E[64,67]. These compounds work by intercepting the ROS and reacting with them to form non-reactive end products in a process known as deactivation.[67]

2.8 Xenobiotics

Xenobiotics are compounds that are foreign to a living organism, in this case, humans.[64] Xenobiotics are immensely diverse in size and shape, which is not surprising given the many sources of compounds, both natural (including natural health products) and anthropogenic that the human body is exposed to.[58] As foreign compounds, xenobiotics are recognized by the organism to be potentially detrimental to its survival; therefore, the organism takes steps to protect itself.[64] The first line of defense for humans consists of a number of transporter systems, such as P-glycoprotein, in the gastrointestinal tract that prevents xenobiotic absorption by

facilitating efflux from the enterocytes into the lumen.[64] If a xenobiotic is absorbed, it must be eliminated through excretion. In humans, excretion of most xenobiotics occurs through the bile and urine.[64] If a xenobiotic is lipophilic it is likely able to diffuse through lipid membranes, making it difficult to excrete. Metabolism of xenobiotics has evolved to primarily serve two functions: (i) to convert xenobiotics to more polar, hydrophilic entities that are more readily excreted and (ii) to attenuate any pharmacological activity.[58,64,68]

2.9 Xenobiotic Metabolism

A number of xenobiotic metabolism pathways have been identified. The enzymes identified in these pathways are often enzymes responsible for the metabolism of endogenous compounds. Xenobiotic metabolism typically occurs in the liver, though other tissues, such as the gastrointestinal tract, lung and kidney, may also contribute to xenobiotic metabolism.

Richard Tecwyn Williams, defined Phase I metabolism as oxidation, reduction and hydrolysis reactions or functionalization processes. Phase I metabolism is primarily catalyzed by cytochrome P450-dependant mixed-functional oxidases.[68] Phase II metabolism is comprised of conjugation reactions for example glucronidation and sulfonation which add a glucuronic acid of sulfonate group to a nucleophilic O or N-atom in a drug via the action of uridine diphosphate glucuronosyltransferase or sulfotransferase. Phase II metabolism normally results in water-soluble metabolites that are readily excreted.[69] Later Phase III metabolism was added to this classification system and encompasses antiporter activity, enzymes that transport drugs out of a cell, like the multidrug resistance-associated protein (MRP).[68,69]

All enzyme systems discussed are subject to great variability in their capacity to metabolize various xenobiotics.[58] Factors including gender, sex, age, disease, diet, exposure to environmental chemicals and genetic polymorphisms all contribute to population variability.[58] This is one of the reasons only a fraction of the population will encounter adverse reactions to a drug or experience increased toxicity.

2.9.2 Phase I metabolism

Phase I metabolism reactions are characterized by the addition or exposure of a polar functional group. Phase I reactions generally consist of oxidation, hydroxylation, reduction and hydrolysis reactions. There are many different classes of phase I enzymes including: Cytochrome P450s (P450), flavin containing monooxygenases (FMOs), alcohol dehydrogenase (AD), aldo- and keto-reductases, aldehyde and xanthine oxidases, peroxidases, amine oxidases and epoxide hydrase.

2.9.2.1 Cytochrome P450

Cytochrome P450 enzymes are a ubiquitous system of heme-thiolate enzymes encountered in all domains in life. They were discovered in 1964 and probably evolved concomitantly with green plants started to liberate O_2 into the atmosphere.[58,64] Cytochromes are proteins that contain a heme group and are membrane bound. All P450 enzymes have a cysteine residue located just prior to the N-terminus of the proximal (L) helix, which is absolutely conserved. This cysteine residue provides a thiolate functional group, which is ligated to the iron of the heme group, without this thiolate the enzyme is inactive.[58] P450 enzymes are monooxygenase enzymes; they insert one atom of oxygen, from O_2, into the substrate creating a hydroxyl (-OH) group while the other atom of oxygen is reduced to water.[58,64]

2.9.2.1.1 Mitochondrial and microsomal cytochrome P450s

There are two classes of P450 enzymes found in humans: microsomal and mitochondrial.[64] Mitochondrial P450 enzymes are located on the inner membrane of the mitochondria and are not implicated in the metabolism of xenobiotics. They are extremely important in the biosynthesis of endogenous compounds such as sterols.[58] Microsomal P450 enzymes (EC 1.14.14.1) are located on the smooth endoplasmic reticulum.[70] They use cytochrome P450 reductases (EC 1.6.2.4.) and cytochrome b_5 reductase (EC 1.6.2.2) to transfer electrons from NADPH. Microsomal P450 enzymes metabolize xenobiotics and are found at highest concentrations in the liver but are also found in other organs that must cope with exposure to foreign compounds such as the skin,

kidney, lung and gut.[58] If cells are homogenized the smooth endoplasmic reticulum forms small vesicles known as microsomes.[70] The microsomes can be collected as a pellet and used as an *in vitro* metabolic system.[70] Microsomes that are made from liver cells contain high levels of xenobiotic metabolizing enzymes and are a valuable tool for studying metabolism and drug interactions.[71]

2.9.2.1.2 Classification of cytochrome P450s

Humans encode approximately 66 functional P450 proteins and 30 pseudo genes. P450 proteins are found in almost every human organ.[58] The cytochrome P450 superfamily is first divided into families, which are, in turn, divided into subfamilies. Each subfamily consists of one or more enzyme isoforms.[58,64] Individual P450 enzymes cannot be properly considered isoenzymes (or isozymes) as isozymes are different enzymes that catalyze the same reaction. For the most part individual P450s catalyze different reactions, though there is some overlapping specificities, so the term isoform was coined.[58] P450 enzymes that belong to the same family share at least a 40% structural homology. Enzymes that belong to the same sub family contain at least 55 % structural homology.[58,64] P450 enzymes are all denoted CYP and then identified as family/subfamily/protein. For instance the notation for the cytochrome P450 enzyme that belongs to family 3, subfamily A, protein 4 is: CYP3A4. Arabic numerators 1-50 are used for animal P450 families, 50-65 for fungal families, 70-100 for plant families and 100 and above are used for bacterial families.[58] Differing alleles of an isozyme are indicated with a star (*) follow by a number, for instance CYP2D6*4.[72]

2.9.2.1.3 Cytochrome P450 metabolism

Families CYP1, CYP2, CYP3 and CYP4 perform xenobiotic metabolism, although CYP4 is minimally involved. The majority (90%) of xenobiotic oxidations are catalyzed by CYP1, CYP2 and CYP3.[64] Other cytochrome P450 families mainly metabolize endogenous substrates. Isoforms CYP1A2, CYP2C8, CYP2C9, CYP2C19, CYP2D6, CYP2E1 and CYP3A4 are responsible for most of the xenobiotic metabolism in humans.[73,74] Out of all the human P450s,

CYP3A4 has the highest level of expression, totaling 34% of all hepatic P450.[58] It is believed that up to half of all xenobiotics are metabolized at least in part by CYP3A4.[58] The CYP2 family displays clinically relevant polymorphisms more frequently than any other P450 family.[75] CYP2D6, 2C19, and 2C9 polymorphisms account for the most frequent variations in phase I metabolism of drugs. For example, a patient taking the anticoagulant warfarin who is homozygous for the CYP2C9*3 allele, would have warfarin metabolism reduced by 90%.[76] This is clinically relevant as warfarin has a narrow therapeutic index. Drug-drug interactions can also differ among individuals based on genetic variation of a polymorphic enzyme.[4]

2.9.2.1.4 Cytochrome P450 metabolism and bioactivation

Cytochrome P450 metabolism can also contribute to the bioactivation of xenobiotics. Electrophiles, reactive oxygen species and radicals can all be formed as a result of P450 metabolism.[58,64] These are all reactive species that can cause cellular damage leading to cell death or cancer. Any factor that influences the metabolism of these chemicals will also affect their toxicity.[64]

2.9.2.1.5 Cytochrome P450 induction and inhibition

Cytochrome P450s can be induced by their own target or by a different environmental factor.[58] The amount of a given P450 enzyme can be increased by up to two orders of magnitude, though the total amount of P450 present generally only increases two or three fold, in the presence of a xenobiotic. P450 may also be upregulated prior to exposure to the xenobiotic due to previous exposure to an environmental factor or in response to disease. This can cause a significant increase of enzyme activity that can lead to a build up of toxic metabolites. Conversely P450 enzymes can be inhibited either reversibly or irreversibly by xenobiotics. If the P450 metabolism pathway is a deactivation pathway, inhibition can lead to increased metabolism via alternate routes. If those alternate pathways are bioactivation pathways this can lead to increased toxicity. Inhibition of P450s can also cause an increase in the concentration of a concomitant drug that is also metabolized by that enzyme. Overdose toxicity is particularly worrisome as the

consequences of such an occurrence can be fatal.[58]

2.9.3 Phase II metabolism

Phase II metabolism involves the conjugation of small polar molecules to xenobiotics or other environmental factors, typically resulting in water-soluble metabolites that are readily excreted.[68] Phase II metabolism is regarded as the detoxification step in the three phase metabolic system of classification,[68,69] but it can also be a critical step for the formation of genotoxic electrophiles.[69] The major reactions included in phase II metabolism are glutathione conjugation, glucuronic acid conjugation, N-acetylation and sulfonation.[58,68]

2.9.3.1 Glutathione conjugation

Glutathione (GSH) is the common name for the tri-peptide γ-L-glutamyl-L-cysteinyl-glycine[58] as shown in Figure 2.9.

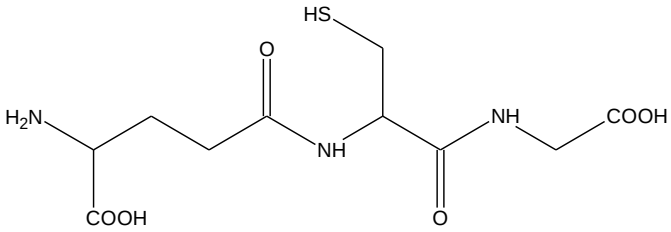

Figure 2.9 Structure of glutathione

GSH is the most common thiol-molecule in all mammalian cells; its concentration in human hepatocyte cytosol is approximately 10 mM.[58] GSH participates in many biochemical processes including maintenance of redox homeostasis and the trapping of electrophiles. GSH is a scavenger molecule that can spontaneously react non-enzymatically with electrophilic and radical species, i.e. quinones and semiquinone radicals. The sulfur atom of the GSH is a "soft" nucleophile (one with easily polarizable electrons) and reacts preferentially with soft electrophiles.[58] GSH is important in protecting the cell against ROS and oxidative stress.

After conjugation of substrate (X) to GSH, the resulting adduct is denoted X-SG as the GSH is always bonded to the substrate at the sulfur atom of the cysteine residue. Though GSH conjugation is normally a detoxification function there are a few instances where conjugation increases toxicity. One example of this is the xenobiotic dichloromethane; its reaction with GSH yields formaldehyde via the intermediate S-chloromethyl-SG. Both the GSH adduct and formaldehyde are more toxic than dichloromethane. The most common case of toxicity associated with this metabolism pathway is not the formation of reactive metabolites, but the depletion of GSH from the cell. This leaves the cell vulnerable to damage from electrophiles and ROS that GSH normally scavenges, it can also cause metabolism to proceed down an alternate, possibly more toxic pathway.[58]

2.10 Quinones

Quinones are a class of cyclic organic compounds containing two carbonyl groups (Figure 2.10). If the carbonyl groups are adjacent to each other, they are in the *ortho*- configuration and called an *ortho*-quinone (o-Q). If a vinyl group separates the carbonyl groups, they are in a *para* configuration (p-Q).

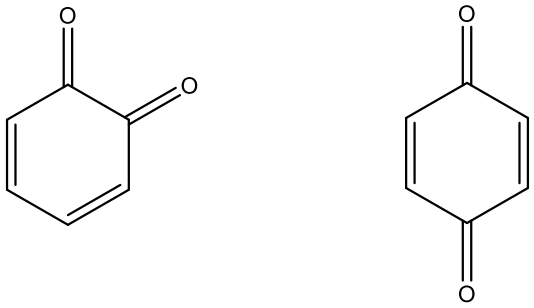

Figure 2.10 Basic structure of an *ortho*-quinone (left) and a *para*-quinone (right).

Quinones and their phenolic precursors (Figure 2.11) are naturally occurring compounds that are ubiquitous in nature.[15]

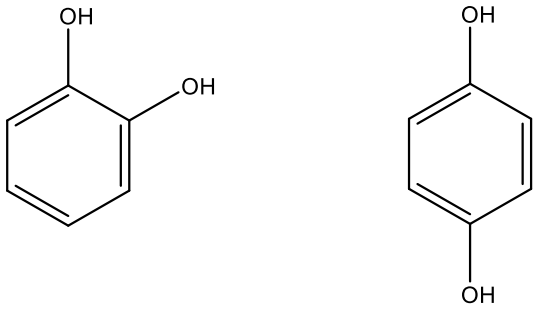

Figure 2.11 Basic structure of the phenolic precursors of an *ortho*-quinone (left) and a *para*-quinone (right).

Humans are exposed to quinones through the consumption of fat, pharmaceutical drugs, natural health products and environmental pollutants such as polycyclic aromatic hydrocarbons.[15,77] Quinones are involved in a vast array of biological and chemical processes, including: the electron transport chain (ETC) in animals and plants, photosynthesis, post-translational modification of proteins and metabolism of cellular signaling molecules.[77]

2.10.1 Quinone toxicity

Quinones can have various toxicological effects *in vivo*, including cytotoxicity, immunotoxicity, and carcinogenesis.[14] Quinones are highly reactive compounds as they are both oxidants and electrophiles.[15] Covalent bonding can cause cytotoxicity if the electrophilic quinones react with nucleophilic groups on cellular macromolecules, like thiol and amine groups in proteins and DNA, forming reversible or irreversible adducts. Irreversible covalent bonding can cause structural or functional changes of cellular macromolecules resulting in cytotoxicity.[14,16]

Quinones are also potent redox active compounds, which can undergo redox cycling with their semi-quinone radicals, generating reactive oxygen species (ROS) and leading to oxidative stress through the formation of oxidized cellular macromolecules, including: lipids, proteins and DNA (Figure 2.12).[14,16]

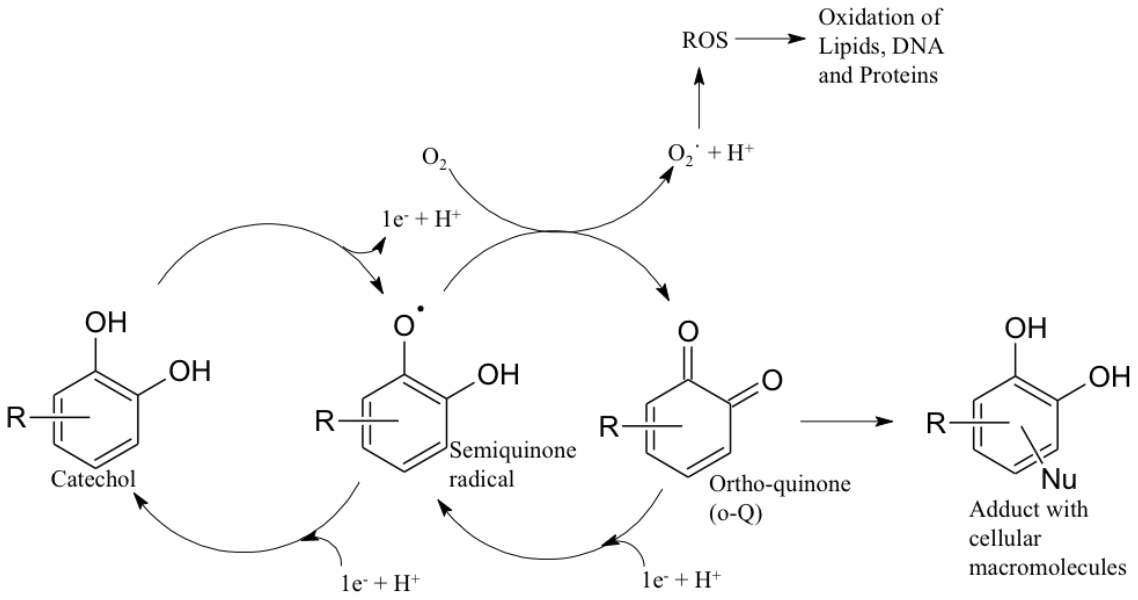

Figure 2.12 Redox cycling of an *ortho*-quinone with its semiquinone radical leads to the formation of reactive oxygen species causing the oxidation of cellular macromolecules leading to oxidative stress. The *ortho*-quinone may also covalently bind to cellular nucleophiles to form adducts

2.10.2 Quinone methides

Quinone methides (QMs) differ structurally from quinones, as one carbonyl group is replaced by a methylene or substituted methylene group.[78] Figure 2.13 shows an example of a *para*-quinone methide (p-QM). QMs have been implicated in the toxicity of certain exogenous compounds including food additives such as butylated hydroxytoluene (BHT).[79]

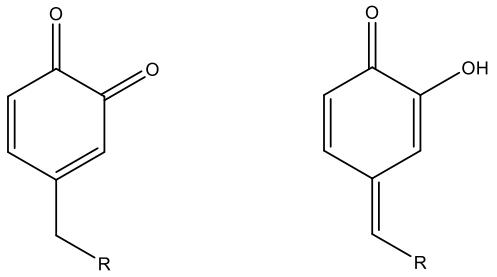

Figure 2.13 General structure of an *ortho*-quinone (left) and *para*-quinone methide (right)

Unlike o-Qs, p-QMs are not implicated in redox cycling processes, instead they are more electrophilic and typically form stable adducts.[14]

2.11 Perspective

Lignans are found in most fiber rich plants and present enormous structural diversity. Interest in lignans and their use as a natural product, arose from their potential health benefits including: changes in blood lipid profiles, antioxidative effects and estrogenic, antiviral, antiestrogenic and anticarcinogenic activities.[6,8-12] However some lignans such as NDGA also present toxicity concerns. To my knowledge there has been no overall structure activity relationship proposed to describe the potential toxicity of lignans in relation to specific structural features. SECO and NDGA are interesting for the purposes of investigating the structure activity relationship of lignans as both have potential pharmacological applications and both are oxidized to reactive intermediates but NDGA is associated with toxicity and SECO is not.

In the drug discovery process, chemical modification is commonly used and is an accepted method to investigate the toxicity and/or pharmacological effects of the constituents of potential drug candidates. The structural features of lignans govern their metabolic pathways and likely have toxicological and pharmacological implications but are poorly understood. The structural features that alter metabolic pathways and allow the formation of reactive intermediates, particularly quinone formation and intramolecular cyclization processes, are of interest. Previously in our lab NDGA analogues were investigated for their stability in aqueous solution, their propensity to form quinone species and the functional groups required for intramolecular cyclization. This research will investigate the effect of the addition of the hydroxyl groups to the two-methyl groups at the γ position on oxidative metabolism of the previous NDGA analogues. These hydroxyl groups are indicated in Figure 2.14.

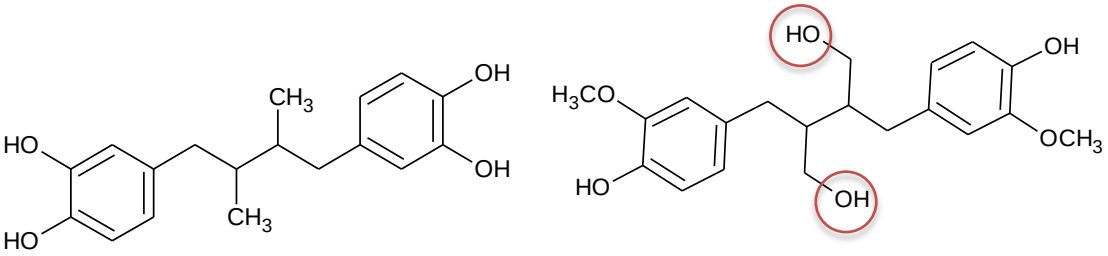

Figure 2.14 Structures of NDGA (left) and SECO (right) with the hydroxyl groups at the γ position in question circled in red.

2.12 Purpose

2.12.1 Rational

Understanding the structural features that guide the mechanistic pathways to toxicity through oxidative metabolism is important for the overall understanding of the structure activity relationship influencing lignan stability and metabolism. To this end several analogues of SECO (SECO-1,2,3,4; Figure 2.15) with altered functional groups were previously synthesized and will be used to investigate substituent effects on: lignan metabolism and formation of reactive quinones and to probe the effect of structure on the pharmacological and toxicological properties of SECO.

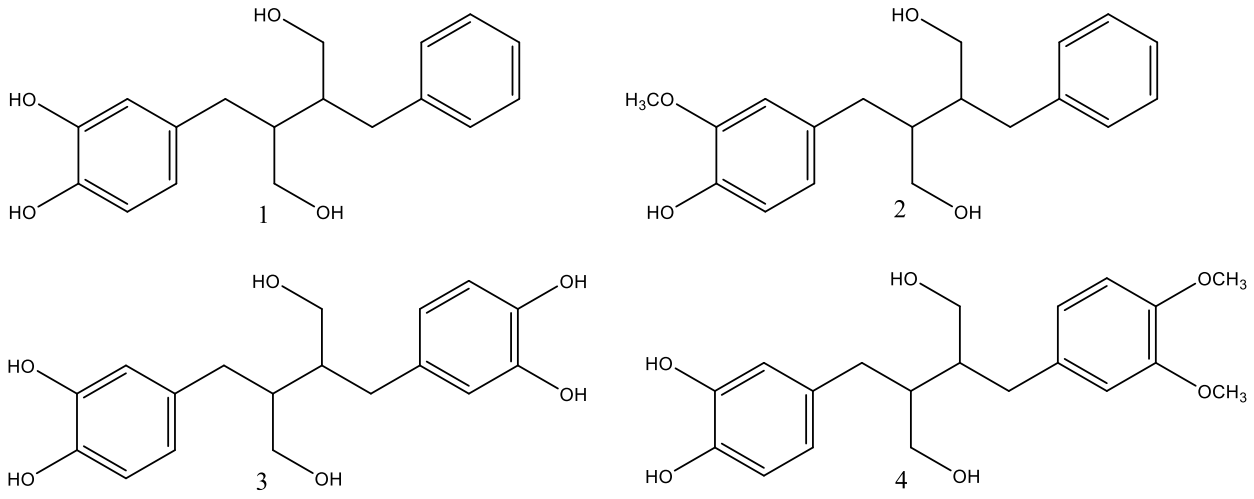

Figure 2.15 Structures of SECO analogues: SECO-1 (1), SECO-2 (2), SECO-3 (3), SECO-4 (4)

These specific analogues were chosen to build on previous research with NDGA analogues (Figure 2.16) with SECO-1 corresponding to NDGA-1.

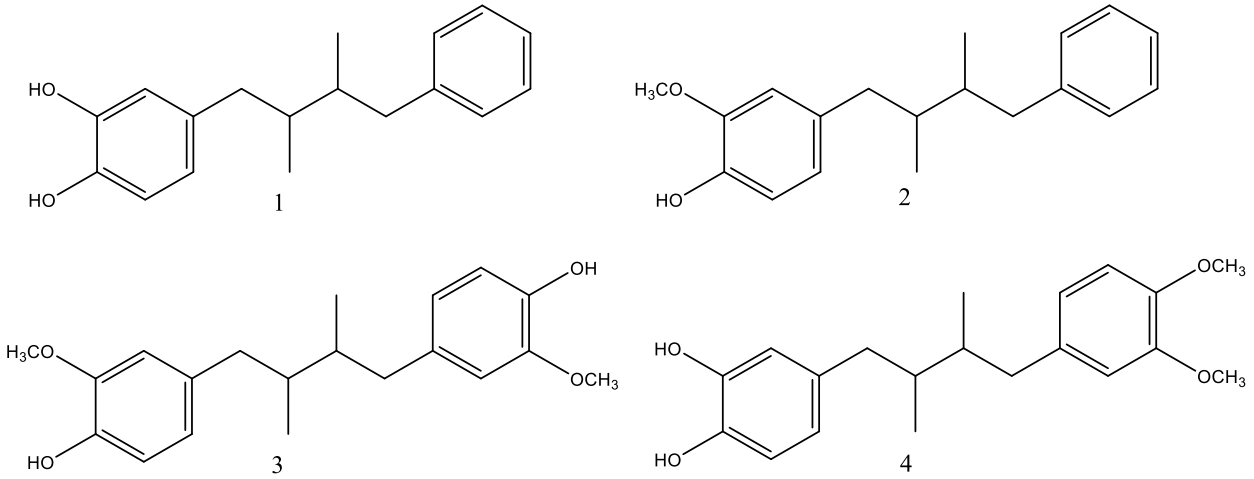

Figure 2.16 Structures of NDGA analogues: NDGA-1 (1), NGDA-2, (2), NDGA-3 (3), NDGA-4 (4)

SECO analogues 1, 2 and 4 were synthetic intermediates isolated during the preparation of the NDGA analogues;[38] SECO-3 was prepared as a direct SECO analogue to NDGA (i.e. a di-catechol lignan). The goals of the NDGA study were to determine the structural features required for dibenzocyclooctadiene formation and how substituents influenced stability. The presence of the γ-OH groups in the SECO analogues introduces the ability for these lignans to be involved in unique intramolecular cyclization reactions, such as that observed for SECO to lariciresinol conversion (see Figure 2.6). As lignans continue to be investigated for their pharmacological properties, an understanding of the influence of the γ-OH groups on lignan stability and metabolism is a crucial component for further development of lignans as potential therapeutic agents.

Autoxidation studies will be performed to determine the stability of each analogue. Enzymatic oxidation experiments will be completed to determine which structural features influence quinone formation. The purpose of this research is to probe the effect of structure on the pharmacological and toxicological properties of lignans.

2.12.2 Hypotheses and Objectives

2.12.2.1 Hypothesis 1

All SECO analogues will form quinones. Catechol analogues will form *ortho*-quinones. Phenol analogues will form *para*-quinone methides

2.12.2.1.1 Objectives 1

1. Determine the rate of autoxidation of the SECO analogues.
2. Determine the *in vitro* hepatic oxidative metabolism and bioactivation of the SECO analogues.

2.12.2.1.1.1 Specific Aims 1

1. Develop a high performance liquid chromatography (HPLC) method for the detection and separation of SECO analogues and autoxidation products.
2. Quantify the stability of the SECO analogues in buffer at pH 6.0 and pH 7.4
3. Identify the autoxidation products using mass spectrometry (MS)

2.12.2.1.1.2 Specific Aims 2

1. Develop an HPLC method for the detection and separation of metabolites.
2. Perform enzymatic and chemical oxidation experiments on the SECO analogues using glutathione as a trapping agent
3. Perform microsomal incubation experiments on the SECO analogues using glutathione as a trapping agent.
4. Identify glutathione adducts and lariciresinol-like metabolites using MS

2.12.2.2 Hypothesis 2

All SECO analogues will inhibit cytochrome P450 isoforms CYP3A4, CYP3A5, CYP2C9 and CYP2C19.

2.12.2.2.1 Objectives 2

1. Determine the ability of the SECO analogues to inhibit cytochrome P450 isoforms CYP3A4, CYP3A5, CYP2C9 and CYP2C19.

2.12.2.2.2.1.1 Specific Aims 1

1. Determine the *in vitro* IC_{50} inhibition values for all of the SECO analogues and SECO against the cytochrome P450 isoforms CYP3A4, CYP3A5, CYP2C9 and CYP2C19. The inhibition study will be carried out by Life Technologies.

3.0 Materials and Methods

3.1 Materials

The following chemicals were purchased from Sigma-Aldrich (St. Louis, MO): $AgNO_3$, dimethyl sulfoxide (DMSO), ethylenediamine-tetracetic acid (EDTA), eugenol, reduced glutathione (GSH), KCl, $MgCl_2$, mushroom tyrosinase, NaOH, reduced nicotinamide adenine dinucleotide phosphate (NADPH) tetrasodium salt, protease inhibitor cocktail (P8215), salicylamide, sodium pyrophosphate ($Na_4O_7P_2$) and sucrose. Formic acid, KOH, Na_2HPO_4, and perchloric acid were obtained from BDH Chemicals (Toronto, ON). Rat Liver Microsomes (0.5mL; 20mg/mL; Lot# RT053C) were purchased from Invitrogen (Life Technologies; Burlington, ON). Dithiolthreitol (DTT), and Pierce® BCA Protein Assay Kit were obtained from Thermo Scientific (Milwaukie, WI). Tris hydrochloride was obtained from EMD Millipore (Billerica, MA). Acetonitrile, ethyl acetate, glycerol, HCl, and methanol were obtained from Fisher Scientific (Fairlawn, NJ); C_2D_3N (acetonitrile-d_3) was obtained from Cambridge Isotope Laboratories Inc. (Andover, MA). Silver oxide (Ag_2O) was freshly prepared from $AgNO_3$ and KOH according to a literature procedure.[80] HPLC runs were performed with HPLC grade acetonitrile from Fisher Scientific (Fairlawn, NJ) and water was filtered using a Millipore, Milli-Q system with a Quantum EX cartridge (Mississauga, ON). LC/MS grade water (Milli-Q H_2O),

methanol and acetonitrile were used for all LC-MS analyses and obtained from Fisher Scientific (Fairlawn, NJ).

3.2 High Performance Liquid Chromatography (HPLC)

HPLC was performed on a Waters Alliance 2695 Separations Module (Milford, MA) using a Waters 2996 Photodiode Array Detector (λ = 280; Milford, MA) and Empower software (2002; Build Number 1154). An Agilent Poroshell 120 EC-C18 4.6 × 50 mm 2.7 μm column (Mississauga, ON) with an injection volume of 10 μL at room temperature was used for compound separation. A linear gradient mobile phase system, solvent A was water with 0.1% formic acid and solvent B was acetonitrile with 0.1% formic acid. Both solvents were filtered through a 0.45 micron filter, sonicated and degassed prior to use. The HPLC gradient outlined in Table 3.1 was used to detect and separate compounds.

Table 3.1 HPLC gradient program employed for the separation of SECO analogues and metabolites

Time (min)	Flow rate (mL/min)	% Solvent A[1]	% Solvent B[2]
0	0.5	85	15
17	0.5	85	15
27	0.5	30	70
30	0.5	10	90
35	0.5	10	90
36	0.5	85	15
39	0.5	85	15
40	0	85	15

[1] water with 0.1% formic acid
[2] acetonitrile with 0.1% formic acid

3.3 SECO Analogue Stability at pH 6.0 and 7.4

A 1 mM solution of each SECO analogue was prepared in a Na_2HPO_4 (50 mM) buffer of the desired pH (6.0 or 7.4). Each sample was vortexed for 5 s and placed in a water-bath heated to 37 °C and shaken at 150 rpm. A pseudo time 0 sample was taken after 15 s on the shaker by removing a 500 μL aliquot and quenched with 20 μL perchloric acid for a final pH ~2 to stop the

reaction. For analysis an internal standard (KA-1-09-2; Figure 3.1) was added and samples were analyzed using the HPLC method described above.[11] The solution was returned to the incubator and samples were taken at 0.25 h, 0.5 h, 1 h, 2 h, 3 h, 4 h, 5 h, 6 h, 7 h, 8 h, 10 h, 12 h, 24 h and 48 h time points.

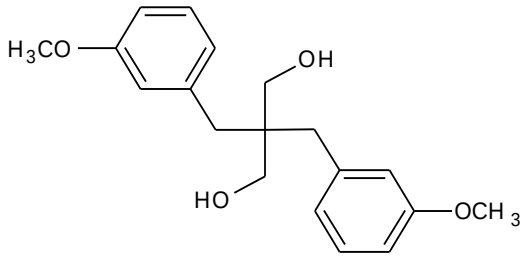

Figure 3.1 Structure of KA-1-09-2 used as the internal standard

3.4 Determination of decomposition products

The major decomposition product of SECO-3 was the only decomposition product present in sufficient quantity that NMR analysis was possible. SECO-3 (1 mM; 5 mg total) was allowed to decompose in Na_2HPO_4 buffer (50 mM; pH 7.4) at 37ºC. The reaction was halted at 8 h with the addition of perchloric acid (200 µL). The pH was checked to ensure that it was less than pH 2. Factions were collected using an Agilent 1200 LC (Santa Clara, CA) and fraction collection based on deviation from baseline. The product fraction was concentrated by using a Buchi R-200 rotary-evaporator with a V-850 Vacuum controller (New Castle, DE) to drive off the acetonitrile. It was then flash frozen using liquid nitrogen and lyophilized using a Labconco Freezone 6 Plus lyophilizer (Kansas City, MO) for more than 24 h. Approximately 1 mg of product was obtained. The product was then analyzed by ^1H nuclear magnetic resonance (NMR) spectroscopy on a Bruker AVANCE DPX-500 spectrometer (Rheinstetten, Germany) and data processed by X-WIN NMR 3.5 software or TopSpin 3.2.

3.5 Silver Oxide Preparation

The procedure employed was based on that outlined in Yu et al., 2004.[80] KOH (0.72 g) was added to 20 mL Milli-Q H_2 and allowed to dissolve completely at room temperature. $AgNO_3$ (2.0 g) was added to 20 mL milli-Q H_2O and stirred for 10 min. The KOH solution was combined

with the $AgNO_3$ solution and stirred for a further 15 min. A black precipitate of Ag_2O forms following the reaction:

$$2KOH + 2AgNO_3 \rightarrow Ag_2O + 2KNO_3 + H_2O$$

The precipitate was filtered and washed with H_2O (3 x 10 mL). Ag_2O is light sensitive so it was covered and dried on a high vacuum pump overnight.[80]

3.6 Silver Oxide Oxidation

This procedure is based on the method outlined in Krol and Bolton, 1997.[81] Stock solutions of each SECO analogue (0.1 M; DMSO) were dissolved in 4 mL acetonitrile to a final concentration of 1 mM. Ag_2O (0.2 g) was added and mixture was placed on a shaker (medium speed) for 15 min at room temperature. The reaction mixture was tremoved from the shaker and allowed to settle. The supernatant (1 mL) was removed and centrifuged at 14 000 rpm for 10 min in an Eppendorf S417C centrifuge (Mississauga, ON). An aliquot of the supernatant (250 μL) was added to Na_2HPO_4 buffer (50 mM; pH 7.4) either with or without glutathione (GSH) (50mM in Na_2HPO_4; pH 7.4; 5:1 GSH/substrate ratio) to a final volume of 5 mL. 500 μL aliquots were used for HPLC analysis using the previously described method. Another 500 μL aliquot was used for mass spectrometry (MS) analysis. UV-Vis spectrophotometry (Agilent 8453; Santa Clara, CA; λ = 200 – 400 nm) was also performed at each stage of the experiment. This experiment was performed with SECO analogues 2 and 3 as well as the model compound eugenol.

3.7 Enzymatic Oxidation using Mushroom Tyrosinase

Oxidation of SECO and its analogues was performed at pH 6.0 utilizing mushroom tyrosinase (EC 1.18.14.1) isolated from the mushroom species *Agaricus bisporus*.[82] Mushroom tyrosinase is catalytically active at pH 6.0 and this protocol is consistent with previous experiments.[82] Mushroom tyrosinase is an enzyme known to exhibit wide substrate specificity and readily oxidizes a number of *o*-diphenolic compounds.[78] GSH was used as trapping system; it will

conjugate to metabolites, specifically quinones produced from the enzymatic oxidation and form GSH adducts.[83] Glutathione S-transferase is not necessary for this reaction to occur. A 5:1 ratio (GSH:substrate) was used, 100 μL of GSH (50 mM) in Na_2HPO_4 buffer (50 mM, pH 6.0) for a final concentration of 5 mM. The position of the GSH in the adduct will determine if an *ortho*-quinone (o-Q) or p-QM was produced.[83] Each SECO analogue (1 mM) was prepared in Na_2HPO_4 buffer (50 mM; pH 6.0) with a final volume of 1 mL with or without GSH (5 mM).

Mushroom Tyrosinase (8 μL of 8.63736 U/μL stock solution) was added to the SECO analogue mixture and vortexed for 5 s. A 500 μL aliquot was immediately removed and quenched with perchloric acid (20 μL) to a final pH ~ 2 to stop the reaction. This was used as time 0. The sample was then centrifuged at 14 000 rpm for 10 min and the supernatant was kept for analysis. The remainder of the reaction mixture was placed in a Boekel Grant ORS 200 water bath (Feasterville, PA) at 37 °C and shaken at 200 rpm for 60 min. The reaction was quenched and centrifuged as described for the time 0 sample. The results of this experiment were analyzed using HPLC as described above, MS and liquid chromatography-mass spectrometry (LC-MS). Experiments were run in triplicate.

3.8 Sample Preparation for Direct Infusion Mass Spectrometry

For samples containing GSH solid phase extraction was used. using a Waters Sep-Pac C18 Vac cartridge (Waters, Milford, MA) and an extraction manifold (Waters, Milford, MA). The cartridge was activated with methanol (5 mL) then washed with Milli-Q H_2O (15 mL). The sample (500 μL) was loaded onto the column and was washed with Milli-Q H_2O (5 mL) to remove salts. Metabolites were washed off the column with methanol (2 x 1 mL).

For samples not containing GSH, liquid-liquid extraction was performed. Ethyl acetate (0.5 mL) was added to the sample and the mixture was inverted (10x) and allowed to settle. The ethyl acetate layer was retained and evaporated on a high vacuum pump overnight. The following morning extraction products were re-dissolved in methanol (0.5 mL). Two different methods were necessary due to the differences in polarity of the metabolites produced.

3.9 Direct Infusion Mass Spectrometry

Mass spectrometry was performed on an AB Sciex 4000 QTRAP mass spectrometer (Framingham, MA) using Analyst software (version 1.6.2). ESI (-) was first used to generate MS^1 full mass spectra with a range of 100 – 700 mass-to-charge ratio (*m/z*). If a GSH adduct was suspected ESI (+) was then used to perform tandem mass spectrometry (MS/MS; MS^2) (see Table 3.2). We previously developed a method of differentiating aromatic and benzylic GSH adducts.[39] This technique was used to perform neutral loss (NL) scans looking for a neutral loss of 129 or 307. Neutral loss of 129 is indicative of an aromatic GSH conjugate, while a neutral loss of 307 is indicative of a benzylic GSH adduct. The precursor ions that are identified by the neutral loss scans were then selected to undergo collision induced dissociation (CID) product ion scans. If the precursor ions are glutathione adducts they show characteristic fragmentation pathways as shown in Figure 3.2.

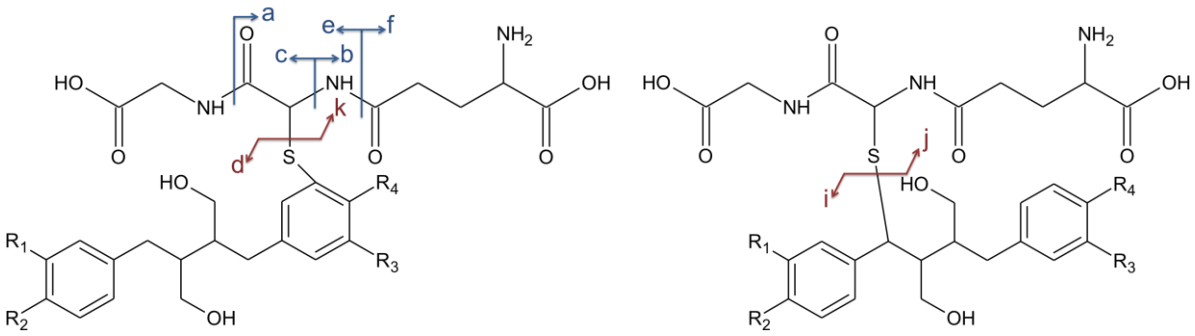

Figure 3.2 Fragmentation pathway of aromatic (left) and benzylic (right) GSH conjugates following collision induced dissociation (CID) for SECO analogues. Developed by Isaac Asiamah.

Table 3.2. Expected *m/z* ESI (+) for the product ions of the GSH adduct fragmentation pathway pictured in Figure 3.2. P represents the parent ion. Developed by Isaac Asiamah.

Fragment Type	Positive m/z	Fragment Type	Positive m/z
a	P-75	**g**	P-232
b	145	**h**	P-249
c	P-146	**i**	308
d	P-275	**j**	P-307
e	P-129	**k**	274
f	130		

3.10 Liquid Chromatography – Mass Spectrometry (LC-MS)

The same liquid chromatography method described in High Performance Liquid Chromatography (HPLC) was used on an Agilent 1200 LC (Santa Clara, CA) with a AB Sciex 4000 QTRAP mass spectrometer (Framingham, MA) using Analyst software (version 1.6.2). ESI (-) MS^1 with a *m/z* range of 100 – 700 and NL (+; 129 and 307) mass spectra were collected. Scans were conducted every 1.5 s.

3.11 Rat Liver Microsome Preparation

The protocol for animal use (20030062) was approved by the University of Saskatchewan UCACS Animal REB . Liver microsomes are subcellular particles derived from the endoplasmic reticulum of hepatic cells.[71] Rat liver microsomes were prepared from the pooled livers of 3 adult male Sprague-Dawley rats using the Krol Lab Preparation of Hepatic Microsomes – Standard Operating Procedure.

3.11.1 Preparation of stock solutions

All stock solutions were prepared in advance and stored at 4°C until use. Milli-Q H_2O was used to make all stock solutions.

A. Homogenization Buffer (100 mL)

50 mM Tris Buffer
150 mM KCl,
0.1 mM Dithiothreitol,
1 mM Ethylenediamine-tetracetic acid
20% Glycerol.
Chill to 4°C and pH to 7.4 with HCl

B. Protease Inhibitor cocktail (Sigma Aldrich; P8215)

Store at -20°C

C. Microsomal Storage Solution (100 mL)

0.25 M Sucrose
Note sucrose solution has a shelf life of 1 week.

D. Microsomal wash solution (100 mL)

50 mM KCl

3.11.2 Microsome preparation

Microsome preparation was performed in a 4 °C cold room. All necessary instruments and solutions were brought to the cold room and chilled prior to commencement. Protease inhibitor cocktail (500 µL) was added to the homogenization buffer. The rat liver was chopped into larger pieces and 2-3 g of liver tissue was weighed out and placed in the 30 mL Wheaton Teflon tissue homogenizer glass sleeve (Millville, NJ). Homogenization buffer (10 mL) was added to the glass sleeve and the teflon tipped pestle of the tissue homogenizer (Wheaton, Millville, NJ) was used

to grind all of the liver into solution. The pestle was then passed through the solution 10 more times taking care that the homogenate remains cold. The homogenate was stored on ice until all of the liver tissue was homogenized. Homogenate was pooled. A Beckman Coulter Optima L-90K ultracentrifuge (Brea, CA) and a Type 60 Ti ultracentrifuge rotor (Beckman Coultre; Brea, CA) were used for all the centrifugation. First a low speed centrifugation at 10,000 rpm (RCF = 10041.8 × g) for 30 min was used to separate out the late cellular particles such as the nucleus, mitochondria and lipid membrane into the pellet. The supernatant was collected and centrifuged at 35,000 rpm (RCF = 123012.4 × g) for 30 min. to separate the smooth and rough endoplasmic reticulum from the cytosol. The supernatant was then removed and the pellet was washed with microsomal wash solution (5 mL). The pellet was again centrifuged at 35,000 rpm (RCF = 123012.4 × g) for 30 min. The resulting pellet was reconstituted in microsomal storage buffer (2 mL). Aliquots (500 μL) were transferred into labeled microfuge tubes and stored at -80 °C.

Rat Liver Microsomes (0.5mL; 20mg/mL; Lot# RT053C) were also purchased from Invitrogen (Life Technologies; Burlington, ON) for method development. Protein concentration was determined using Pierce® BCA Protein Assay Kit

3.12 Rat Liver Microsome Oxidation

Niemeyer *et al*., 2003, established that SECO undergoes oxidative metabolism when incubated with liver microsomes (rat and human).[10] The major product of SECO's metabolism was lariciresinol though there were also at least 5 other minor products detected.[10] Rat liver microsomal incubations with SECO have also been performed by Jacobs and Metzler, 1999, this method was modified to be consistent with previous microsomal incubations done in the Krol lab.[84] This experiment was run with and without a GSH trapping system, where a 10:1 ratio (GSH:substrate) was utilized. The following stock solutions were prepared: 0.1M stock solutions of the SECO analogues in methanol or dimethyl sulfoxide (DMSO); $MgCl_2$ (100 mM); β-nictotinamide adenine dinucleotide 2'-phosphate reduced salt hydrate (NADPH) (10 mM) in pH 7.4 Na_2HPO_4 buffer (50 mM); GSH (50 mM) in pH 7.4 Na_2HPO_4 buffer (50 mM); pH 7.4 Na_2HPO_4 buffer (50 mM) ; $Na_4O_7P_2$ (100mM) (sodium pyrophosphate; SPP). The final volume of the reaction mixture was 500 μL and contained: 0.5 mg/mL of microsomal protein, 0.5 mM of

the test compound, 5 mM $MgCl_2$, 5 mM GSH and 10 mM SPP. This reaction mixture was pre-incubated (5 min) in a Boekel Grant ORS 200 water bath (Feasterville, PA) at 37 °C and shaken at 200 rpm. The reaction was initiated with the addition of NADPH (50 μL of 10 mM; 1 mM final concentration). The reaction was terminated after 60 min by addition of ice-cold acetonitrile (20 μL). The sample was then centrifuged at 14 000 rpm for 10 min and the supernatant was kept for analysis. The results of this experiment were analyzed using HPLC, MS and LC-MS methods and sample preparations described above. Experiments were performed in triplicate and no NADPH and boiled microsomes (60 s prior to addition to the assay) were used as negative controls. .

3.13 Cytochrome P450 Inhibition

We contracted Life Technologies to run IC_{50} inhibition assays, using their SelectScreen® Biochemical P450 Profiling Services (Madison, WI). This screen uses P450 Baculosomes® containing a single human P450 isozyme and rabbit NADPH-cytochrome P450 reductase, prepared from insect cells with recombinant baculovirus and Vivid® Substrates. The Vivid® Substrates have low fluorescence until cleaved via metabolism by cytochrome P450, generating a highly fluorescent metabolite. Inhibitors are identified by their ability to prevent formation of a fluorescent signal.

All SECO analogues and SECO were prepared at a 100X concentration (50 mM) in 100% DMSO and sent to Life Technologies (Madison, WI). The 100X concentration was then diluted to a 3X working concentration in potassium phosphate (100 mM; pH 7.4). The final well content of DMSO was 1%.

3.14 Statistical Analysis

GraphPad Prism 6 (La Jolla, CA) was used for statistical analysis. Linear regression analysis was used to determine if slopes were statistically different from zero, to determine stability and to determine kinetic parameters. Kinetic parameters under unstable conditions were also calculated using a non-linear regression fit to a phase 1 decay model. $P < 0.05$ was deemed significant.

4.0 Results

4.1 SECO Analogue Stability

The autoxidation of catechols is pH dependent, therefore the stability of the SECO analogues must be probed to determine if they have a dissociation constant at or near physiological pH.[85] Stability studies were performed on all SECO analogues (1 mM) at pH 6.0 and pH 7.4 in Na_2HPO_4 buffer (50 mM) at 37°C. A pilot study was conducted for 6 h, and two subsequent 8 h trials were run. This time frame was originally chosen as it was consistent with previous NDGA analogue studies. It was discovered that 8 h trials were insufficient to determine kinetic decomposition parameters (k and $t_{1/2}$) so the duration of the trials was extended to 48 h. For conditions under which the analogues were deemed stable only one 48 h trial was performed to conserve starting material and the data from the 6 and 8 h trials was included in the statistical analysis. For the conditions under which analogues were deemed unstable only 48 h trial data was used. SECO-3 could not be detected past 10 h, no calibration curves were prepared, instead the relative change in peak area was followed. HPLC analysis as described in section 3.2 were performed monitoring decrease in starting material at $\lambda = 280$. The SECO analogues that were unstable and decomposed, yielded multiple products. For SECO-3 the formation of a major decomposition product was followed. Stability experiments revealed that all SECO analogues were stable at pH 6.0 as no change in substrate peak areas was observed over 8h. SECO-2 was stable at pH 7.4, however SECO analogues 1, 3 and 4 were not stable at pH 7.4 with $t_{½}$ of 9.00, 1.73 and 7.03 h respectively (Table 4).

4.1.1 Pseudo zero time-point

During the pilot studies it was discovered that if an analogue was unstable, when the time 0 sample was collected after vortexing but prior to being put in the water bath, the time 0 SECO analogue peak consistently had a smaller area than the 30 min time point (Figure 4.1). We attempted to solve this problem by incubating the Na_2HPO_4 buffer (50 mM) at 37°C for 5 min prior to the addition of the SECO analogues, however this did not fully resolve the problem. Instead, a pseudo t = 0 was collected by waiting 15 s after the sample was placed in the water

bath, which resolved the discrepancy. Starting material, t = 0 and pseudo t = 0 were all analyzed by HPLC and the mass-to-charge ratio was determined by MS. All three samples were consistent with the starting material. Therefore, a pseudo t = 0 point was used for all trials.

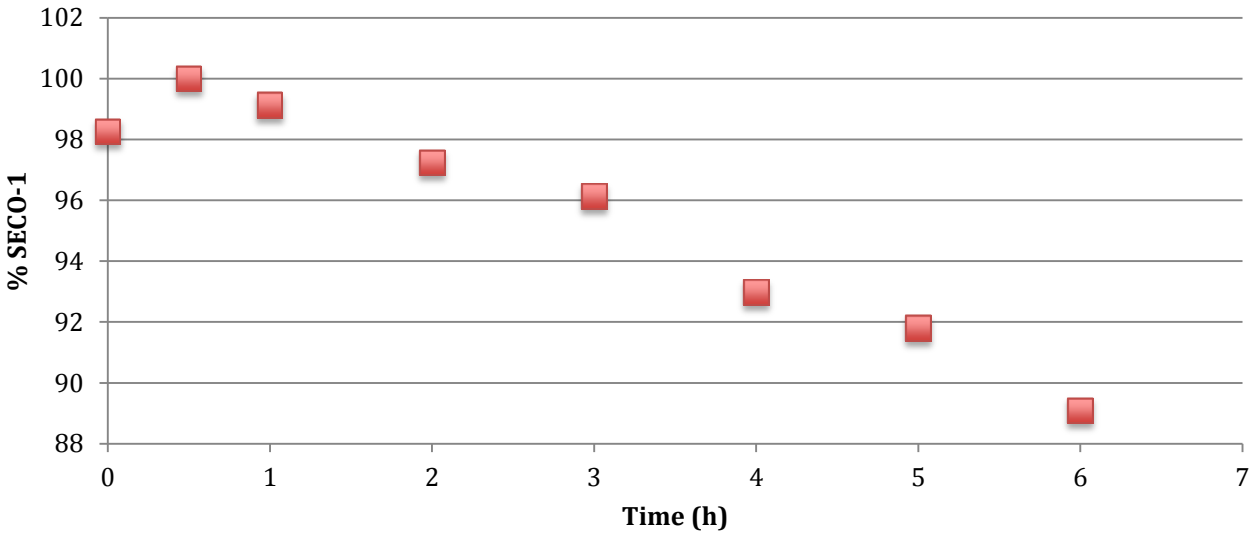

Figure 4.1 1 mM SECO-1 analogue in Na_2HPO_4 buffer (50 mM; pH 7.4) over time (h) at 37°C. Absorbance at λ = 280 nm. The peak area under the curve was normalized to the internal standard (KA-1-09-2).

4.1.2 HPLC analysis of SECO analogue decomposition

The following column types were tested for SECO analogue separation: C8, C18, CN, Hilic and NH_2. The C18 column was determined to demonstrate superior resolution, retention time and peak shapes. Mobile phase starting conditions of 95%, 90% and 85% Milli-Q water with 0.1% formic acid were investigated. 85% Milli-Q water with 0.1% formic acid was decided upon due to solubility issues with SECO-1. This also agrees with the precedent set with previous flaxseed lignan experiments. Different run-times, flow rates and gradients were tested. The first runs were on a Nova-Pak ® C18 3.9 × 150 mm column using salicylic acid as the internal standard (Figure 4.2). It was discovered, based on the mass-to-charge ratio determined by MS, that the SECO-3 originally used was not the correct structure. When the correct SECO-3 analogue was used the retention times of SECO-3 and the internal standard were too similar (RT_{SECO-3} = 3.6 min and

$RT_{salicylic\ acid}$ = 3.9 min) therefore the internal standard was switched to KA-1-09-2 (Figure 3.1). None of the data collected with the previous internal standard was used. After analysis by MS, it was also found that the originally used SECO-1 was not actually SECO-1 but a furan decomposition product. SECO-1 was re-synthesized and none of the furan data is included. Originally a dual wavelength HPLC detector was used to detect UV absorbance, but was subsequently changed to a photodiode array HPLC detector to obtain greater flexibility in data collection. None of the data collected with the dual wavelength detector is included in this thesis.

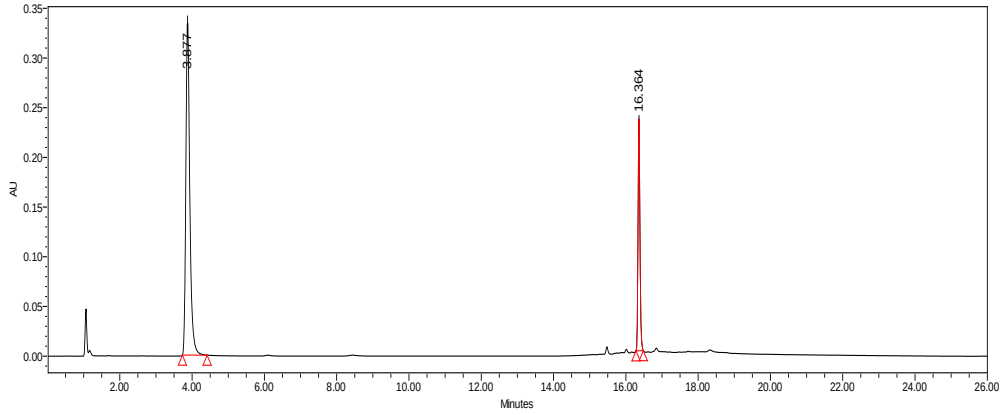

Figure 4.2 Chromatogram of SECO-1 (RT = 16.4 min) using a Nova-Pak ® C18 3.9 × 150 mm column and salicylic acid (RT = 3.9 min) as the internal standard (IS) at λ = 280 nm.

Using the Nova-Pak ® C18 3.9 × 150 mm column it was difficult to detect metabolites particularly in the absence of GSH, especially given the impurities found in the blank from the column that could not be removed. The starting material disappeared but no metabolites were detected (Figure 4.3). Further method development was done to attempt to find the metabolites and to increase the retention time of SECO-3. The 40 min method described in the methods section is the method used for all reported data including stability studies.

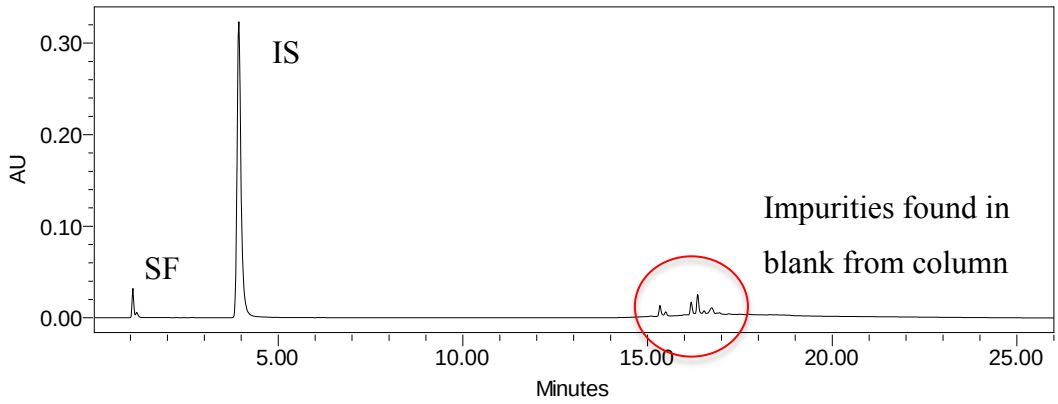

Figure 4.3 Chromatogram of SECO-1 using Nova-Pak ® C18 3.9 × 150 mm column and salicylic acid (RT = 3.9 min) as the internal standard (IS) at λ = 280 nm after 1 h MT oxidation in Na_2HPO_4 buffer (50 mM; pH 6.0) at room temperature. SF = solvent front. Impurities found in blank from column indicated with red circle.

In January 2015 an Agilent Poroshell 120 EC-C18 4.6 × 50 mm 2.7 µm column became available. The Poroshel column has a tighter particle size distribution which greatly improves chromatographic separation. The application of this column to the research project significantly improved the quality of the data generated and allowed for the separation of metabolites and increased the retention time of SECO-3 allowing for the detection of SECO-3 GSH adducts. All metabolism studies and LC-MS analysis, were conducted on this column. For the stability studies, one trial at pH 7.4 data and two trials at pH 6.0 were conducted using the Nova-Pak ® C18 3.9 × 150 mm column. Data from both columns was used, as there was a limited amount of starting material available (Table 4.1). The method developed for the Agilent Poroshell 120 EC-C18 4.6 × 50 mm 2.7 µm column is reported in the methods (section 3.2). All SECO analogues presented as single peaks in HPLC chromatograms for both columns.

Table 4.1 Summary of retention times for SECO analogues and the internal standards employs chromatography method described in section3.2.

Analogue	RT (min)	λ (nm)
SECO-1[a]	21.1	282
SECO-1[b]	23.8	282
SECO-2[a]	22.5	281
SECO-2[b]	24.9	281
SECO-3[a]	3.6	281
SECO-3[b]	5.5	281
SECO-4[a]	15.1	282
SECO-4[b]	22.2	282
IS[a]	24.3	272
IS[b]	26.6	272
salicylic acid[a]	3.9	280

a = Nova-Pak ® C18 3.9 × 150 mm column

b = Poroshell 120 EC-C18 4.6 × 50 mm 2.7 µm column

Below is a representative chromatogram of SECO-3 (RT = 5.4 min) at time = 0 (Figure 4.4) and time = 8 h (Figure 4.5) at λ = 280 nm. Decomposition of SECO-3 generated multiple products, a major peak (RT = 1.7 min) is observed (Figure 4.5).

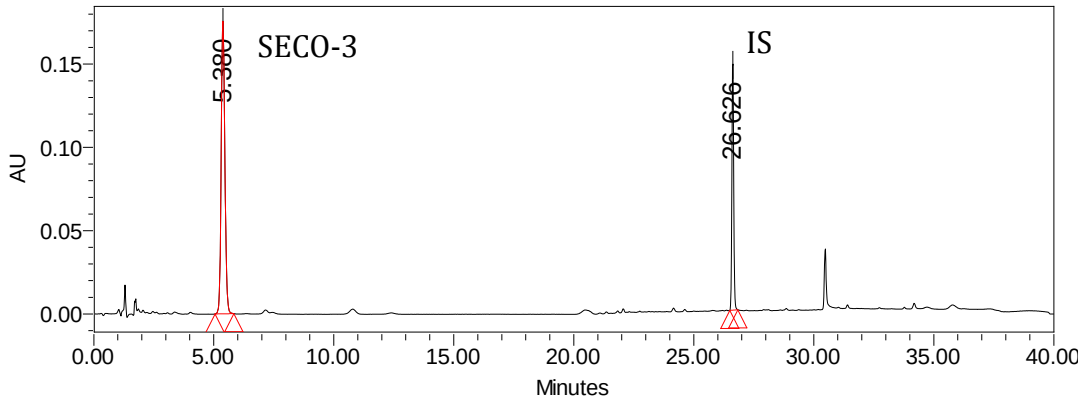

Figure 4.4 Chromatogram of SECO-3 stability at pH 7.4 time point t = 0 h showing SECO-3 and KA-1-09-2 as the internal standard (IS) at λ = 280 nm.

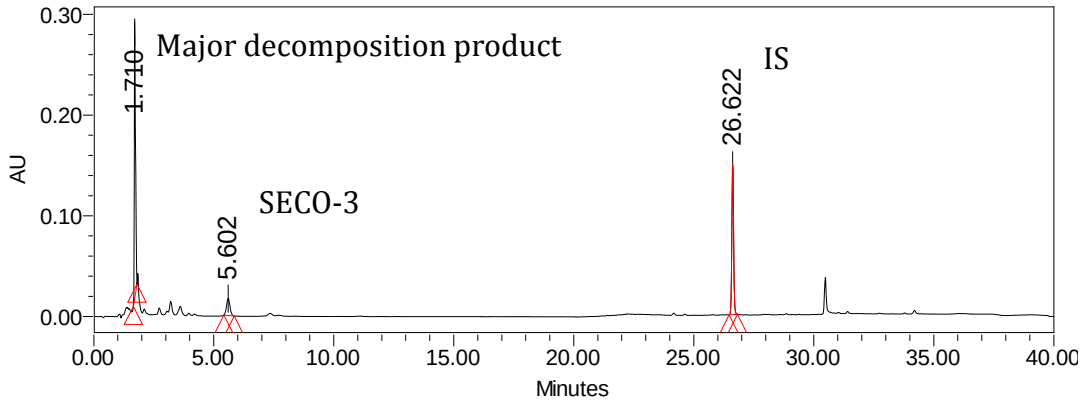

Figure 4.5 Chromatogram of SECO-3 stability at pH 7.4 time point t = 8 h showing KA-1-09-2 as the internal standard (IS), SECO-3 and the major SECO-3 decomposition product at λ = 280 nm.

The disappearance of the starting material (SECO-3) and the appearance of the major decomposition product was plotted in Figure 4.6. Tracking the formation of the major decomposition product past the eight hours shown in Figure 4.6 reveals its slow decomposition with 8 h as its peak concentration.

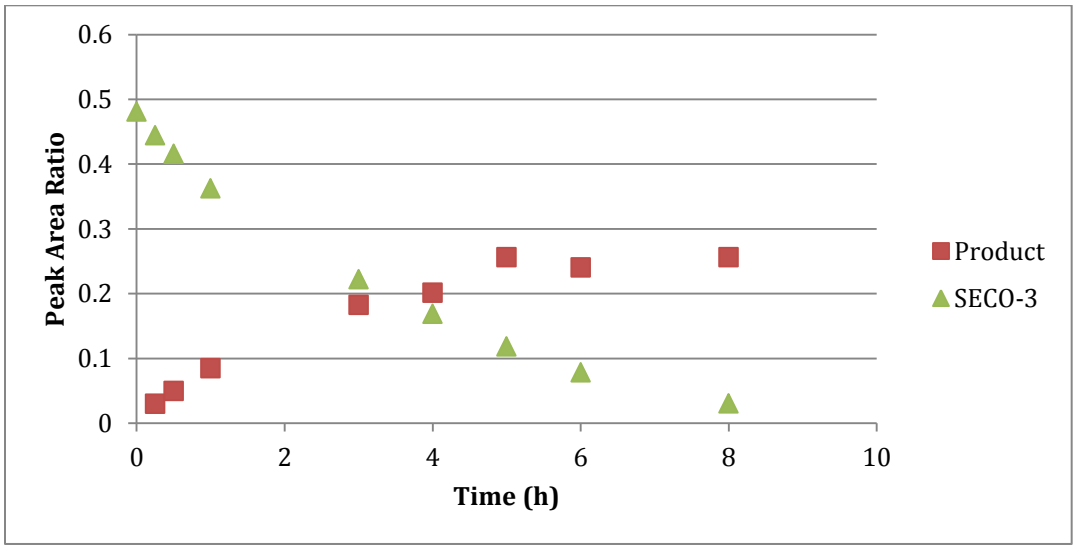

Figure 4.6 The disappearance of the starting material and the appearance of a product for SECO-3 in Na_2HPO_4 buffer (50 mM; pH 7.4) at 37ºC.

Unlike SECO-3, autoxidation of SECO-1 and SECO-4 did not show evidence of a major peak. Representative chromatographs of SECO-4 (RT = 21.8 min) at t = 0 (Figure 4.7) and t = 24 h (Figure 4.8), λ = 280 nm, are shown below. After 24 h there is a decrease in starting material and the appearance of multiple products.

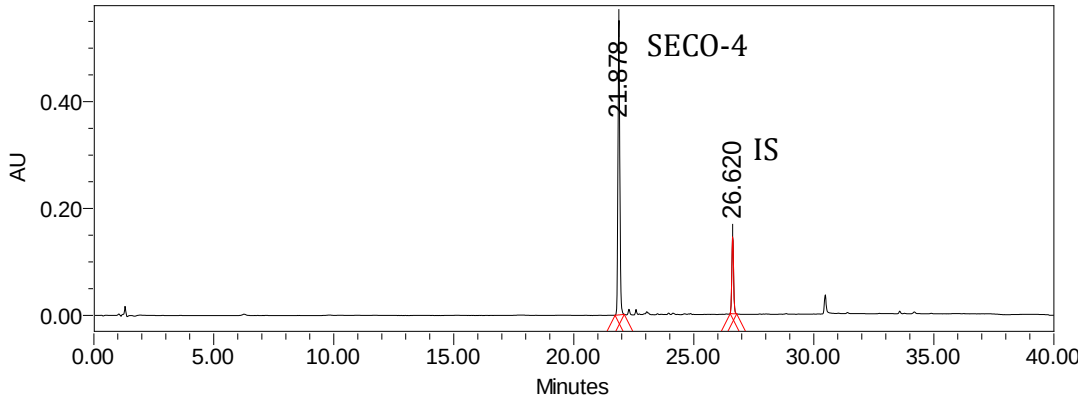

Figure 4.7 Chromatogram of SECO-4 stability at pH 7.4 time point t = 0 h showing SECO-4 and internal standard (IS) at λ = 280 nm.

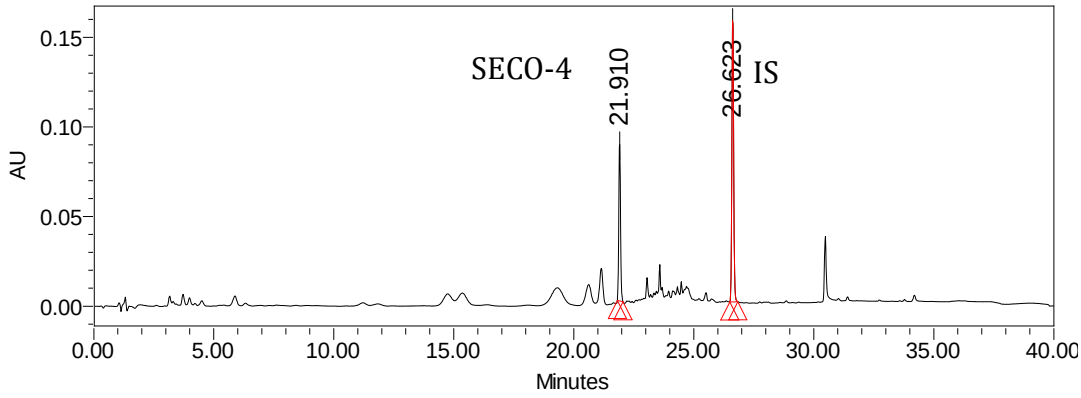

Figure 4.8 Chromatogram of SECO-4 stability at pH 7.4 time point t = 24 h showing SECO-4, internal standard (IS) and multiple products at λ = 280 nm.

4.1.3 Determination of decomposition products.

The major decomposition product of SECO-3 was the only decomposition product present in sufficient quantity that NMR analysis was possible. The major decomposition product of SECO-3 was consistent with the formation of an NDGA like, dibenzocyclooctadiene derivative (Figure 4.9). ^{1}H NMR (500 MHz, CD_3CN): δ (ppm) 1.31 (2H, s), 1.44 (2H, s), 2.06 (3H, s), 2.67 (5H, s), 3.73 (2H, s), 3.75 (2H, s), 6.64 (2H, m), 6.72 (2H, m).

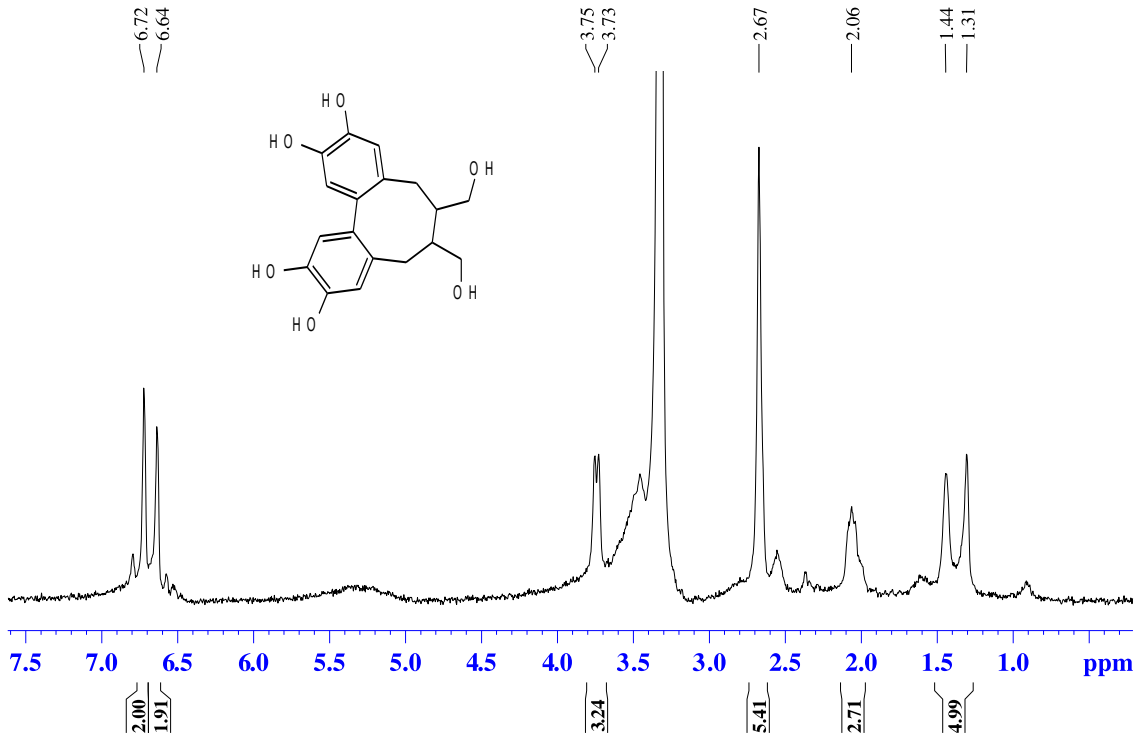

Figure 4.9 ^{1}H nuclear magnetic resonance (NMR), 500 MHz on a Bruker AVANCE DPX-500 spectrometer.

SECO-1 and SECO-4 do not form a major dibenzocyclooctadiene like product. Both SECO-1 and SECO-4 form multiple minor decomposition products, none of which were present in sufficient concentration for NMR identification. MS and LC-MS data suggests other types of cyclized products may be present (Figure 4.10).

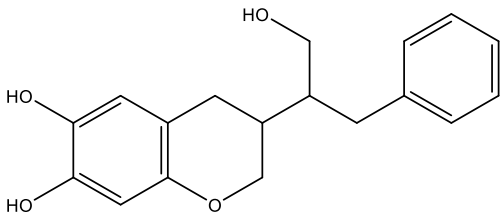

Figure 4.10 Possible structure of a SECO-1 decomposition product

4.1.4 Statistics

GraphPad Prism 6 software was used for all statistical analysis. Duplicates from each trial were averaged and each trial was used as an independent replicate. Eight trials were completed to get four trials of usable data for both pH 6.0 and 7.4. Trials were eliminated from the pool of data for technical issues, for example: HPLC problems part way through the analysis and a power outage in the middle of one of the trials. Variability was introduced into the data due to multiple factors including: trials run over the course of 18 months, different batches of buffer and starting materials, and the use of two different HPLC columns to collect data. The peak area ratio of sample to internal standard was used for all statistical analyses. Two different statistical analyses were performed on the trial data; a linear transformation followed by a linear regression and a non-linear regression fit to a phase 1 decay model. The results of both analyses were comparable therefore the results of the linear regression are reported to compare with results from similar work with NDGA analogues. The results from the non-linear regression analysis are reported in appendix A.

4.1.4.1 Linear transformation

Integrated rate law for 1st order kinetics

$$\ln[A] = -kt + \ln[A]_o$$

Solve for $t_{1/2}$

$$t_{\frac{1}{2}} = \frac{\ln 2}{k}$$

This calculation can be used to determine the kinetic parameters manually without using statistical software and is an accepted method for determining k and $t_{½}$ in simple, non-enzymatic systems. It is also based on this law that the flowing linear transformation was chosen:

$$y = \ln([A]/[A_o])$$

Though only the unstable data were 1st order reactions, a linear transformation was necessary to account for some of the variability between trials for statistical analysis.

At pH 6.0 one trial was run to 48 h, the rest were terminated at 6 h to conserve starting material. None of the SECO analogues had slopes statistically different from 0 (all $P > 0.05$; Figure 4.11) at pH 6.0. Therefore all of the analogues were considered to be stable at pH 6.0

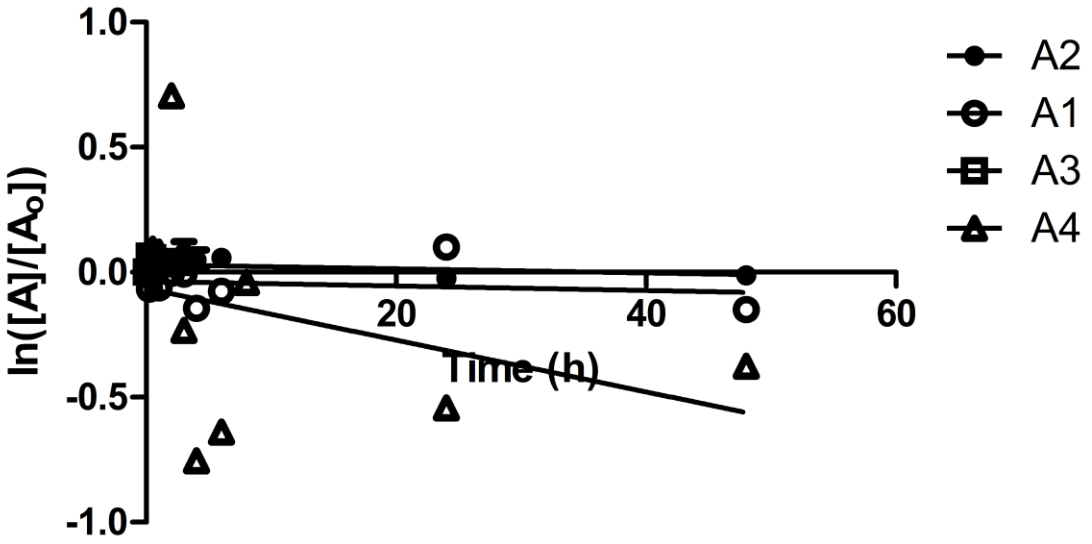

Figure 4.11 Linear regression lines for 1 mM SECO analogues: SECO-1 (A1), SECO-2 (A2), SECO-3 (A3) and SECO-4 (A4), in 50 mM Na_2HPO_4 buffer, pH 6.0 at 37°C. Change in concentration was determine from the peak area under the curve, normalized to the internal standard (KA-1-09-2), a linear transformation was applied and plotted as a function of time (h). Error bars = ± 1 SE.

SECO-2 was also stable at pH 7.4, with a slope not statistically different from 0 ($P > 0.05$). SECO -1, -3 and -4 had slopes statistically different from zero ($P < 0.0001$, Figure 4.12) and are therefore not stable at pH 7.4. SECO-1, -3 and -4 all show characteristics of 1st order kinetics.

For SECO-2 only one replicate was done to 48 h, 3 other replicates were only run until 8 h. The shorter time scale required fewer time points meaning a lower starting volume was required translating to using less starting material, saving it for other experiments. For all other analogues all replicates were run 48 h.

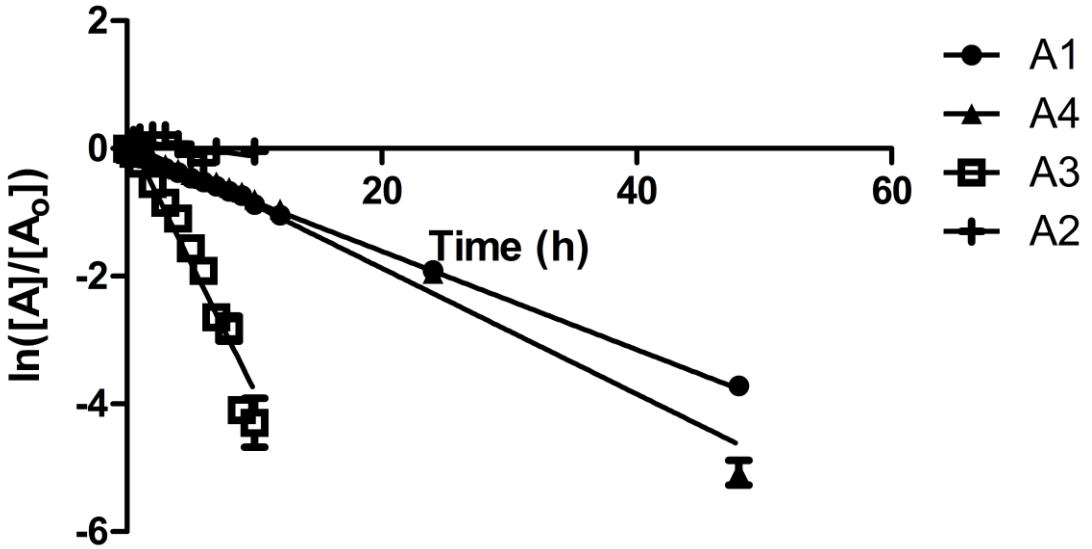

Figure 4.12 First-order regression lines for 1 mM SECO analogues: SECO-1 (A1), SECO-2 (A2), SECO-3 (A3) and SECO-4 (A4), in 50 mM Na_2HPO_4 pH 7.4 at 37°C over time (h). Change in concentration was determined from the peak area under the curve, normalized to the internal standard (KA-1-09-2) and plotted as a function of time (h). Error bars = ± 1 SE.

Table 4.2 shows a summary of kinetic parameters for the unstable SECO analogues at pH 7.4 determined via linear transformation and linear regression.

Table 4.2 Summary of kinetic data for SECO analogue autoxidation at pH 7.4 using a linear transformation and linear regression analysis.

	SECO-1	SECO-2	SECO-3	SECO-4
$k\ (h^{-1})$	0.08	*	0.40	0.10
$t_{1/2}$ (h)	9.00	*	1.73	7.03
R^2	0.98	*	0.94	0.98

* No change in starting material was observed over 48 h, therefore kinetic parameters were not determined

4.2 Mushroom Tyrosinase Oxidation

Mushroom tyrosinase (MT) oxidation was used to generate *ortho*-quinone (o-Q) standards of the SECO analogues. Oxidation was conducted in a 50 mM Na_2HPO_4 buffer, pH 6.0, at room temperature in the presence and absence of a GSH trapping system. Due to the structure of SECO-2 and the mechanism of action of MT it was predicted that SECO-2 would not be oxidized by mushroom tyrosinase. HPLC, MS and LC-MS analysis validated this prediction. SECO-1, -3 and -4 oxidation generated aromatic GSH adducts in the presence of GSH.

4.2.1 GSH trapping system

HPLC was used to generate chromatograms of the SECO analogues (Figure 4.13) and their metabolites (Figure 4.15). ESI (-) was used to generate MS^1 full mass spectra with a range of 100 – 700 mass-to-charge ratio (*m/z*). An ion with the *m/z* 606.4 was suspected to be a GSH adduct as it was the predicted mass. ESI (+) was then used to perform neutral loss (NL) scans looking for a neutral loss of 129 or 307. The NL (+) 129, indicative of an aromatic GSH conjugate, indicated a *m/z* 608.3. The precursor ion *m/z* 608 was selected to undergo a collision induced dissociation (CID) product ion scan (+) and generated the characteristic fragmentation of an aromatic GSH adduct. LC-MS ESI (-) MS^1 full mass spectra with a range of 100 – 700 mass-to-charge ratio

(*m/z*) were generated from which smaller ranges of *m/z* were extracted to compare with HPLC results.

SECO-1 data shown is representative of SECO-3 and SECO-4 pattern of oxidation. Chromatograms of SECO-1 from HPLC (Figure 4.13) and LC-MS (Figure 4.14) analysis.

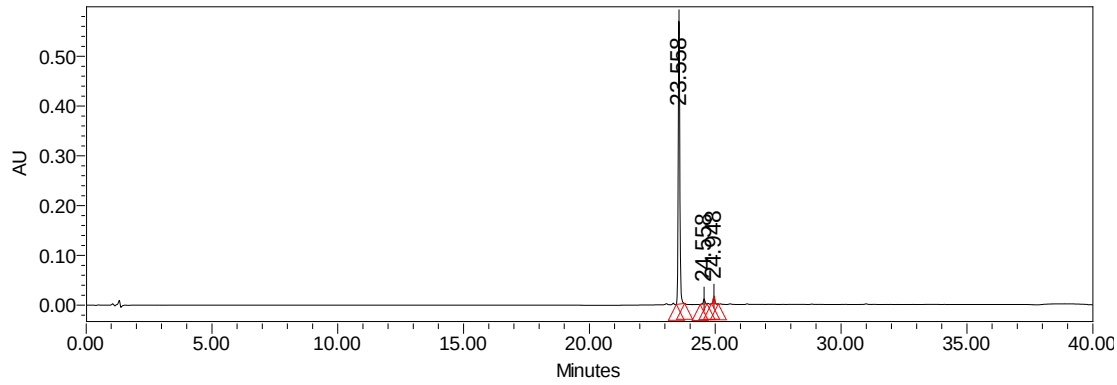

Figure 4.13 HPLC chromatogram of SECO-1, λ = 280 nm.

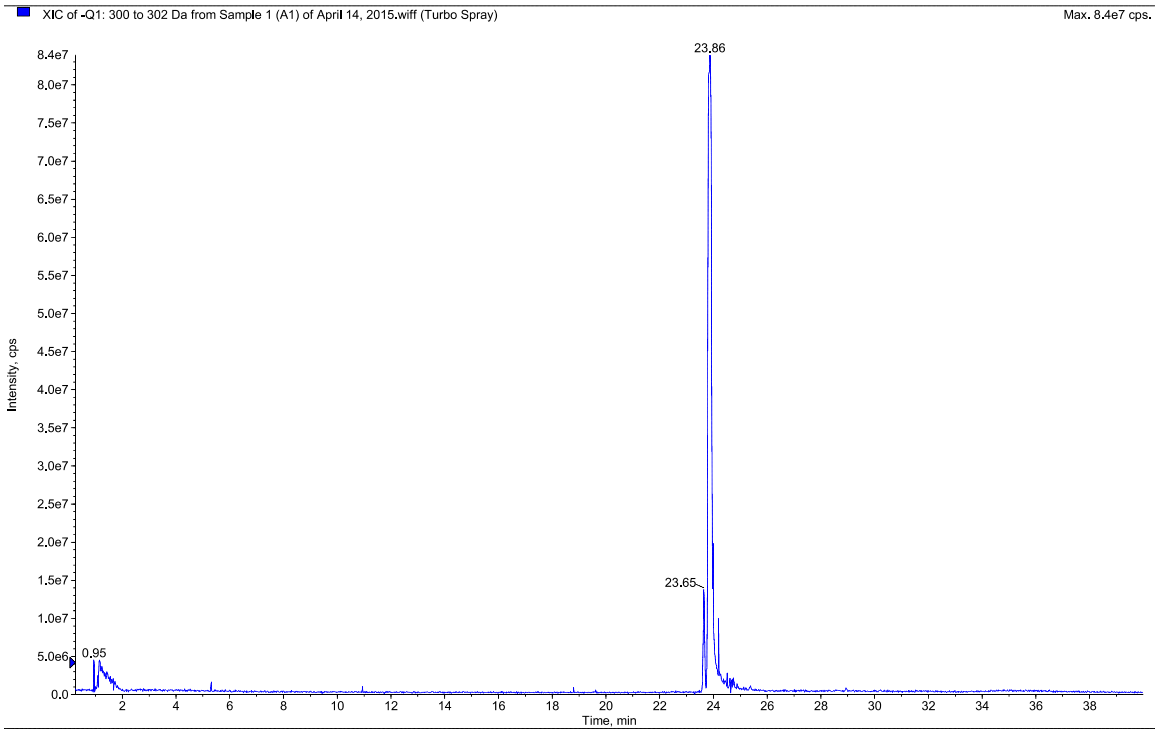

Figure 4.14 LC-MS ESI (-) MS[1] scan of SECO-1, *m/z* 300-302 range isolated from overall range of *m/z* 100 to 700.

After 1 h incubation with mushroom tyrosinase in 50 mM Na_2HPO_4 pH 6.0 at room temperature with 5:1 GSH trapping system, SECO-1 shows multiple pairs of metabolites (Figure 4.15).

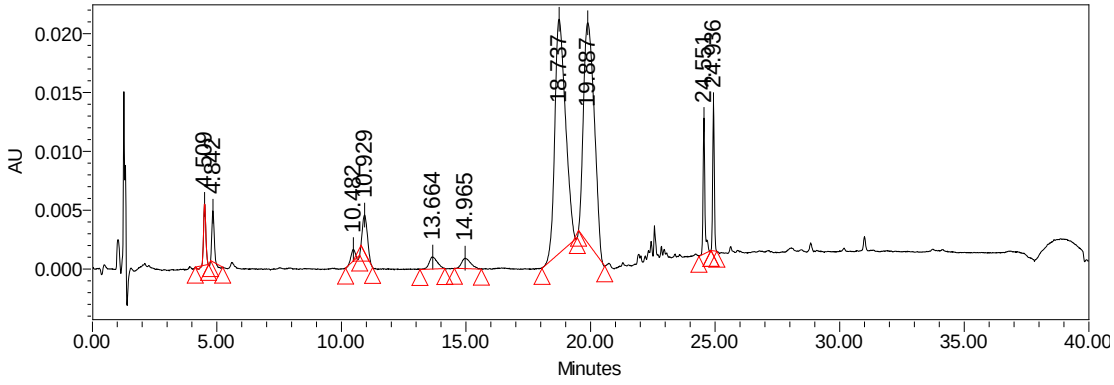

Figure 4.15 HPLC chromatogram SECO-1 after mushroom tyrosinase oxidation with GSH present at λ = 280 nm. The peaks at 10.4, 10.9, 18.8 and 19.8 min are consistent with GSH adducts due to the characteristic shift in maximum absorbance. The peaks at 24.5 and 24.9 min are impurities present in starting material that are not metabolized.

These identified peaks also show the characteristic shift in absorbance from the λ_{max} = 280 nm of the starting material to absorbance maxima at approximately 253 nm and 293 nm observed for GSH adducts (Figure 4.16).

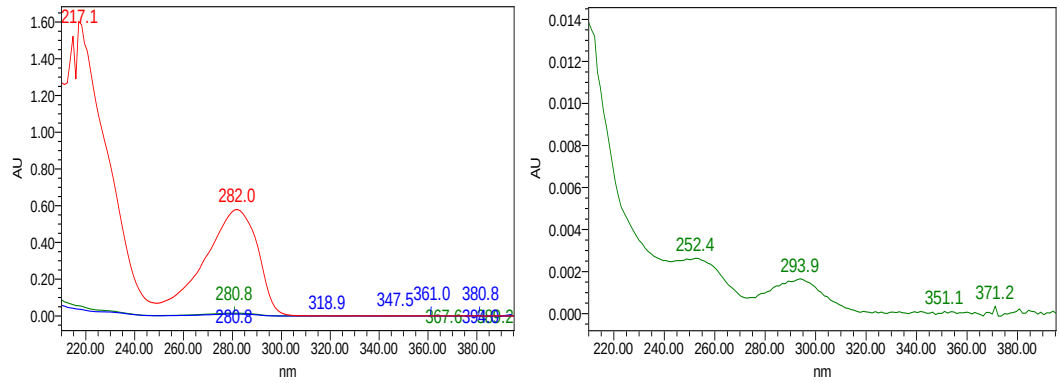

Figure 4.16 Characteristic shift in absorbance spectra from starting material (left; red) with local absorbance maxima at approximately 280 nm (SECO-1 = 282.0 nm) to a GSH adduct (right; green; RT = 18.7 min) with two local absorbance maxima at approximately 253 nm and 294 nm (SECO-1 = 252.4 nm and 293.9 nm).

NL(+) 129 and 307 scans were done to determine if aromatic or benzylic GSH adducts, respectively, were present. The (+) NL 129 scan indicated a precursor ion with an *m/z* of 608.4 (Figure 4.17). No precursor ions were identified in the (+) 307 scans.

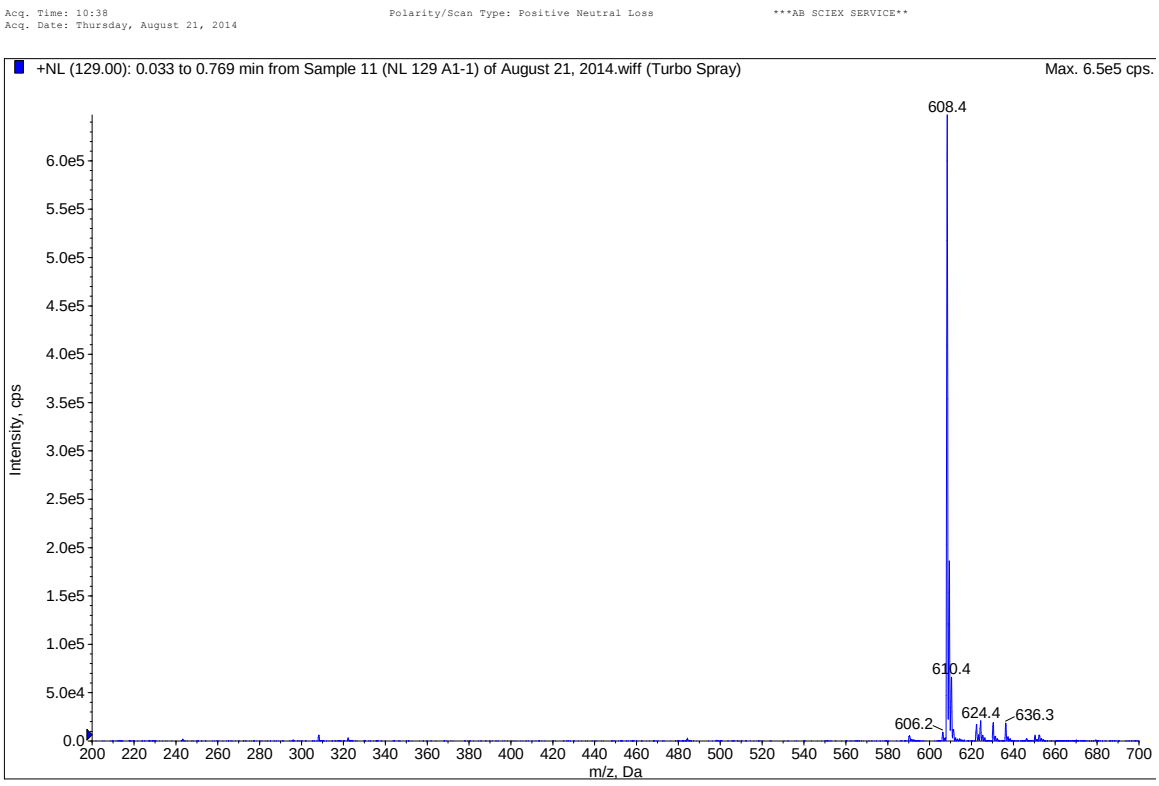

Figure 4.17 Direct infusion ESI (+) NL 129 scan of SECO-1 oxidized with mushroom tyrosinase, trapped with a 5:1 GSH trapping system.

The *m/z* range indicated by the NL scan (*m/z* 605-607) was isolated from the overall range of *m/z* 100 to 700 (Figure 4.18) and compared to the HPLC chromatogram. The identified LC-MS peaks with RT of 10.1, 10.6, 18.0 and 18.8 min correspond with the 10.4, 10.9, 18.8 and 19.8 min peaks respectively identified as having the characteristic shift in absorbance maximum in the HPLC-UV chromatogram.

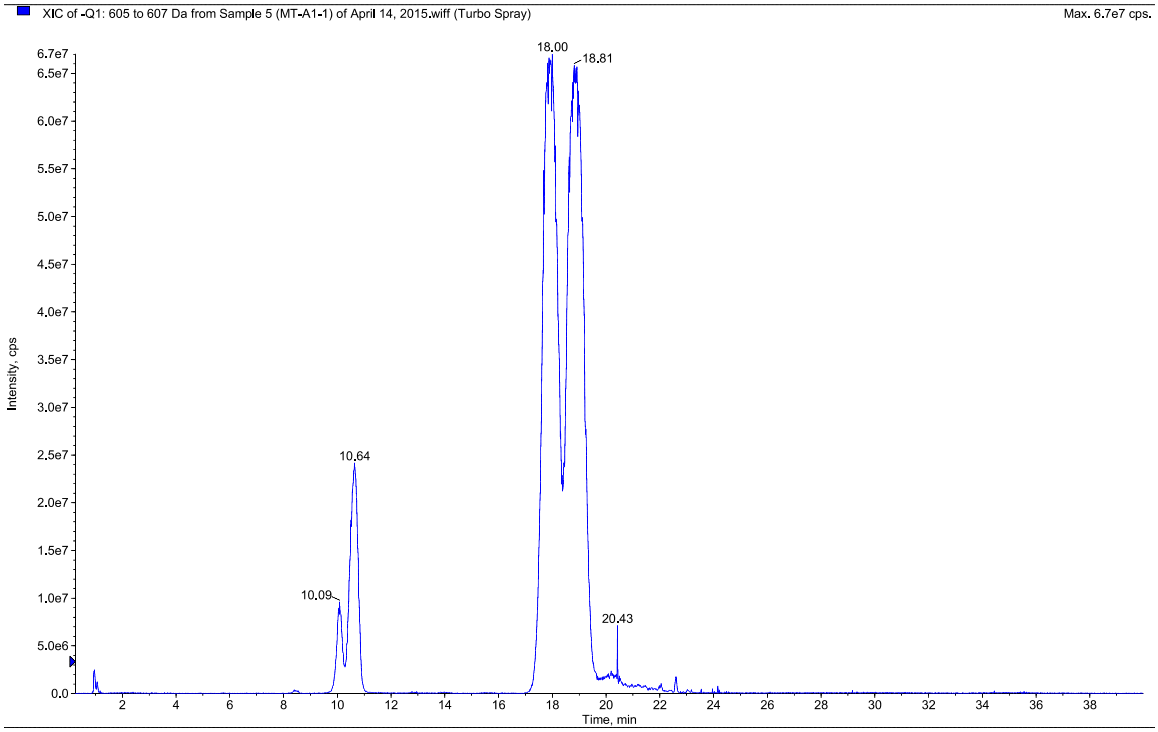

Figure 4.18 LC-MS ESI (-) MS^1 scan of SECO-1 after mushroom tyrosinase oxidation with GSH trapping system present, *m/z* 605-607 range isolated from overall range of *m/z* 100 to 700.

A product ion scan (*m/z* = 608.3) of SECO-1 after MT oxidation in the presence of GSH was consistent with the suggested structure showing some of the characteristic fragmentation patterns of GSH by ESI (+) *m/z* 75, 129, 146, 232, 249 and 275 (Figure 4.19).

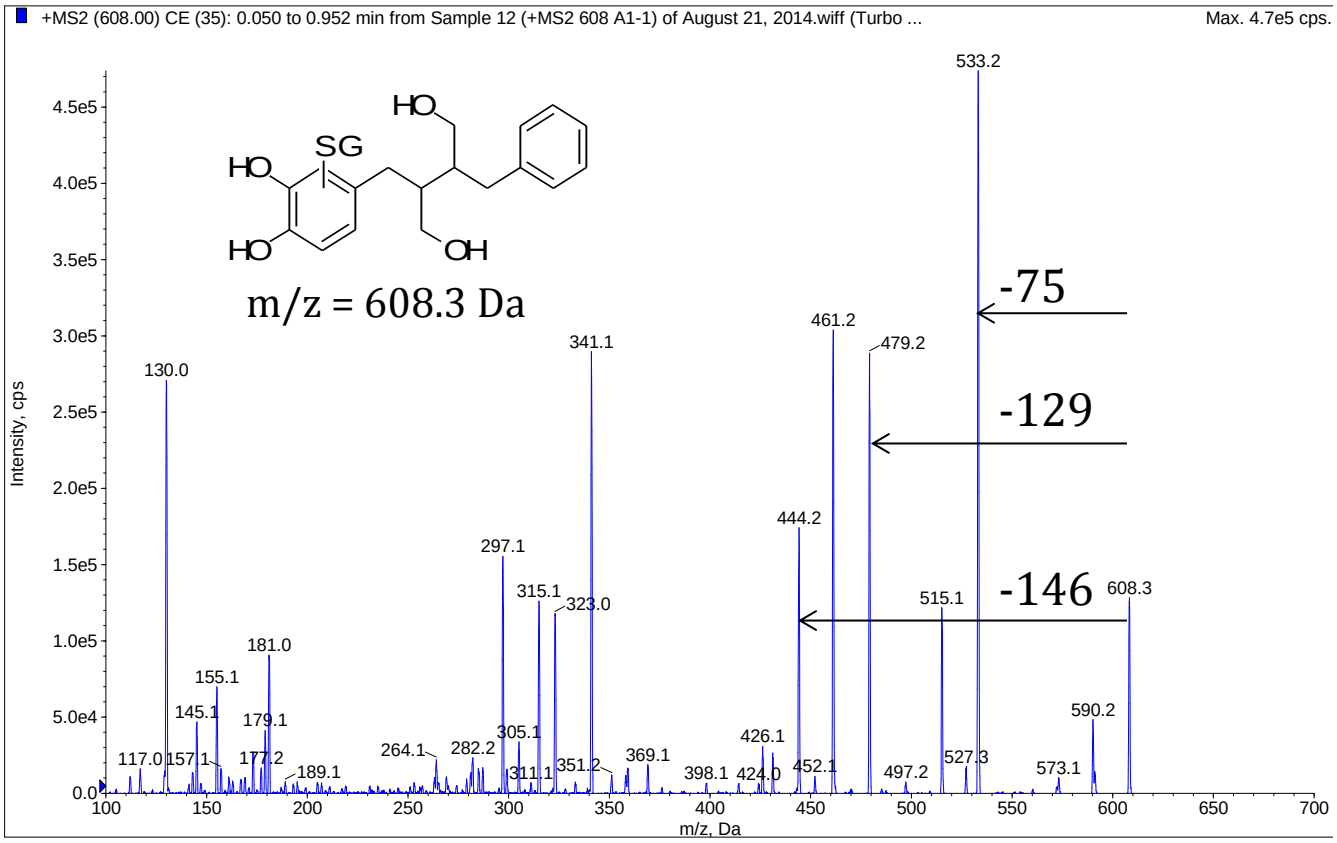

Figure 4.19 Product ion scan of a SECO-1 glutathione adduct (*m/z* = 608.3) consistent with the suggested structure showing some of the characteristic fragmentation pattern of GSH in ESI (+) *m/z* 75, 129 and 146.

4.2.2 No GSH trapping system

After 1 h incubation with mushroom tyrosinase in Na_2HPO_4 buffer (50 mM; pH 6.0) at room temperature with no trapping system, SECO-1 showed multiple metabolites with similar retention times (Figure 4.20). None of the peaks shown in this chromatogram were observed in previous experiments with the NovaPak column. The solution changes from colourless to yellow in the absence of a GSH trapping system. SECO-3 and SECO-4 demonstrate similar metabolite profiles.

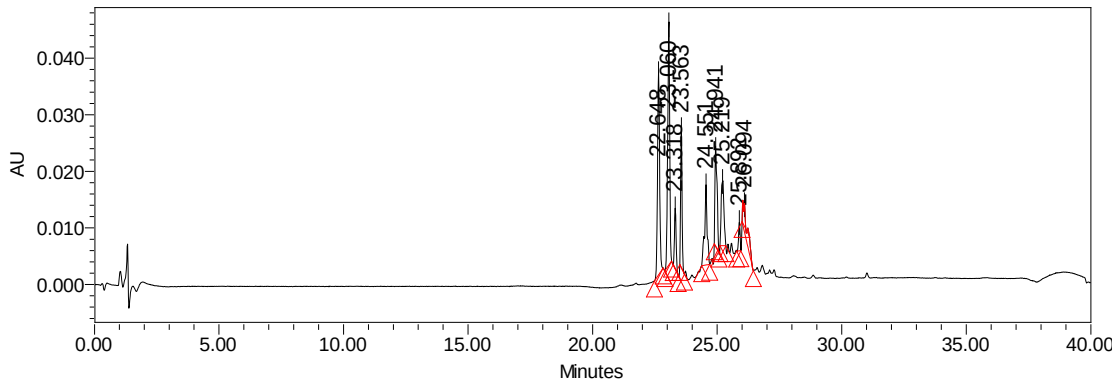

Figure 4.20 HPLC chromatogram of SECO-1 after mushroom tyrosinase oxidation in the absence of GSH trapping system at λ = 280 nm. None of the peaks shown in this chromatogram were observed in previous experiments with the NovaPak column.

These peaks correspond to an addition in mass of 14 Da as shown by LC-MS (Figure 4.21).

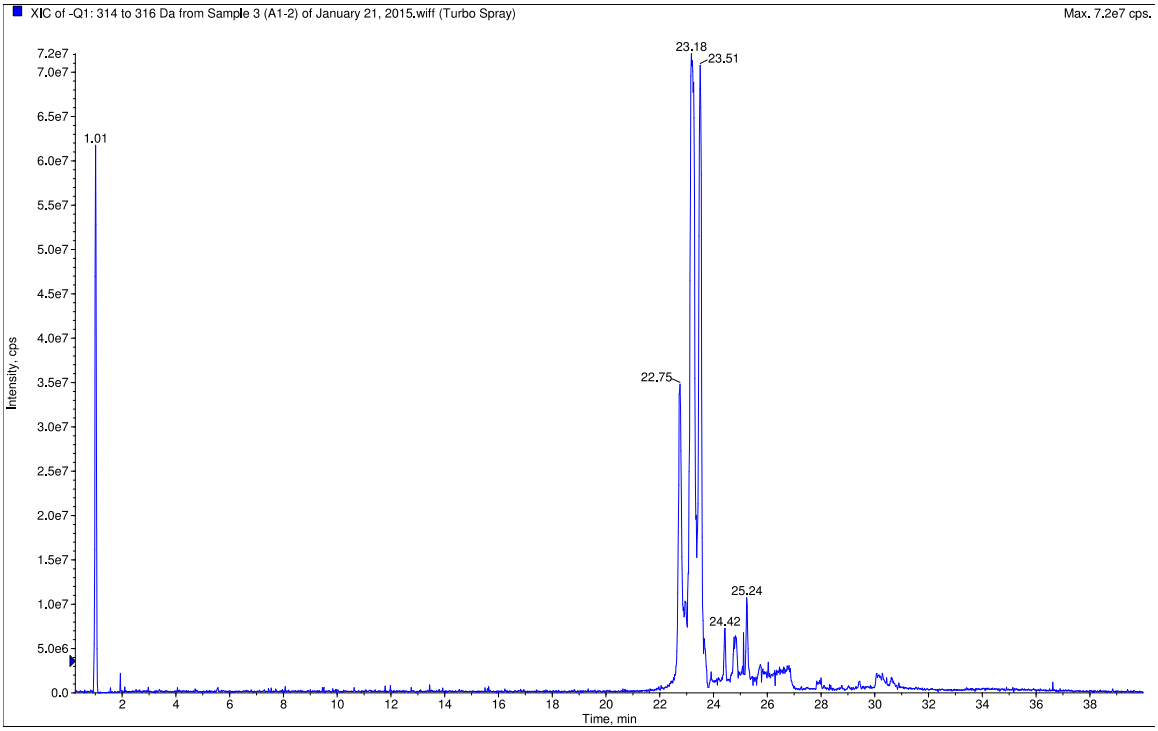

Figure 4.21 LC-MS ESI (-) MS[1] scan of SECO-1 after mushroom tyrosinase oxidation with no GSH trapping system present, *m/z* 314-316 range isolated from overall range of *m/z* 100 to 700.

The 14 Da difference corresponds to addition of an oxygen atom and loss of 2 hydrogens.

SECO-3 and SECO-4 follow the same pattern of metabolism as SECO-1. In the presence of GSH, aromatic GSH adducts are formed. In the absence of GSH there is an addition of 14 Da. The *m/z* (-) and the RT (min) of the metabolites are reported in Table 4.3. SECO-2 is not metabolized by mushroom tyrosinase so only starting material is reported.

Table 4.3. Summary of LC-MS data for mushroom tyrosinase oxidation of SECO analogues.

Analogue	Oxidation	*m/z* (-)	RT (min)	NL (+)
SECO-1	Starting material	301	23.8	N/A
	In presence of GSH	608	10.1	129
		608	10.6	129
		608	18.0	129
		608	18.8	129
	In absence of GSH	315	22.7	N/A
		315	23.1	N/A
		315	23.5	N/A
SECO-2	Starting material	315	24.9	N/A
SECO-3	Starting material	333	5.5	N/A
	In presence of GSH	638	2.2	129
		638	2.5	129
	In absence of GSH	347	2.8	N/A
		347	3.2	N/A
		347	3.5	N/A
		347	4.0	N/A
SECO-4	Starting material	361	22.2	N/A
	In presence of GSH	666	5.1	129
		666	5.4	129
		666	8.3	129
		666	11.8	129
	In absence of GSH	375	15.3	N/A
		375	18.8	N/A
		375	19.4	N/A
		375	21.2	N/A

4.3 Rat Liver Microsomes

Rat liver microsome (RLM) oxidations were conducted to investigate the *in vitro* hepatic oxidative metabolism and bioactivation of the four SECO analogues. Oxidation was conducted with 0.5 mg/mL of microsomal protein, 0.5 mM of the test compound, 5 mM $MgCl_2$, 5 mM GSH and 10 mM SPP in a 50 mM Na_2HPO_4 pH 7.4 buffer in a water bath at 37°C. The DMSO content was 0.5%. All SECO analogues were metabolized by RLM. In the presence of GSH, GSH adducts were detected. Demethylation reactions also occurred. Incubations carried out in the absence of NADPH and using boiled microsomes were used as negative controls. Results consistent with autoxidation were observed, no additional metabolism occurred.

4.3.1 SECO-1

RLM oxidation of SECO-1 formed products with RT of 10.1, 10.7, 18.0 and 19.0 min (Figure 4.23).

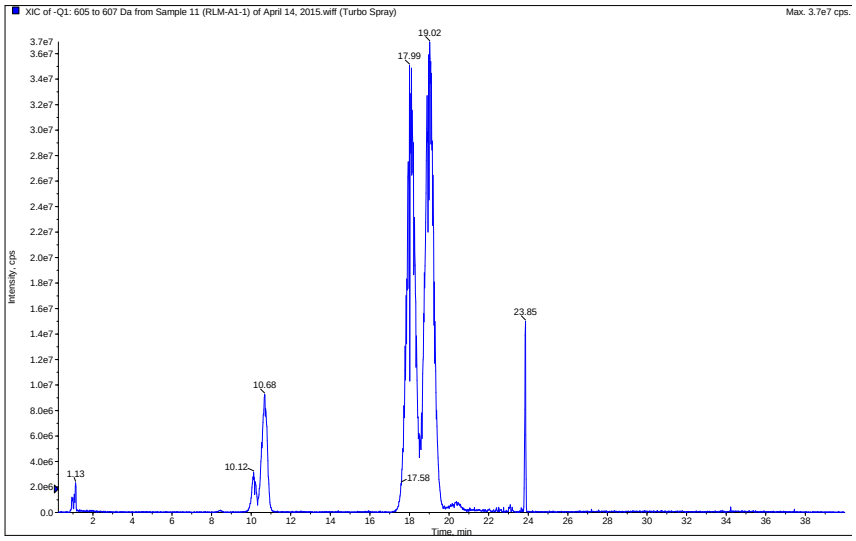

Figure 4.22 LC-MS ESI (-) MS^1 scan of SECO-1 after rat liver microsome oxidation with GSH trapping system present, *m/z* 605-607 range isolated from overall range of *m/z* 100 to 700.

These products corresponded to the standard GSH adducts generated by SECO-1 oxidation by MT with RT of 10.1, 10.6, 18.0 and 18.8 min respectively (Table 4.4).

Table 4.4 LC-MS retention times of aromatic GSH adducts generated from mushroom tyrosinase and rat liver microsome oxidation of SECO-1 in the presence of GSH.

SECO-1 aromatic GSH adduct	MT	RLM
RT (min)	10.1	10.1
	10.6	10.7
	18.0	18.0
	18.8	19.0

NL (+) 129 and product ion scans were used to confirm the presence of aromatic GSH adducts.

In the absence of GSH there was a decrease in starting material of approximately 34% as determined by HPLC. HPLC shows one potential product (RT = 1.7 min; Figure 4.24) that may be obscured by NADPH in the LC-MS analysis, however this product would not account for the total decrease. This particular chromatogram was run without an internal standard to preclude the possibility of it obscuring a metabolite.

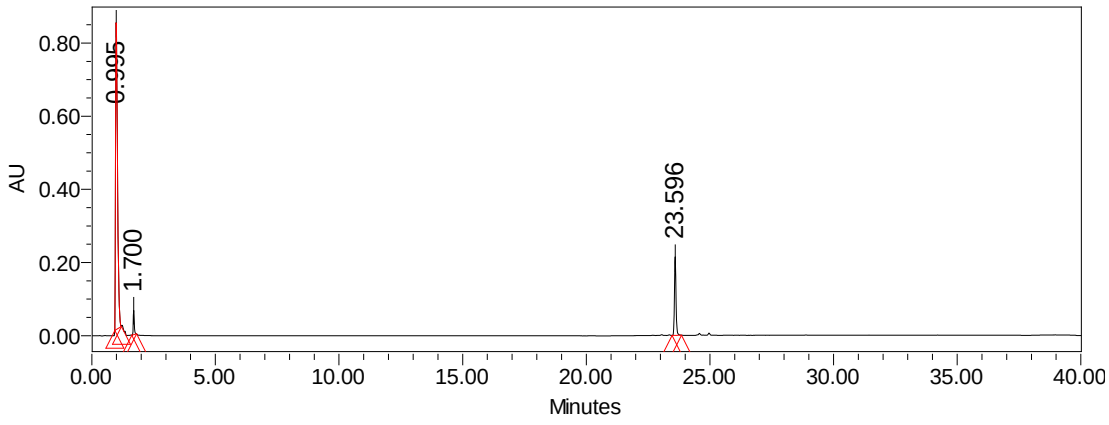

Figure 4.23 HPLC chromatogram (λ = 282 nm) of SECO-1 after rat liver microsome oxidation in the absence of GSH.

No major products were detected by LC-MS, however there was weak evidence of SECO-1 cyclization (RT = 24.7 min; Figure 4.25) by LC-MS.

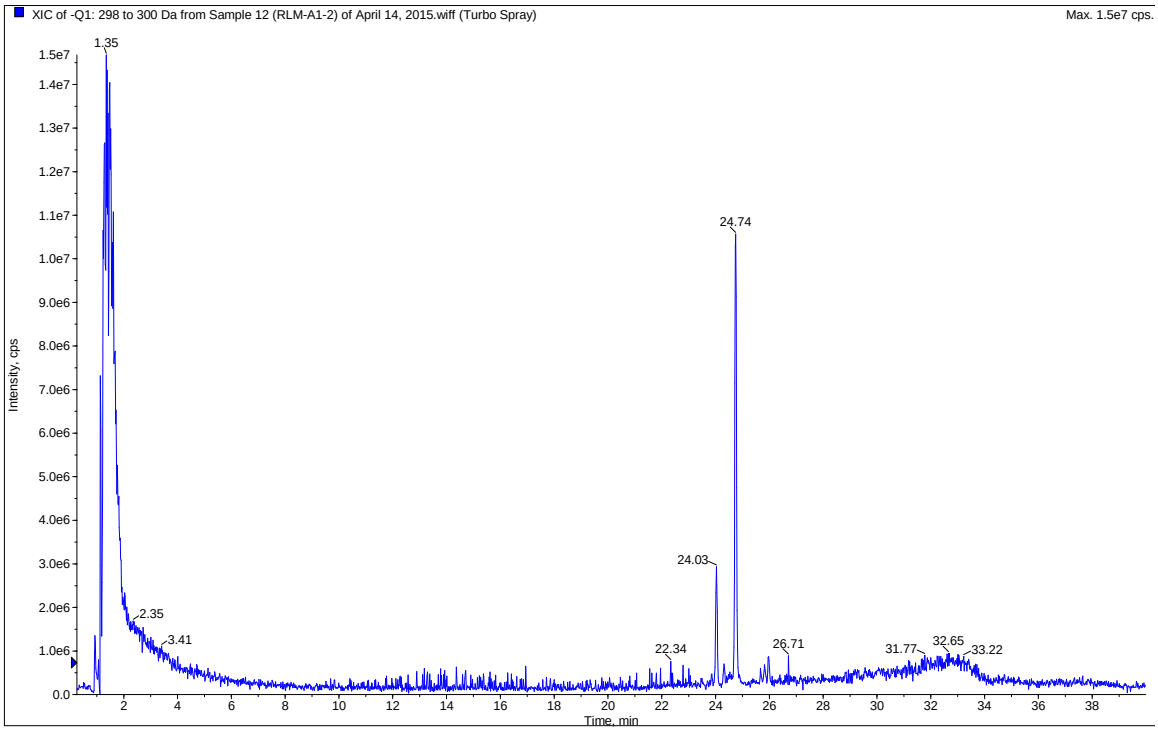

Figure 4.24 LC-MS ESI (-) MS[1] scan of SECO-1 after rat liver microsome oxidation in the absence of GSH trapping system, *m/z* 298-300 range isolated from overall range of *m/z* 100 to 700.

The two possible cyclo-SECO-1 structures consistent with *ortho*-quinone formation are shown in Figure 4.26.

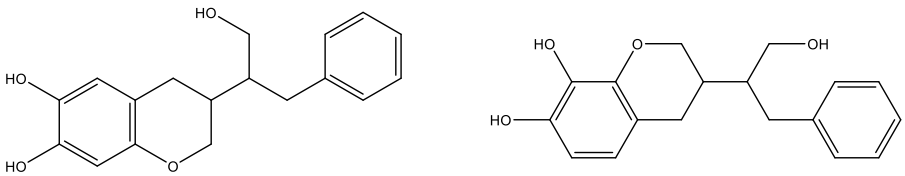

Figure 4.25 Possible structures of potential SECO-1 cyclized metabolites.

4.3.2 SECO-2

SECO-2 was metabolized by RLM. A precursor ion of *m/z* = 646.0 (Figure 4.27) was identified by NL (+) 307. A mass charge ratio of 646.0 corresponds to the expected *m/z* of a SECO-2 GSH adduct with the addition of a sodium ion.

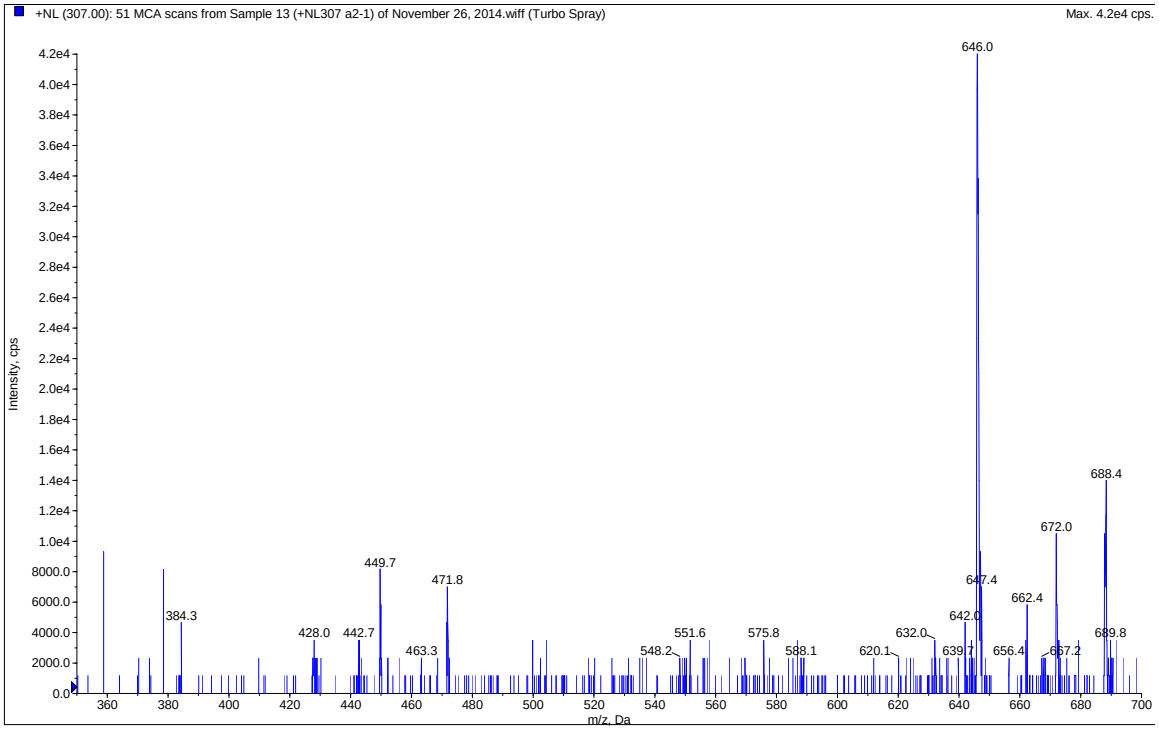

Figure 4.26 Direct infusion ESI (+) NL 307 scan of SECO-2 after rat liver microsome oxidation in the presence of 10:1 GSH trapping system.

When the collision energy was increased, this precursor ion corresponded with a metabolism product (no sodium) with RT of 22.9 min (Figure 4.28).

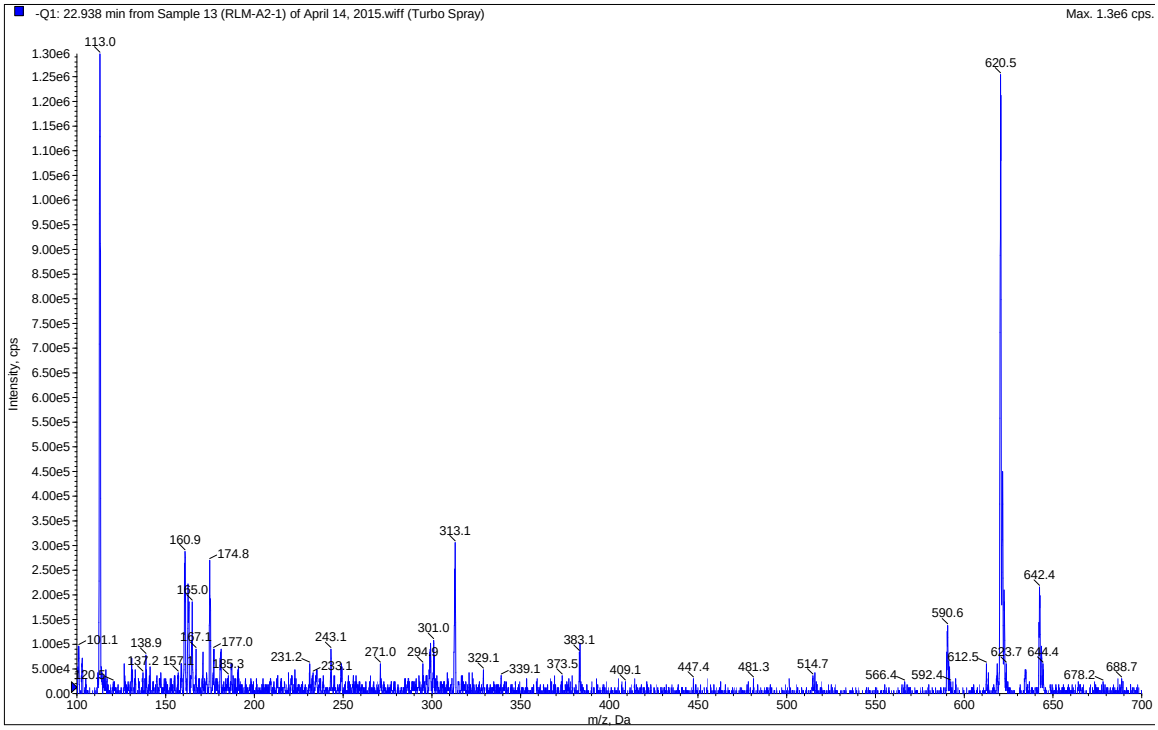

Figure 4.27 LC-MS ESI (-) MS[1] scan of SECO-2 after rat liver microsome oxidation in the presence of GSH trapping system, ionization at 22.9 min.

This indicates a benzylic GSH adduct (Figure 4.29).

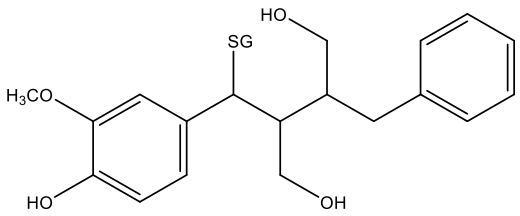

Figure 4.28 Structure of SECO-2 GSH adduct at the benzyl position.

Peaks consistent with dealkylation (SECO-1), with subsequent oxidation to an o-Q and trapping with GSH were detected (Figure 4.30). These peaks had *m/z* = 606.5 and RT consistent with SECO-1 aromatic GSH adducts (Table 4.5). NL (+) 129 and product ion scans were attempted, however these products were not present in sufficient quantity for reliable results.

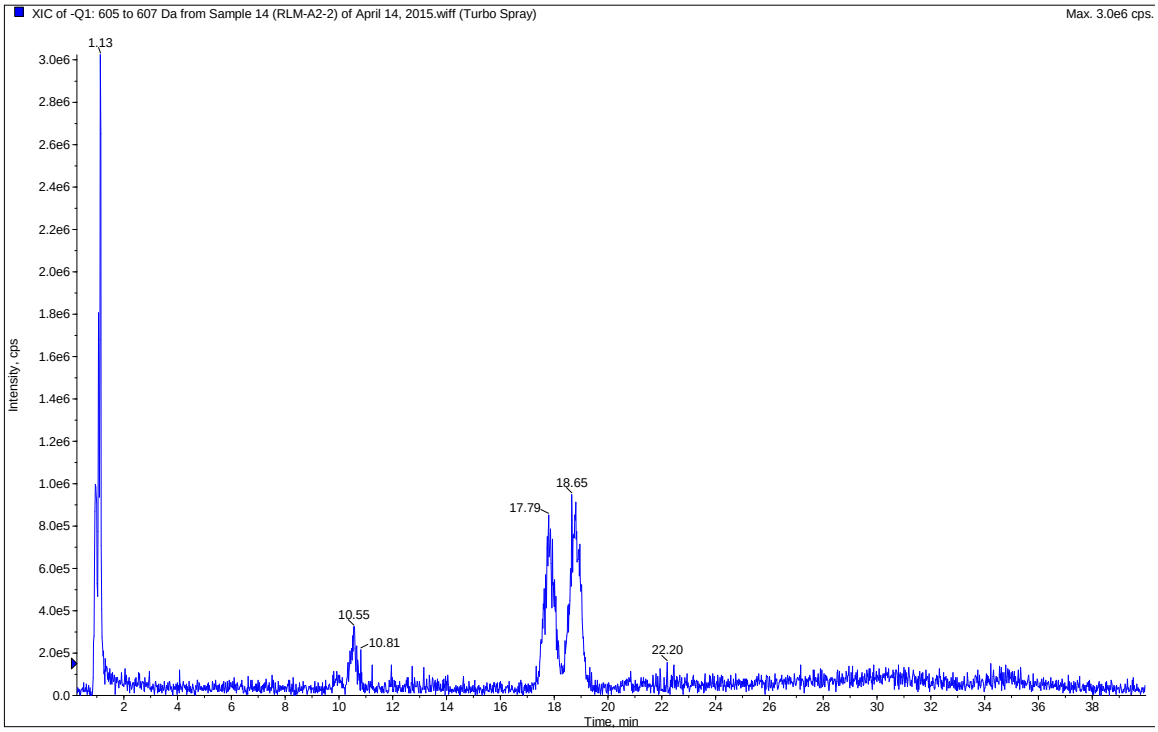

Figure 4.29 LC-MS ESI (-) MS[1] scan of SECO-2 after rat liver microsome oxidation with GSH trapping system present, *m/z* 605-607 range isolated from overall range of *m/z* 100 to 700.

Table 4.5 Comparison of the retention times for the SECO-1 aromatic GSH adducts and the suspected GSH adducts from SECO-2 dealkylation followed by oxidation and trapping with GSH resulting from rat liver microsome oxidation.

RLM	SECO-1	SECO-2
RT (min)	10.1	10.5
	10.7	10.8
	18.0	17.8
	19.0	18.7

In the absence of the GSH trapping system a product with an *m/z* = 313.5 (Figure 4.31), ESI (-) with a RT = 28.5 min was detected (Figure 4.32).

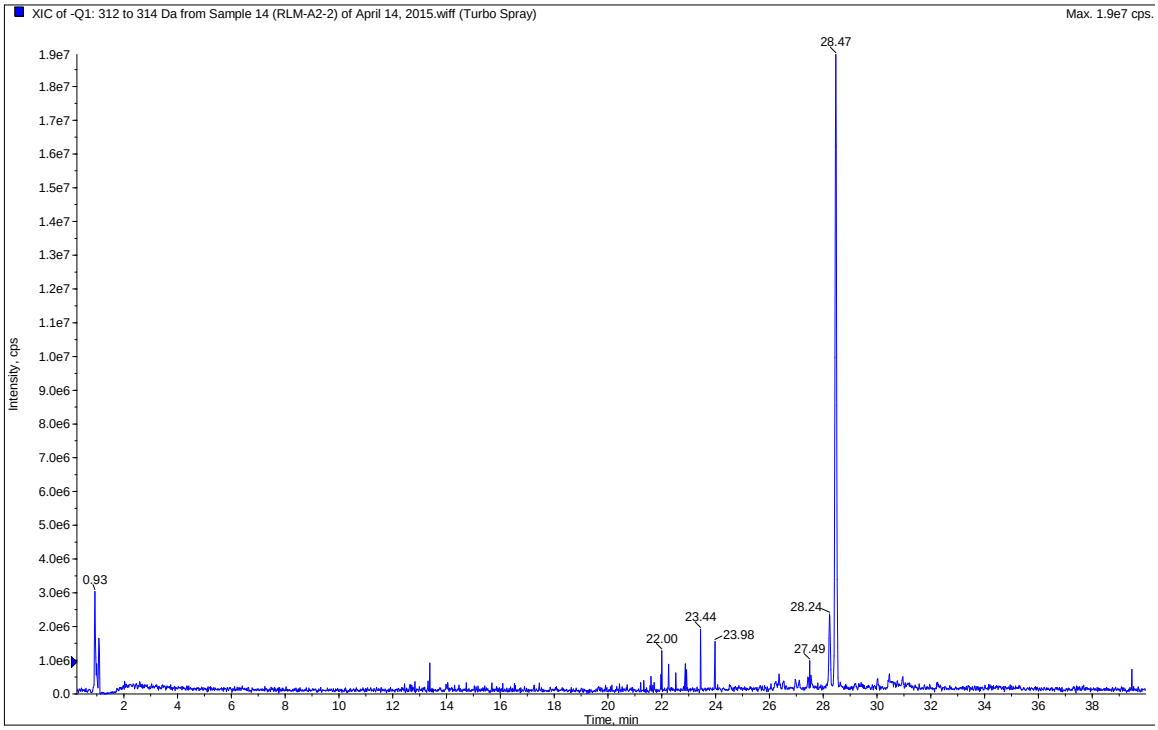

Figure 4.30 LC-MS ESI (-) MS^1 scan of SECO-2 after rat liver microsome oxidation in the absence of GSH trapping system, *m/z* 312-314 range isolated from overall range of *m/z* 100 to 700.

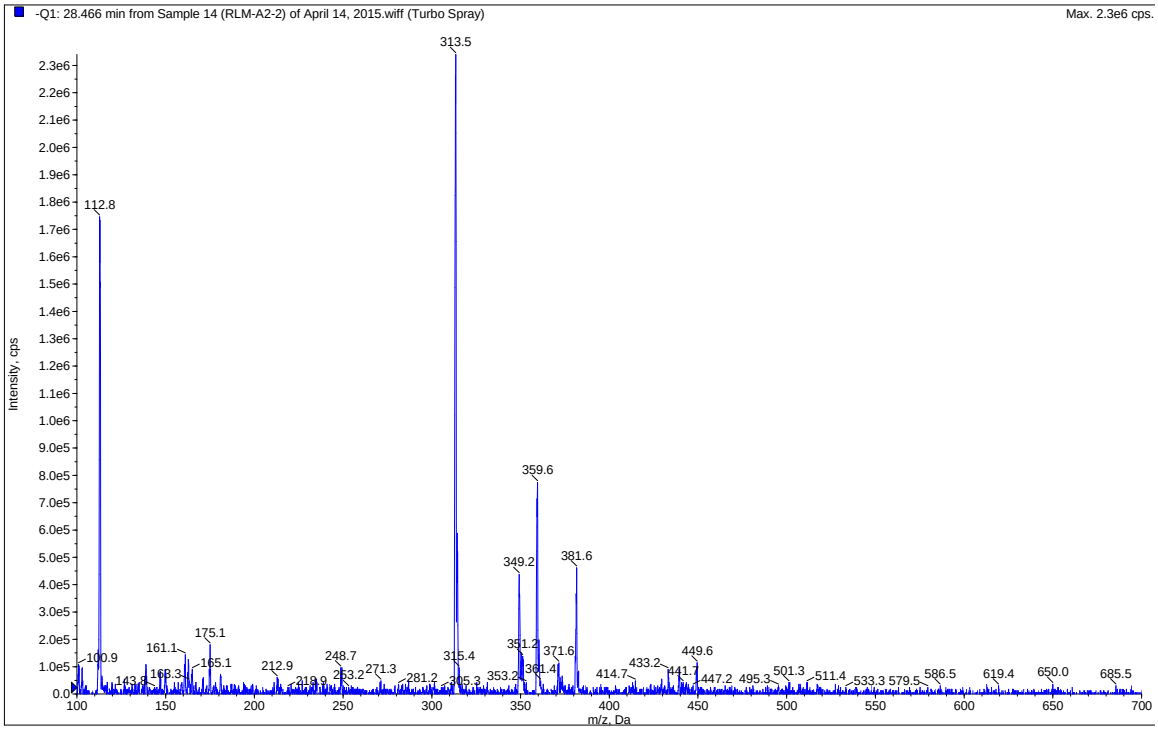

Figure 4.31 LC-MS ESI (-) MS^1 scan of SECO-2 after rat liver microsome oxidation in the presence of GSH trapping system, ionization at 28.5 min isolated from 40 min chromatograph.

This product was consistent with what is expected for a lariciresinol-like metabolite (Figure 4.33).

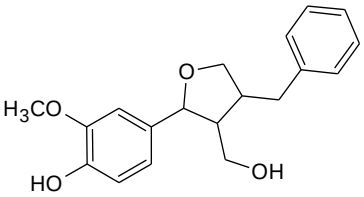

Figure 4.32 Structure of SECO-2 lariciresinol-like metabolite

There is also evidence of a dealkylated product. This metabolite would have the same structure as SECO-1 and has the expected *m/z* = 301.1 and RT = 23.8 (Figure 4.34).

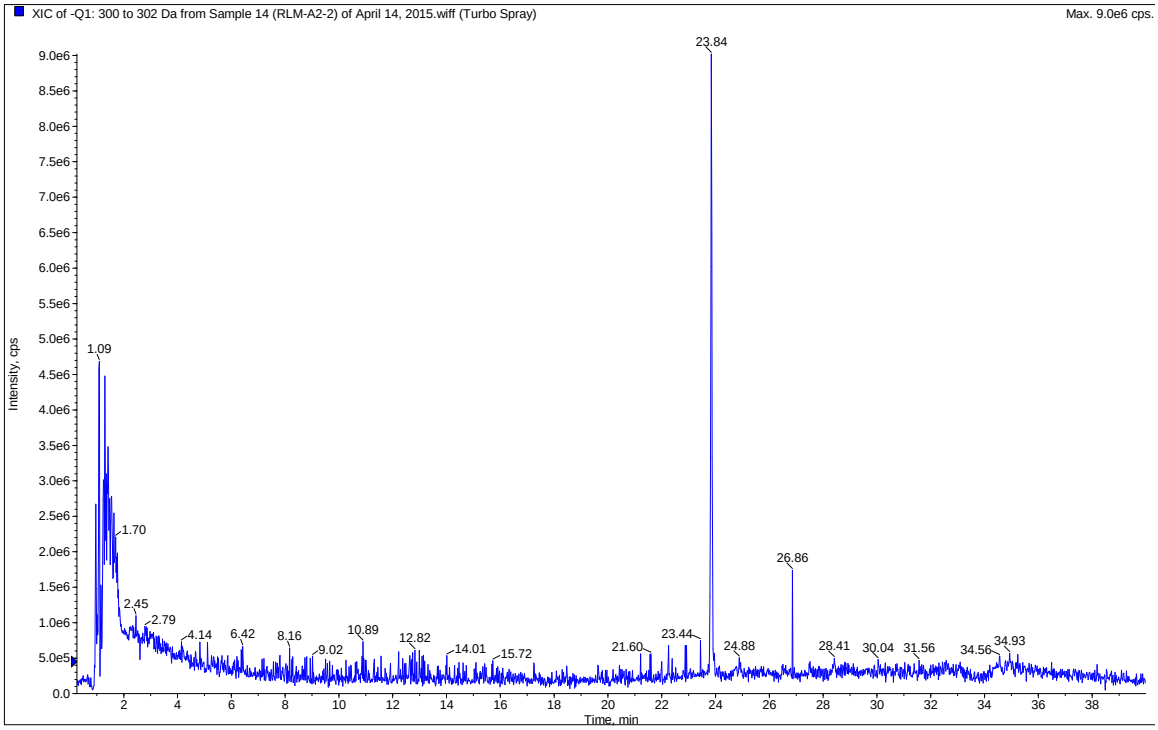

Figure 4.33 LC-MS ESI (-) MS[1] scan of SECO-2 after rat liver microsome oxidation in the absence of GSH trapping system, *m/z* 300-302 range isolated from overall range of *m/z* 100 to 700.

4.3.3 SECO-3

Like SECO-1, SECO-3 forms aromatic GSH adducts with RT = 2.4 and 2.6 min which are consistent with the aromatic GSH adducts formed by MT oxidation (Table 4.6).

Table 4.6 LC-MS retention times of aromatic GSH adducts generated from mushroom tyrosinase and rat liver microsome oxidation of SECO-3 in the presence of GSH.

SECO-3	MT	RLM
RT (min)	2.2	2.4
	2.5	2.6

In the absence of GSH, we observed metabolites with RT = 24.9 and 25.8 min with an *m/z* = 331 (Figure 4.35). These retention times do not correspond to the previously observed dibenzocyclooctadiene like product observed in the stability studies.

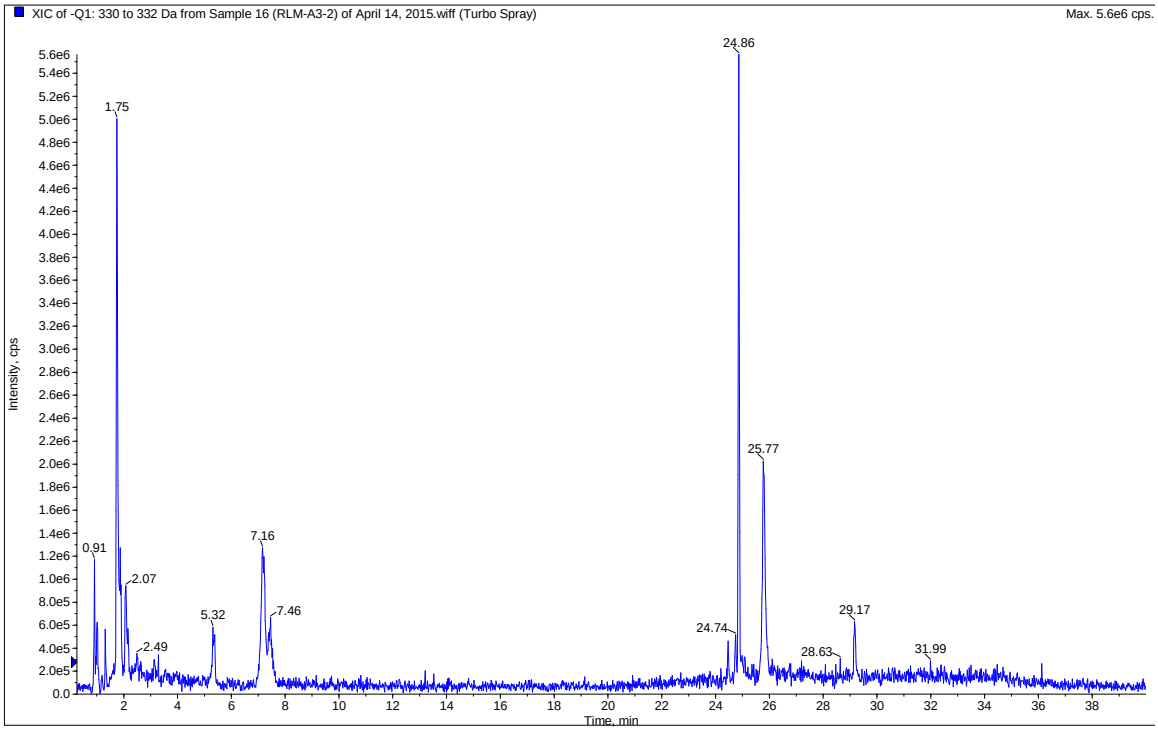

Figure 4.34 LC-MS ESI (-) MS[1] scan of SECO-3 after rat liver microsome oxidation in the absence of GSH trapping system, *m/z* 330-332 range isolated from overall range of *m/z* 100 to 700.

A *m/z* of 331 would be expected for cyclo-SECO-3 metabolites (Figure 4.36).

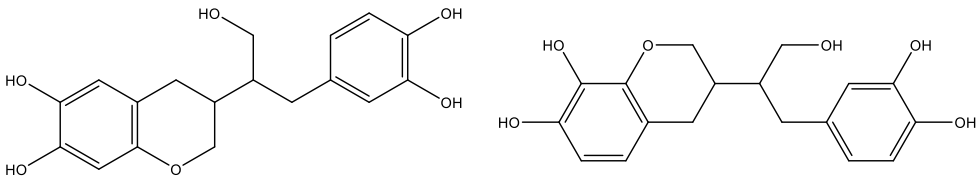

Figure 4.35 Structures of possible SECO-3 rat liver microscome metabolism products in the absence of GSH that would possess a *m/z* = 301 in ESI (-)

There is weak evidence of a metabolite with a RT = 1.75 min with a *m/z* = 331 in the absence of GSH that agrees with the dibenzocyclooctadiene seen in the decomposition reactions (Figure 26). It is difficult to confirm because the dibenzocyclooctadiene RT and that of NADPH (RT = 1.2 min) are similar. This 1.75 min peak with *m/z* = 331 is also observed in the no NADPH control.

4.3.4 SECO-4

Like SECO-1 and SECO-3, SECO-4 forms aromatic GSH adducts with RT = 5.1, 5.4 and 8.4 min which are consistent with the aromatic GSH adducts formed by MT oxidation (Table 4.7). The only difference is that with MT oxidation there is evidence of a GSH adduct with RT = 11.8 min that is not observed with RLM oxidation.

Table 4.7 LC-MS retention times of aromatic GSH adducts generated from mushroom tyrosinase and rat liver microsome oxidation of SECO-4 in the presence of GSH.

SECO-4	MT	RLM
RT (min)	5.1	5.1
	5.4	5.4
	8.3	8.4
	11.8	-

As with SECO-2 there is evidence of dealkylation (Figure 4.37) RT = 10.5 and 17.9 min *m/z* = 347 in the absence of GSH.

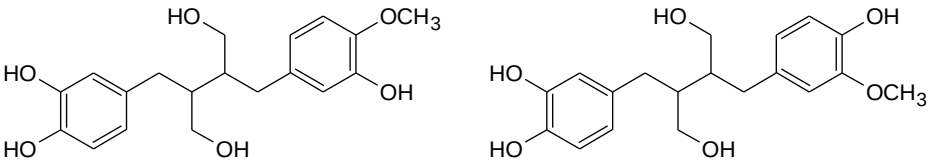

Figure 4.36 Possible structures of SECO-4 dealkylation metabolites.

In the presence of GSH we observed peaks with RT = 3.6 and 5.8 min, *m/z* = 652 that are consistent with dealkylated GSH adducts (Figure 4.38).

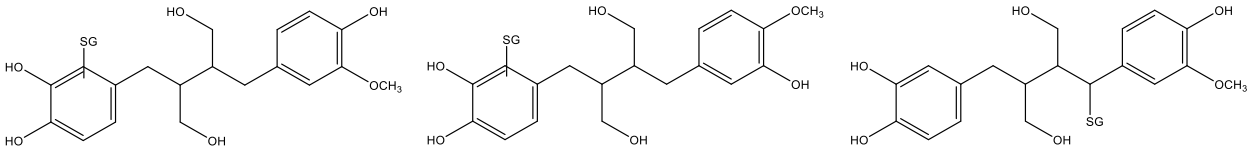

Figure 4.37 Possible structures for GSH adducts of dealkylation SECO-4 metabolites.

In the absence of GSH there is evidence of a dealkylated cyclic product *m/z* = 345, RT = 24.7 min (Figure 4.39)

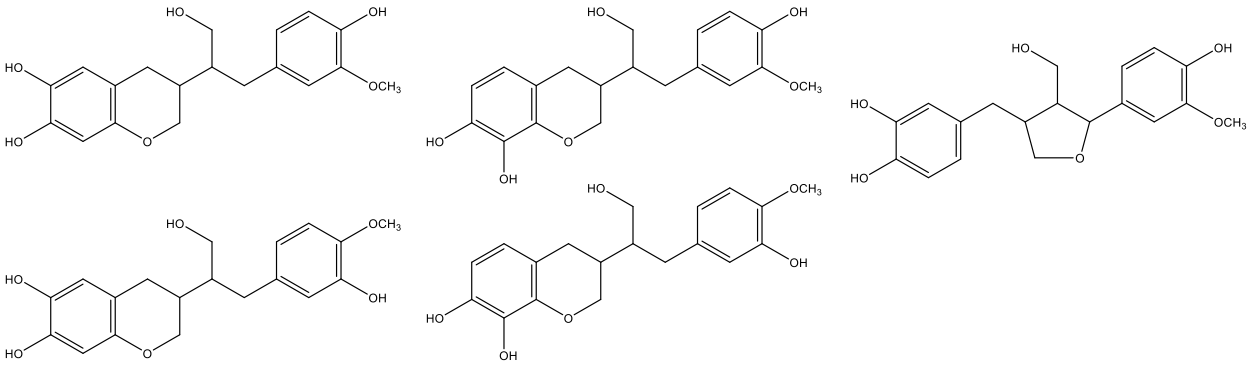

Figure 4.38 Possible structures for cyclic dealkylated metabolites from SECO-4 RLM oxidation.

Peaks consistent with two dealkylation reactions, forming SECO-3, and subsequent oxidation to an o-Q and trapping with GSH were detected. These peaks had *m/z* of 606.5 and retention times consistent with SECO-3 aromatic GSH adducts (Table 4.8). NL (+) 129 and product ion scans were attempted, for both the suspected single and double dealkylated GSH adducts, however these products were not present in sufficient quantity for reliable results.

Table 4.8 LC-MS retention times of aromatic GSH adducts generated from rat liver microsome oxidation of SECO-3 compared to retention time of SECO-4 metabolism products the *m/z* = 638 in the presence of GSH.

RLM	SECO-3	SECO-4
RT (min)	2.4	3.0
	2.6	3.6

4.3.5 Summary

Below (Table 4.9) is a summary of the retention times, m/z and NL results for the rat liver microsome oxidation of all of the SECO analogues.

Table 4.9 Summary of the retention times, m/z and NL of the starting materials and the metabolites detected from rat liver microsome oxidation experiments.

Analogue	Oxidation	m/z (-)	RT (min)	NL (+)
SECO-1	Starting material	301	23.8	N/A
	In presence of GSH	608	10.1	129
		608	10.7	129
		608	18.0	129
		608	19.0	129
	In absence of GSH	301	23.8	N/A
		299	24.7	N/A
SECO-2	Starting material	315	24.9	N/A
	In presence of GSH	620	22.9	307
		608	10.5	-
		608	10.8	-
		608	17.8	-
		608	18.7	-
	In absence of GSH	301	23.8	N/A
		313	28.5	N/A
SECO-3	Starting material	333	5.5	N/A
	In presence of GSH	638	2.4	129
		638	2.6	129
	In absence of GSH	331	1.7	N
		331	24.8	N/A
		331	25.8	N/A
SECO-4	Starting material	361	22.2	N/A
	In presence of GSH	666	5.1	129
		666	5.4	129
		666	8.3	129
		652	3.6	-
		652	5.8	-
		638	3.0	-
		638	3.6	-
	In absence of GSH	347	10.5	N/A
		347	17.9	N/A
		345	24.7	N/A

4.4 Inhibition

All of the SECO analogues and SECO were sent to Life Technologies for P450 inhibition studies. IC_{50} values were determined using their SelectScreen® Biochemical P450 Profiling Services. All SECO analogues and SECO were prepared at a 100X concentration (50 mM) and diluted to a 3X working concentration in 100 mM potassium phosphate pH 7.4. The IC_{50} assay results are summarized in Table 4.10.

Table 4.10 Summary of SECO and SECO analogue IC_{50} values for cytochrome P450 isoforms CYP3A4, CYP3A5, CYP2C9 and CYP2C19

IC_{50} (μM)	CYP3A4 [a]	CYP3A4 [b]	CYP3A5 [a]	CYP3A5 [b]	CYP2C9	CYP2C19
SECO	99.2	303	61.4	396	24.6	47
SECO-1	25.6	4.75	28.2	70.8	82.9	6.83
SECO-2	20.7	34.6	23.4	48.5	6.04	0.424
SECO-3	37.5	46.5	21.4	47.9	99.3	105
SECO-4	62.5	100	45.5	135	185	114

a = BOMCC
b = DBOMF

In cytochrome P450 inhibition assays the *in vitro* experimental conditions, including the choice of probe substrate, can have a significant impact on the results of the assay.[86] Under the same assay conditions, different probe substrates may provide different results.[86] These differences are most notable for the CYP3A subfamily.[86] The interactions between CYP3A4 and its substrates and inhibitors are complex. The complex effects are attributed to the binding of multiple substrates within the active site of the enzyme.[87] Consequently the interactions, in this case inhibition, observed with one probe may not be representative of those observed with other substrates.[87] It is therefore recommended that two or more probe substrates are used for evaluation of CYP3A mediated interactions.[86,87] The effects of different probe substrates may impact the accurate assessment of drug interaction potential and extrapolation from *in vitro* to *in vivo*.[86,87] For this reason, two different probes, BOMCC and DBOMF, were used to determine the IC_{50} for CYP3A4 and CYP3A5.

5.0 Discussion

Since the lignan skeleton remains a target for pharmacological applications, a greater understanding of the structural features responsible for lignan pharmacological and toxicological activities is necessary. Previously the structure-activity relationship of NDGA oxidative metabolism was investigated using NDGA analogues. Unlike NDGA, SECO has two additional hydroxyl groups, one at each γ position on the lignan backbone. What is not known is the effect of these hydroxyl groups on the oxidative metabolism of lignans. Based on the previous study[38] four areas of interest were identified: *ortho*-quinone (o-Q) formation, *para*-quinone methide (p-QM) formation, cyclization to dibenzocyclooctadiene and intramolecular cyclization as a method of mediating toxicity

A major limitation of this study was the lack of structural information from NMR analysis. There was not enough starting material available for scale up and the reactions did not produce enough individual metabolite for NMR analysis. NMR data was only collected for one product, the major SECO-3 autoxidation product. Despite a modest scale up and most of the starting material being converted to this single product there was very little product collected, less than 1 mg. This made for a poor signal to noise ratio in the NMR analysis. All structural information reported is based on MS and LC-MS data.

5.1 High Performance Liquid Chromatography (HPLC) Method Development

A challenge for HPLC analysis of SECO lignans is having a retention time sufficient to observe both polar and non-polar metabolites. This is important because a wide variety of metabolites are possible and expected. GSH addition would result in a metabolite that is more polar than starting material. Cyclization to a lariciresinol like metabolite or to a 6-membered ring would result in a metabolite that is less polar than the starting material. During the original phase of method development a Nova-Pak ® C18 3.9 × 150 mm column was determined to provide the optimal resolution and retention times for the SECO analogues. The retention time of SECO-3 (RT = 3.6 min) was not ideal as many of the more polar metabolites, such as the GSH adducts, would likely elute in the solvent front. This was confirmed when metabolites were not detected in mushroom tyrosinase studies though a decrease in starting material was observed.

In January 2015 an Agilent Poroshell 120 EC-C18 4.6 × 50 mm 2.7 µm column became available and the Nova-Pak ® C18 3.9 × 150 mm separation method was modified for the new column. The Agilent Poroshell 120 EC-C18 4.6 × 50 mm 2.7 µm column, possessing a tighter particle size distribution, showed an improved retention time for SECO-3 (RT = 5.5 min). Even for analogues where metabolites were detected, such as SECO-1, the resolution, separation and detection of metabolites was significantly improved as shown in Figure 5.1.

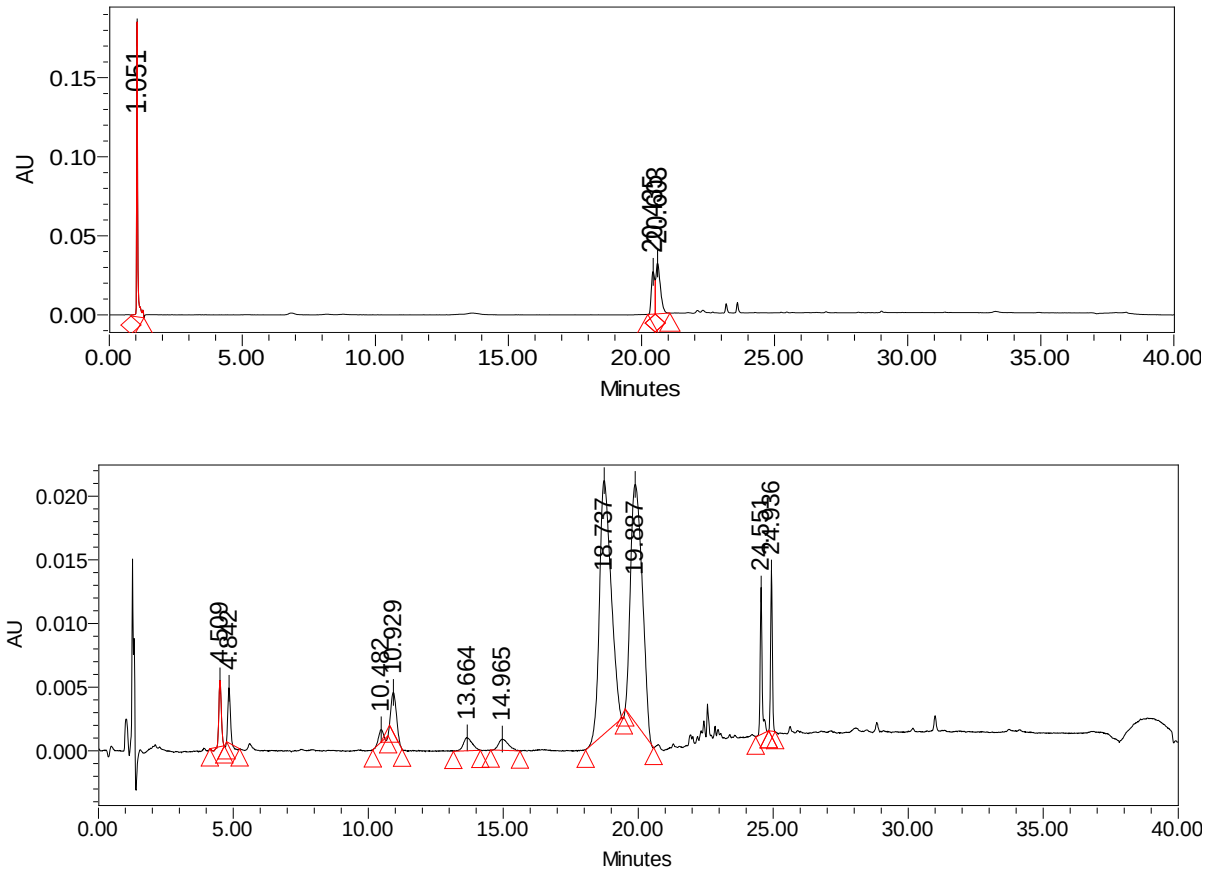

Figure 5.1. Comparison of Nova-Pak ® C18 3.9 × 150 mm column (top) and Agilent Poroshell 120 EC-C18 4.6 × 50 mm 2.7 µm column (bottom) after mushroom tyrosinase oxidation of SECO-1. λ = 280 nm.

5.2 SECO Analogue Stability

If a compound is to be used as a pharmaceutical agent it is imperative to understand its physiological stability. A compound with a short half-life under physiological conditions may not reach the site of effect. If a compound's stability is not determined under the *in vitro* experimental conditions, incorrect conclusions as to the compounds pharmacological activity may be drawn. If the compound is unstable and no effect is observed it may be due to the absence of the compound because of decomposition and not the ability of the compound to produce the tested effect. Alternatively, effects attributed to the starting material may in fact be a result of one or more of the decomposition products. Olson et al. (2008) observed the instability of quercetin in Dulbecco's modified eagle medium which was incubated under normal cell culture conditions.[88] It was posited that the quercetin breakdown products were actually responsible for the proapoptotic effects normally attributed to quercetin.[88] NDGA, NDGA analogues and flavonols, a related family of polyphenols, have all demonstrated instability in aqueous buffer systems.[38,89] Therefore, the stability of the SECO analogues under physiological assay conditions needed to be determined.

Stability studies were also useful for separating the effects of the potentially competing processes of autoxidation and enzyme oxidation. The half-life of the decomposition will determine if autoxidation will be a concern on the time scale of our experiments and to determine if metabolites of autoxidation products need to be considered. The half-life of the SECO analogues may also be an indication of whether they are suitable for future cell culture studies. The half-life of the compound needs to be substantially longer than the incubation period. SECO-3, whose $t_{1/2}$ = 1.73 h at pH 7.4, for example is not likely appropriate for cell culture studies, unless experimental conditions are utilized which minimize autoxidation.

All of the SECO analogues were stable at pH 6.0 but only SECO-2, the sole phenol analogue, was stable at pH 7.4. The autoxidation potential of catechols and phenols is pH dependent with stability inversely proportional to pH.[90] Therefore, it is reasonable that the catechol analogues are stable at pH 6.0 but not 7.4. In this investigation there was no evidence of phenol instability. This is contrary to previous research on NDGA analogues, illustrated in Figure 5.2, where phenol

analogue instability at pH 7.4 was observed. The half-life of NDGA analogue A2 was 5.49 h and the half-life of A3 was 6.70 h.[39]

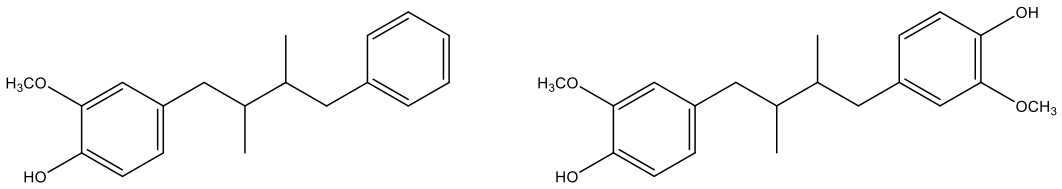

Figure 5.2 Structure of previously studied NDGA phenol analogues: A2 (left) and A3 (right)

Due to the observation that analogues with a phenol substituent on the aromatic ring were stable and those with a catechol substituent were not, it was expected that SECO-3 with catechol substituents on both aromatic rings would have the shortest half-life. SECO-3 does indeed have the shortest half-life ($t_{1/2}$ = 1.73 h) and is consistent with the previously reports for NDGA and NDGA analogue 6, which have catechol substituents on both aromatic rings ($t_{1/2}$ = 3.94 and 1.47 h respectively).[39]

SECO-3 was the only SECO analogue where there was evidence of a dibenzocyclooctadiene decomposition product, consistent with the NDGA study that posited the need for catechol moieties on both aromatic rings for this type of cyclization to occur.[38] The formation of and decomposition of the dibenzocyclooctadiene was also consistent. SECO-3 dibenzocyclooctadiene concentration peaked at 8 h. NDGA and NDGA analogue 6 (Figure 5.3) both had dibenzocyclooctadiene concentration that peaked at 9 h.[39]

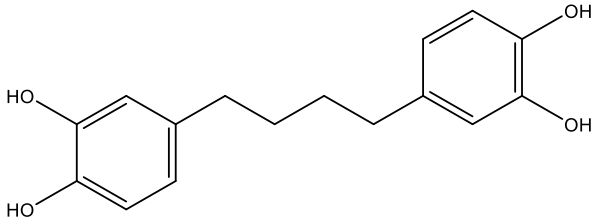

Figure 5.3 Stucture of NDGA analogue 6

Though the half-life of SECO-3 is consistent with those seen in the NDGA study, the $t_{½}$ of SECO-1 and SECO-4 are longer than observed for all of the NDGA analogues. This could speak to a possible stabilization effect of the two hydroxyl groups in the SECO analogues when

cyclization to a dibenzocyclooctadiene does not occur. Since dibenzocyclooctadiene formation can occur in some lignans, it is possible that the lignan analogues may adopt conformations in solution that favour a stabilizing interaction between the alcohols and the catechols. The precise nature of such a stabilizing conformation however is unclear.

The half-lives of SECO-1 and SECO-4 are similar but not the same. There is approximately a 2 h difference, which opens up the possibility that the substituents on the opposite aromatic ring influence the overall lignan stability. Interestingly the stability trend observed for SECO-1 and SECO-4 differs from that for the analogues of NDGA (NDGA-1 and NDGA-4). NDGA -1 ($t_{1/2}$ 4.22 h) is more rapidly autoxidized than NDGA-4 ($t_{1/2}$ 4.62 h). For the SECO analogues analyzed using the same linear transformation it is the opposite, SECO-1 has a longer half-life ($t_{1/2}$ = 9.00 h) than SECO-4, ($t_{1/2}$ = 7.03 h). It should be noted that the NDGA calculations were performed using Excel, while this study used GraphPad for statistical analysis. Unexpectedly, in both methods of analysis, linear and non-linear regression, the SECO catechol analogues consistently displayed greater stability than the NDGA catechol analogues. How the alcohol groups on the side chain influence lignan stability is not known and will require further study.

5.3 Silver Oxide Oxidation

Silver oxide oxidation is accepted standard method of generating *para*-quinone methides.[91,92] This protocol was intended to be used to generate p-QM standards, however, the silver oxide oxidation experiments with the SECO analogues were not successful in producing GSH adducts. The silver oxide oxidation protocol was successful in generating GSH adducts for the model compound eugenol (Figure 5.4), which is consistent with Thompson *et al*., 1990.[93]

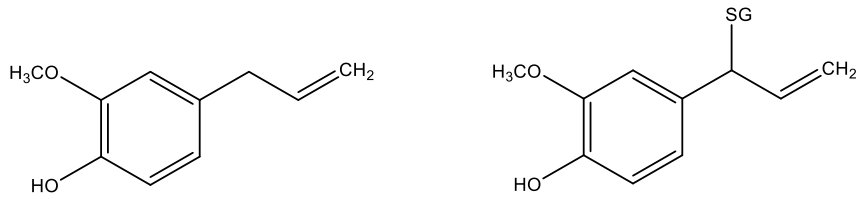

Figure 5.4 Eugenol (left) and Eugenol-SG adduct (right) formed after silver oxide oxidation. Adduct location determined by MS.

When the reaction was followed by UV-Vis spectrophotometry, a change in maximum absorbance from approximately 280 nm was observed to longer wavelength, approximately 350 nm, consistent with p-QM formation.[78] Working concentrations agreed with the eugenol pilot studies and should have been sufficiently dilute for solubility. Addition of the oxidation mixture to buffer for trapping with GSH resulted in loss of absorbance, likely as a result of insolubility, implying that the SECO p-QMs were excessively hydrophobic. In an effort to overcome this presumed hydrophobicity, the quinone methides were extracted with ethyl acetate, however this was also unsuccessful. There have been consistent solubility issues with these lignans and ultimately the use of this method to make standards was unsuccessful. The concentrations of lignan used should have been sufficiently low to avoid quinone polymerization and precipitation. The alcohol groups may impart a unique property to the lignans and requires further investigation.

5.4 Mushroom Tyrosinase Oxidation

Tyrosinase (EC 1.14.18.1) is a copper-enzyme, widely distributed in nature.[94,95] Tyrosinase catalyzes the hydroxylation of monophenols to *ortho*-diphenols and the oxidation of *ortho*-diphenols to *ortho*-quinones, using molecular oxygen.[94,95] Diphenols are better mushroom tyrosinase substrates than monophenols.[96] Mushroom tyrosinase (MT) experiments were conducted to create *ortho*-quinone standards, as tyrosinase-catalyzed oxidation of a catechol is a common method for generating *ortho*-quinones.[78,81,91,97]

SECO-2 is the only analogue that does not contain a catechol moiety and was the only analogue not metabolized by MT. MT is capable of carrying out an *ortho* hydroxylation reaction to form a catechol, but this was not observed in either the presence or absence of GSH. Hydroxylation may occur below our limit of detection.

SECO-1, SECO-3 and SECO-4 all followed the same pattern of metabolism. In the presence of GSH, the analogues are first oxidized to *ortho*-quinones and then trapped with GSH (Figure 5.5). All of the catechols formed aromatic GSH adducts as confirmed by mass spectrometry; NL (+)

129 and product ion scans. There was no evidence of either cyclization or hydroxylation, however it is possible that cyclization and/or hydroxylation was below our limit of detection.

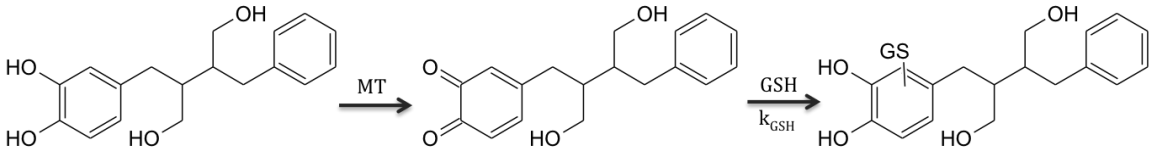

Figure 5.5 Proposed reaction scheme for mushroom tyrosinase mediated oxidation of SECO-1 in the presence of GSH

In the absence of the GSH trapping system SECO-1, SECO-3 and SECO-4 were metabolized to multiple (3, 4 and 4, respectively) metabolites that showed an addition of 14 Da to their respective starting material molecular masses by MS. Given the possible MT reactions, the 14 Da addition is in accordance with cyclization and the addition of an oxygen atom. Figure 5.6 illustrates a possible SECO-1 metabolite. MT is capable of hydroxylating a catechol at the *ortho* position; an intial *ortho*-quinone that undergoes intramolecular cyclization would produce a catechol, which would be anticipated to be a favourable MT substrate and consistent with our results.

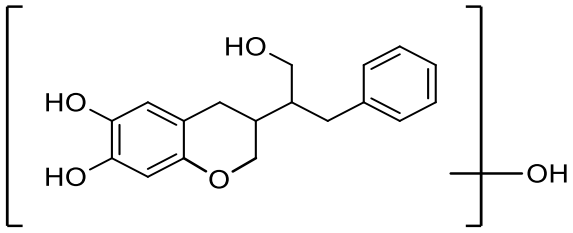

Figure 5.6 Possible SECO-1 metabolite structure; accounts for the addition of 14 Da.

Figure 5.7 illustrates two possible reaction pathways for MT oxidation in the absence of GSH that would account for the additional 14 Da.

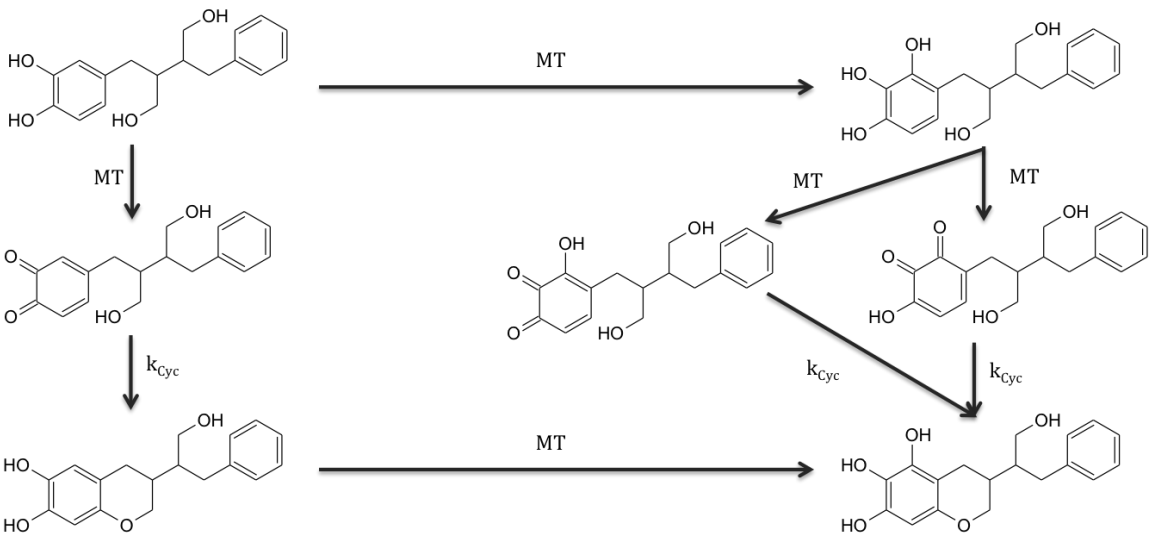

Figure 5.7 Possible reaction schemes for the mushroom tyrosinase mediated oxidation of SECO-1, SECO-3, SECO-4 in the absence of GSH.

Note that in Figure 5.7, hydroxylation is shown at one of the possible *ortho* positions for simplicity. An alternative 6-membered ring cyclization product is also possible *ortho* to the catechol OH, however based on the most reactive site in previous lignan catechols, we suspect that the structures as shown are the most likely.[98] Due to the absence of hydroxylation in SECO-2 and in the presence of GSH, cyclization most likely occurs prior to hydroxylation. For the proposed reaction schemes to occur, GSH addition (an intermolecular reaction) must out compete cyclization, an intramolecular reaction ($k_{cyc} < k_{GSH}$). Thiols are superior nucleophiles to alcohols, which may explain the ability of GSH to compete with intramolecular cyclization, although other steric or electronic factors may also contribute.

5.5 Microsomal Oxidation

5.5.1 Assay Development and Pilot Study

Rat liver microsome experiments were carried out to investigate the *in vitro* oxidative metabolism of the SECO analogues. The development of the microsomal oxidation assay protocol was time consuming, as SECO is a relatively poor cytochrome P450 substrate. We first thought that something had occurred during microsome preparation that caused the destruction of P450 activity. To investigate this possibility rat liver microsomes (0.5mL; 20mg/mL; Lot#

RT053C) were purchased from Invitrogen (Life Technologies), which did not resolve this issue. Another possibility was the presence of NADPH-pyrophosphatase which degrades NADPH and is present in rat liver microsomes, but which is not found in human liver microsomes.[99] The original protocol did not contain a NADPH-pyrophosphatase inhibitor.[99] NADPH-pyrophosphatase catalyzes the reaction:

$$NADPH + H_2O \rightarrow NMNH + ADP$$

As no NADPH regenerating system was included, the NADPH dependent-P450 reactions decreased, causing the metabolism of the SECO analogues to fall below our detection limits. NADPH-pyrophosphatase can be inhibited with the addition of sodium pyrophosphate.[99] Overloading the reaction with NADPH allowed for the detection of metabolism with both our model compound eugenol and with the SECO analogues. NADPH is over 35,000 times more expensive than sodium pyrophosphate, therefore sodium pyrophosphate was added to the assay protocol to decrease the amount of NADPH necessary for each reaction. Previous research in our lab did not detect the metabolism of phenols, possibly due to the absence of NADPH-pyrophosphatase inhibition.

Eugenol was used as a model compound in rat liver microsome assay protocol pilot studies. When eugenol was oxidized in the presence of GSH it formed a benzyl GSH adduct (Figure 5.8), which was consistent with the results of Thompson et al. 1990.[93]

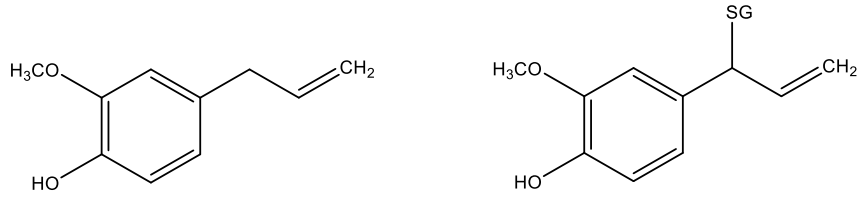

Figure 5.8 Structure of eugenol (left) and the structure of the eugenol benzylic GSH adduct (right).

5.5.2 Reaction Pathway 1

Figure 5.9 illustrates the proposed RLM mediated oxidation reaction pathway 1 for SECO-1 and SECO-2.

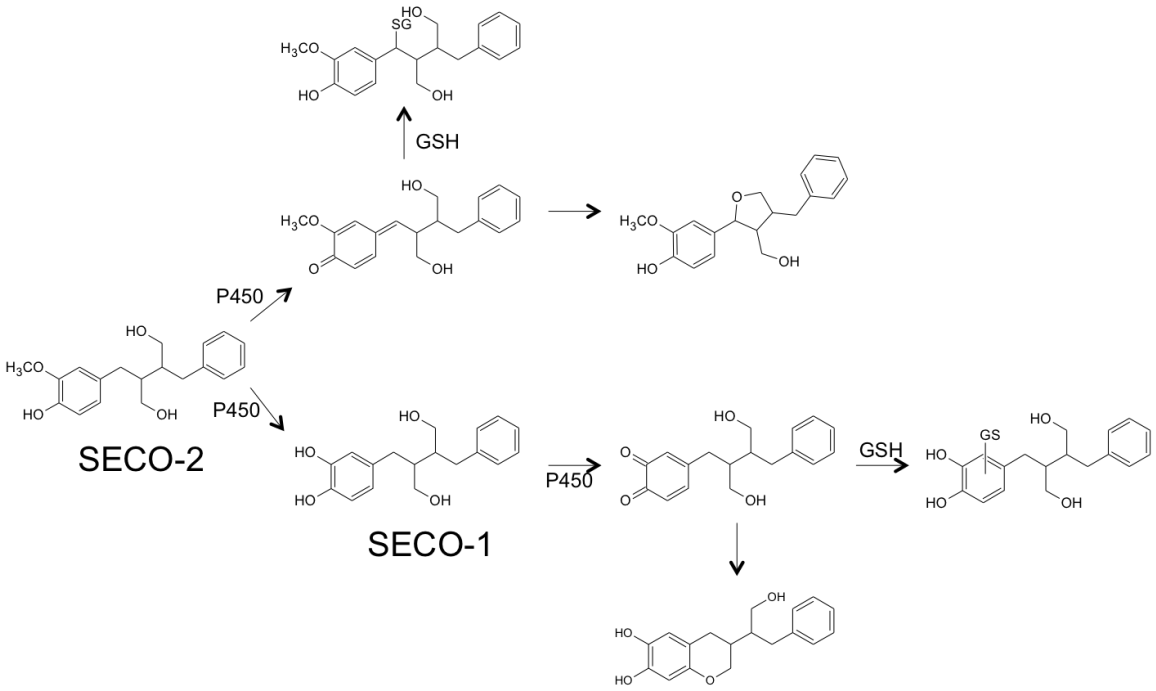

Figure 5.9 Scheme 1: Reaction pathway 1 proposed for the rat liver microsome (P450) mediated oxidative metabolism of SECO-1 and SECO-2

SECO-1 has the simplest reaction pathway. In the presence of GSH, SECO-1 is oxidized to an *ortho*-quinone and trapped with GSH to form aromatic GSH adducts as determined by MS. These adducts agree with MT standards that were previously discussed. In the absence of GSH there were no major metabolism products detected. There was weak evidence of cyclization found (RT = 24.7 min) only detected by MS and a possible product (RT = 1.7 min) only detected by HPLC, however, these could not account for the decrease in starting material observed. Only one cyclization product (6'-position) is illustrated in Figure 5.9 for simplicity, though we acknowledge that the 2'-isomer is also possible as shown in Figure 4.25. One possible explanation for the loss of starting material to unobserved products is that SECO-1 could be metabolized to a dicarboxylic acid derivative that would be anticipated to elute in the solvent

front, and could not be characterized.[98] Diacids are known to be generated from o-Q by reaction with HOO^- that produces a neutral diacid following acidification and isolation.[100]

A benzylic GSH adduct was detected (NL (+) 307) upon SECO-2 oxidation in the presence of GSH. This indicates the formation of a p-QM prior to trapping. In the absence of GSH a metabolite with a *m/z* in agreement with a cyclization product was observed. Cyclization to the aromatic ring is also possible, with these structures shown in Figure 5.10, but given what is known about SECO metabolism, the lariciresinol-like cyclization is most likely and is shown in scheme 1.

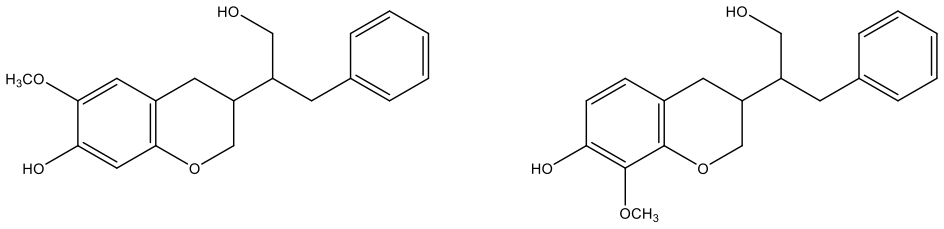

Figure 5.10 SECO-2 cyclization to the aromatic ring

In addition to oxidation to a p-QM, cytochrome P450 catalyzes a dealkylation reaction forming SECO-1. In the presence of GSH, metabolites with a RT and *m/z* that agree with the SECO-1 aromatic GSH adducts and the SECO-1 MT standards were observed. Unfortunately, the conversion was low and there was not enough of these metabolites to be reliably detected using NL (+) 129 scans to confirm whether they were aromatic GSH adducts.

5.5.3 Reaction Pathway 2

Figure 5.11 illustrates the proposed RLM mediated oxidation reaction pathway 3 for SECO-3 and SECO-4.

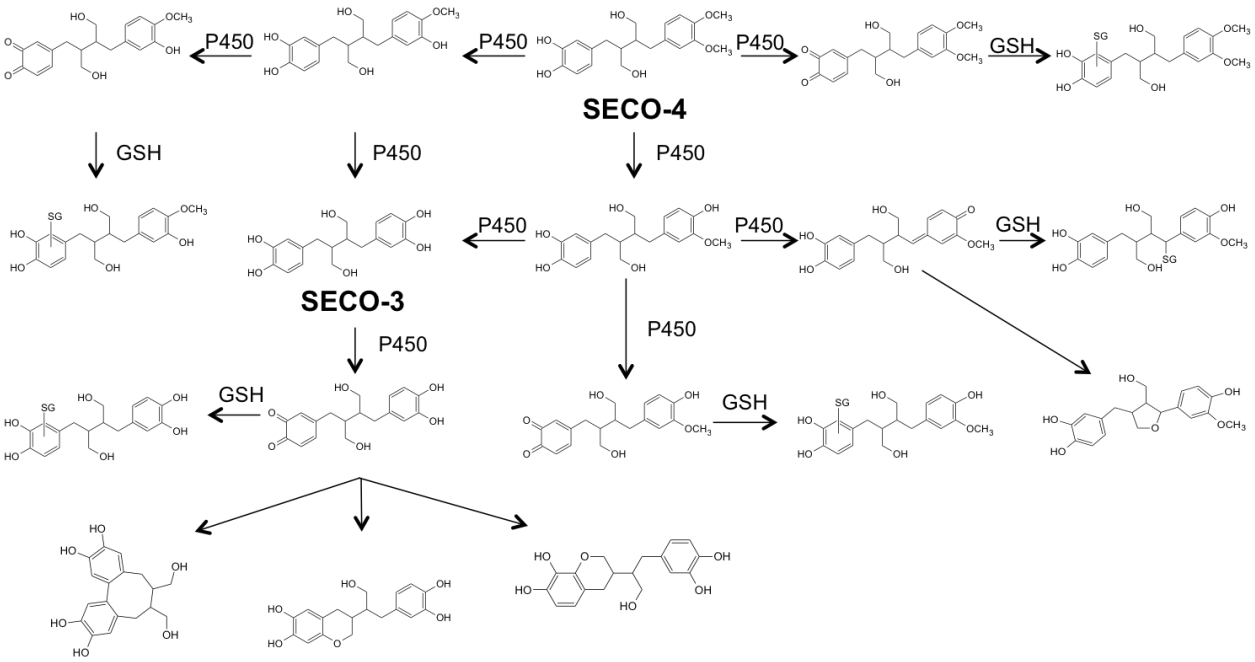

Figure 5.11 Scheme 2: Proposed reaction pathway 2 for the rat liver microsome mediated oxidative metabolism of SECO-3 and SECO-4

SECO-3 and SECO-4 demonstrate the same basic reactions as SECO-1 and SECO-2 for RLM mediated oxidation: dealkylation and oxidation to a quinone. However, because of the increased number of substituents on the aromatic rings there exists an increased number of possible metabolites.

In the presence of GSH, SECO-3 generated aromatic GSH adducts (NL (+) 129) that agreed with the previously created MT standards. In the absence of GSH, 3 metabolites were detected with RT of 1.7, 24.8 and 25.8 min. The 1.7 min peak is consistent with the dibenzocyclooctadiene decomposition product observed in the stability studies (Figure 4.9). This metabolite was difficult to detect in the presence of NADPH as the RT of NADPH was 1.2 min and overlaps with the dibenzocyclooctadiene signal. This metabolite was also detected in the no NADPH control and was likely a result of autoxidation and not enzyme oxidation. There are two potential cyclization products for SECO-3 involving the alcohol side-chain, both shown in Figure 5.11, that agreed with the two RT and *m/z* observed. What product corresponds to which elution time is unknown at present. Because there were multiple metabolites and because we have not

conducted their individual quantitation it is difficult to determine if a dicarboxylic acid was another potential metabolite.

Oxidation of SECO-4 in the presence of GSH produced aromatic (NL (+) 129) GSH adducts consistent with MT generated standards. These adducts were the major metabolites detected. In the presence of GSH, SECO-4 metabolism also generated an additional 4 possible GSH adducts; two metabolites with the expected *m/z* for dealkylated GSH adducts and two with that of double dealkylated GSH adducts. The RT of the double dealkylated GSH adducts agreed with the RT of the SECO-3 aromatic GSH adducts, but there was insufficient metabolite produced for NL confirmation.

In the absence of GSH there is evidence of two single dealkylation products, RT = 10.5 and 17.9 min. There are two possible single dealkylation products (Figure 4.35) though assigning specific structures a retention time is not currently possible. Conversely, there are 5 possible single dealkylation and cyclization metabolites (Figure 4.38), but only one product (RT = 24.7 min) with the predicted *m/z* is detected. If the catechol was oxidized to an o-Q followed by cyclization, multiple products would be expected. However, if dealkylation occurs in the para-position and that phenol is oxidized to a p-QM followed by cyclization to a lariciresinol like product only one metabolite is expected. Therefore, only the p-QM cyclization to a lariciresinol like metabolite is included in Figure 5.11. Given oxidation to the p-QM, it is reasonable to postulate that one of the previously discussed single dealkylation GSH adducts is a benzyl adduct however this cannot be presently confirmed.

All SECO analogues formed quinones. Catechol analogues formed o-Q and phenol analogues formed p-QM. There was no evidence of isomerization from an o-Q to a p-QM in any of our results, which is in agreement with the previous NDGA study.[38]

The proposed reaction schemes are only possible if the intermolecular reaction of GSH addition outcompetes the intramolecular reaction of cyclization ($k_{cyc} < k_{GSH.}$). Theoretically if the quinones are able to react with GSH then it is possible for them to react covalently with cellular macromolecules such as DNA and proteins, making cyclization a poor detoxification

mechanism. To my knowledge this is the first time anyone has reported GSH outcompeting cyclization to a lariciresinol like metabolite with this class of compound. In the case of SECO-2, though oxidation to a p-QM was expected, addition of GSH at the benzylic position was not. Previous attempts at trapping SECO oxidized to a p-QM with GSH failed, generating only lariciresinol, which was generated as the intramolecular reaction out competed the intermolecular reaction of GSH addition.[2] Rat liver microsome oxidation of SECO was repeated and the previously generated results were confirmed. No GSH adducts were detected and a metabolite consistent with lariciresinol was the major metabolite in both the presence and absence of GSH. No dealkylation was detected. This could be due to a difference in the cytochrome P450 isoforms that metabolize SECO versus the SECO analogues.

5.6 Inhibition

SECO has many potential pharmacological uses including: reduction in serum cholesterol levels, delaying the onset of type II diabetes, the treatment/prevention of cardiovascular diseases, and decreased formation of breast, prostate and colon cancers. A number of pharmaceutical drugs are currently used to treat these conditions such as: Docetaxel, Doxorubicin, Cabazitaxel, Abiraterone, Enzalutamide, Atorvastatin, Rosuvastatin, Fluvastatin, Simvastatin, Lovastatin and Pravastatin. All of these drugs that undergo P450 metabolized are metabolized by subfamilies CYP3A and CYP2C. As we were interested in studying potential drug interactions, isoforms CYP3A4, CYP3A5, CYP2C9 and CYP2C19 were selected for inhibition screening.

The choice of probe substrate can have a significant impact on the results of an *in vitro* cytochrome P450 inhibition assay.[86] Different probe substrates may not provide the same result, even when all of the other assay conditions are kept constant.[86] These differences are most notable for the CYP3A subfamily.[86] The effects of the complex interactions between CYP3A4, its substrates and inhibitors are attributed to the binding of multiple substrates within the active site of the enzyme.[87] Consequently the effect, in this case inhibition, observed with one probe may not be representative of those observed with other substrates.[87] It is therefore recommended that two or more probe substrates are used for evaluation of CYP3A mediated interactions.[86,87] For this reason, two different probes, BOMCC and DBOMF, were used to determine the IC_{50} for

CYP3A4 and CYP3A5. IC_{50} is the concentration of an substrate which is needed to inhibit a biological or biochemical process by 50%. The effects of different probe substrates may impact the accurate assessment of drug interaction potential and extrapolation from *in vitro* to *in vivo*.[86,87]

In general, the SECO analogues were mediocre cytochrome P450 inhibitors, consistent with previously reported lignan IC_{50} values.[2] Notably, analogues with substituents on only one aromatic ring tended to be stronger inhibitors than those with substituents on both aromatic rings.

SECO was previously reported to have an IC_{50} value of 373 μM.[2] This agrees with our results from the CYP3A4 and CYP3A5 DBOMF IC_{50} assay of 303 and 396 μM respectively, which form a range around the previously reported CYP3A IC_{50}. The CYP3A probe-substrate interactions were significant for SECO with the BOMCC assay returning IC_{50} values of 99.2 and 61.4 μM.

None of the SECO analogues are particularly good CYP3A inhibitors, with the exception of SECO-1 in the DBOMF assay against CYP3A4. Given that this is the outlier the inhibition may be due to probe-substrate interaction. SECO-2 was the best inhibitor of CYP2C9 and 2C19 activity, with the IC_{50} of CYP2C19 in the nM range. SECO-1 was also a good inhibitor of 2C19.

Some of the tested analogues (SECO-1 and SECO-2) demonstrated inhibition against various P450 isoforms with IC_{50} values in the low μM to high nM range. This could translate into *in vivo* consequences including drug interactions with co-administered drugs and toxicity. SECO-1 and SECO-2 may be better inhibitors as they are the most lipophilic of the analogues, which could make them better cytochrome P450 substrates. SECO-2, the most non-polar of the analogues, is also the most stable of the analogues which could influence inhibition.

SECO-4 was the weakest inhibitor of cytochrome P450 activity. SECO-3 is the most polar analogue, however, SECO-3 is less stable than SECO-4 and its stability under the specific assay conditions is unknown. Some of the inhibition attributed to SECO-3 may be an artifact of a decomposition product, such as a dibenzocyclooctadiene. The IC_{50} of NDGA against CYP3A is

reported to be 97.3 μM whereas the IC_{50} of dibenzocyclooctadiene is 36.8 μM.[2] The dibenzocyclooctadiene is the better inhibitor. Enterolactone, a mammalian lignan whose structure is shown in Figure 2.5, has phenol substituents on both aromatic rings. It like SECO-3 and SECO-4 is a poor inhibitor of CYP3A.[2] This trend points towards lignans with substituents on both aromatic rings being poorer inhibitors of cytochrome P450 activity than those with substituents on only one ring.

Moclobemide is used to treat depression and social anxiety and is a known *in vivo* CYP2C19 inhibitor with clinical significance.[101,102] Moclobemide, as shown in Figure 5.11, shares certain structural characteristics with SECO-2 that may be relevant.

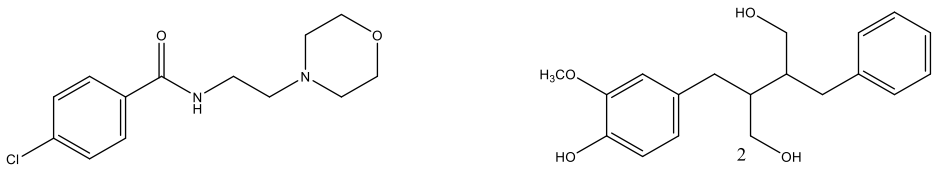

Figure 5.12 Structures of SECO-2 (right) and moclobemide (left)

CYP2C19 polymorphisms are known to cause large differences in the pharmacokinetics of a number of clinically important drugs.[103] Inhibition of CYP2C19, especially in poor metabolizers, can have clinically relevant consequences. For instance, phenytoin plasma concentrations and toxicity has been shown to increase and increased risk of toxicity from tricyclic antidepressants is likely.[101]

Though there has been a limited number of studies on the endogenous role of CYP2C19, it has been shown to be involved in the metabolism of endogenous steroid hormones including: estrone, estradiol, progesterone and testosterone.[104] This study does not suggest inhibition on the level of clinically relevant inhibition of metabolism of endogenous steroid hormones in an adult human. However, a tentative link between CYP2C19 metabolism and fetal brain development and adult personality, depression in particular, has been drawn.[105-108] The impact of an inhibitor of CYP2C19 on a fetus undergoing brain development that is already a poor metabolizer is unknown.

6.0 Conclusions

Quinones are a class of compounds that can have various toxicological effects *in vivo*, including cytotoxicity, immunotoxicity, and carcinogenesis. All of the SECO analogues tested formed quinones. Phenol analogues were metabolized to *para*-quinone methides (p-QM) and catechol analogues to *ortho*-quinones (o-Q). There was no evidence of isomerization from o-Q to p-QM. Interestingly GSH conjugation was competitive with intramolecular cyclization. In the presence of GSH no cyclization products were detected. To the best of my knowledge this is the first time GSH addition has been reported to be competitive with intramolecular cyclization in this class of lignan. As these quinones react with GSH it is a possibility that these quinones will react with cellular macromolecules such as DNA and proteins in a cellular environment leading to toxicity.

Based on our results cyclization to a lariciresinol (k_{lar}) is more likely to occur than cyclization to a 6-membered ring (k_{ring}). This may be because $k_{lar} > k_{ring}$. Lariciresinol-like cyclization decreases the chances of phenol toxicity *in vivo,* however, due to dealkylation to a catechol and GSH out competing cyclization, it does not preclude the possibility. Based on these results, design of lignans that can undergo side-chain cyclization is a poor mitigation strategy for quinone-mediated toxicity from this class of lignan.

Dibenzocyclooctadiene formation requires the presence of catechol moieties on both 6-membered rings of the lignan, in agreement with previous studies on NDGA and its analogues. This process was not enzyme mediated but instead a result of autoxidation. Indeed, P450 oxidation appears to have resulted in *ortho*-quinone formation and minimized dibenzocyclooctadiene formation. This observation provides further support for a radical-mediated, rather than *ortho*-quinone-mediated, mechanism for spontaneous dibenzocyclooctadiene formation.[38, 39]

Every SECO analogue and SECO itself demonstrated inhibition against all tested cytochrome P450 isoforms. Those with substituents on both aromatic rings tended to be poorer inhibitors than those with substituents only on one. The IC_{50} results for SECO inhibition of CYP3A agree with previously reported results. Some of the analogues demonstrated inhibition with IC_{50} values in the low μM to high nM range against some of the P450 isoforms. This may translate into *in*

vivo effects especially with concerns of drug interactions with potential co-administered drugs such as Docetaxel and Doxorubicin. If lignans from this class of compound are to be developed for pharmaceutical use P450 inhibition testing will be an important component of safety assessments.

7.0 Future Research

The major shortcoming of the metabolite study was the inability to obtain sufficient product to confirm the structures by NMR. More of the SECO analogue starting materials could be made so the assays performed in this study could be scaled up with the hope of gathering NMR data to confirm the structures of the metabolites suggested by MS. Even with scale up it may be difficult to collect enough of some of the metabolites detected as the conversion is low so preparation of a synthesized standard may be necessary for some of the metabolites, especially for cyclization products. This will be especially helpful for metabolites generated in the absence of GSH, as no standards were generated for these metabolites. It would be of particular interest to determine where cyclization occurs after a single SECO-4 dealkylation.

The loss of starting material in the autoxidation studies also requires further study. The formation of diacid metabolites which elute rapidly by HPLC is anticipated, which will require further optimization of HPLC parameters.

The specific cytochrome P450 isoforms responsible for the metabolism of SECO and the SECO analogues could be identified. This could elucidate a possible explanation for the different pattern of metabolism observed between SECO and the analogues. This could be carried out using supersomes.

The formation of quinones infer toxicity, however toxicity studies using for example HEPG2 or isolated hepatocytes would provide support for this hypothesis. It is anticipated that lignan stability would be inversely correlated to toxicity, although lignan stability in the study conditions would also need to be confirmed.

8.0 References

1. Ipsos-Reid. Natural Health Product Tracking Survey - 2010 Final Report. 2011; http://epe.lac-bac.gc.ca/100/200/301/pwgsc-tpsgc/por-ef/health/2011/135-09/report.pdf. Accessed July 16, 2015.
2. Billinsky J, Maloney K, Krol E, Alcorn J. A Comparison Between Lignans from Creosote Bush and Flaxseed and Their Potential to Inhibit Cytochrome P450 Enzyme Activity. In: Vallisuta O, Olimat SM, eds. *Drug Discovery Research in Pharmacognosy* 2012.
3. Caccia S, Pasina L, Nobili A. How pre-marketing data can be used for predicting the weight of drug interactions in clinical practice *European Journal of Internal Medicine.* 2013;24:217-221.
4. U.S. Food and Drug Administration. Drug Interaction Studies — Study Design, Data Analysis, Implications for Dosing, and Labeling Recommendations. In: Services USDoHaH, ed 2012.
5. Toure A, Xueming X. Flaxseed Lignans: Source, Biosynthesis, Metabolism, Antioxidant Activity, Bio-Active Components and Health Benefits. *Comprehensive Reviews in Food Science and Food Safety.* 2010;9:261-269.
6. Zhang W, Wang X, Liu Y, et al. Dietary flaxseed lignan extract lowers plasma cholesterol and glucose concentrations in hypercholesterolaemic subjects. *The British Journal of Nutrition.* 2008;99:1301-1309.
7. Landete JM. Plant and mammalian lignans: A review of source, intake, metabolism, intestinal bacteria and health. *Food Research International.* 2012;46:410-424.
8. Xia Y, Bi W, Zhang Y. Synthesis of Dibebzylbutanediol lignans and their Anti-HIV, Anti-HSV, Anti-tumor Activities. *Journal of the Chilean Chemical Society.* 2009;54:428-431.
9. Adolphe JL, Whiting SJ, Juurlink BH, Thorpe LU, Alcorn J. Health effects with consumption of the flax lignan secoisolariciresinol diglucoside. *The British Journal of Nutrition.* 2010;103:929-938.
10. Niemeyer HB, Honig DM, Kulling SE, Metzler M. Studies on the Metabolism of the Plant Lignans Secoisolariciresinol and Matairesinol. *Journal of Agricultural and Food Chemistry.* 2003;51:6317-6325.
11. Mukker JK, Kotlyarova V, Singh RS, Alcorn J. HPLC method with fluorescence detection for the quantitative determination of flaxseed lignans. *Journal of Chromatography B.* 2010;878:3076-3082.
12. Hu C, Yuan YV, Kitts DD. Antioxidant activities of the flaxseed lignan secoisolariciresinol diglucoside, its aglycone secoisolariciresinol and the mammalian lignans enterodiol and enterolactone in vitro. *Food and Chemical Toxicology.* 2007;45:2219-2227.
13. Raffaelli B, Hoikkala A, Leppälä E, Wähälä K. Enterolignans. *Journal of Chromatography B.* 2002;777:29-43.
14. Bolton JL, Trush MA, T.M. P, Dryhurst G, Terrence JM. Role of Quinones in Toxicology. *Chemical Research in Toxicology.* 2000;13:135-160.
15. Monks TJ, Jones DC. The metabolism and toxicity of quinones, quinonimines, quinone methides, and quinone-thioethers. *Current Drug Metabolism.* 2002;3:425-438.

16. O'Brien PJ. Molecular Mechanisms of Quinone Cytotoxicity. *Chemico-Biological Interactions.* 1991;80:1-41.
17. Khan IA, Smillie T. Implementing a "Quality by Design" approach to assure the safety and integrity of Botanical Dietary Supplements. *Journal of Natural Products.* 2012;75:1665-1673.
18. Health Canada. About Natural Health Product Regulation in Canada. 2012; http://www.hc-sc.gc.ca/dhp-mps/prodnatur/about-apropos/index-eng.php. Accessed July 16, 2015.
19. Health Canada. About Natural Health Products. 2012. http://www.hc-sc.gc.ca/dhp-mps/prodnatur/about-apropos/cons-eng.php. Accessed July 16, 2015.
20. Jordan SA, Cunningham DG, Marles RJ. Assessment of herbal medicinal products: challenges, and opportunities to increase the knowledge base for safety assessment. *Toxicology and Applied Pharmacology.* 2010;243:198-216.
21. Bates DW, Cullen DJ, Laird N, et al. Incidence of adverse drug events and potential adverse drug events: Implications for prevention. *Journal of the American Medical Association.* 1995;274:29-34.
22. Bennett BS, Lipman AG. Comparative study of prospective surveillance and voluntary reporting in determining the incidence of adverse drug reactions. *American Journal of Hospital Pharmacy.* 1977;34:931.
23. Cullen DJ, Bates DW, Small SD, Cooper JB, Nemeskal AR, Leape LL. The incident reporting system does not detect adverse drug events: a problem for quality improvement. *The Joint Commission Journal on Quality Improvement.* 1995;21:541.
24. Desikan R, Krauss MJ, Dunagan WC, Rachmiel EC, Bailey T, Fraser VJ. Reporting of Adverse Drug Events: Examination of a Hospital Incident Reporting System *Advances in Patient Safety.* 2004;1:145-160.
25. Sharav O, Shim YY, Okinyo-Owiti DP, Sammynaiken R, Reaney MJT. Effect of Cyclolinopeptides on the Oxidative Stability of Flaxseed Oil. *Journal of Agricultural and Food Chemistry.* 2014;62:88-96.
26. The history of flax. 2011; http://mfga.ca/flax-facts/the-history-of-flax/. Accessed July 22, 2015.
27. Prasad K. Flaxseed: a source of hypocholesterolemic and antiatherogenic agents. *Drug News & Perspecive.* 2000;13:99-104.
28. Canadian Grain Commission. Quality of western Canadian flaxseed 2014. 2014; https://www.grainscanada.gc.ca/flax-lin/harvest-recolte/2014/hqf14-qrl14-2-en.htm. Accessed July 20, 2015.
29. Johnsson P. *Phenolic Compounds in flaxseed: chromatographic and spectroscopic analyses of glucosidic conjugates*: Deptartment of Food Science, Uppsala; 2004.
30. Sigma-Aldrich. Material Safety Data Sheet: Secoisolariciresinol. 2014; http://www.sigmaaldrich.com/MSDS/MSDS/DisplayMSDSPage.do?country=CA&language=en&productNumber=60372&brand=FLUKA&PageToGoToURL=http%3A%2F%2Fwww.sigmaaldrich.com%2Fcatalog%2Fproduct%2Ffluka%2F60372%3Flang%3Den. Accessed July 20, 2015.
31. Moss GP. Nomenclature of Lignans and Neolignans (IUPAC Recommendations 2000). *Pure and Applied Chemistry.* 2000;72:1493-1523.

32. Masuda T, Akiyama J, Fujimoto A, Yamauchi S, Maekawa T, Sone Y. Antioxidation reaction mechanism studies of phenolic lignans, identification of antioxidation products of secoisolariciresinol from lipid oxidation. *Food Chemistry.* 2010;123:442-450.
33. Kotylarova V. *Pharmacokinetics of flaxseed lignans in the rat*, University of Saskatchewan; 2011.
34. Canadian Cancer Society's Advisory Committee on Cancer Statistics. Canadian Cancer Statistics 2013. Toronto, ON: Canadian Cancer Society; 2013.
35. Billinsky JL, Krol ES. Nordihydroguaiaretic acid autoxidation produces a schisandrin-like dibenzocyclooctadiene lignan. *Journal of Natural Products.* 2008;71:1612-1615.
36. Youngren JF, Gable K, Penaranda C, et al. Nordihydroguaiaretic acid (NDGA) inhibits the IGF-1 and c-erbB2/HER2/neu receptors and suppresses frowth in breast cancer cells. *Breast Cancer Research and Treatment.* 2005;94:37-61.
37. Lu J-M, Nurka J, Weakley SM, et al. Molecular mechanisms and clinical applications of nordihydroguaiaretic acid (NDGA) and its derivatives: An update. *Medical Science Monitor.* 2010;16:93-100.
38. Asiamah I, Hodgson HL, Maloney K, Allen KJ, Krol ES. Ring substitution influences oxidative cyclisation and reactive metabolite formation of nordihydroguaiaretic acid analogues. *Bioorganic & Medicinal Chemistry.* 2015;23:7007-7014.
39. Asiamah I. *Synthesis of nordihydroguairetic acid (NDGA) analogues and their oxidative metabolism*, University of Saskatchewan; 2015.
40. Lu JM, Nurko J, Weakley SM, et al. Molecular mechanisms and clinical applications of nordihydroguaiaretic acid (NDGA) and its derivatives: an update. *Medical Science Monitor.* 2010;16:93-100.
41. Lambert J, Dorr R, Timmermann B. Nordihydroguaiaretic Acid: A Review of Its Numerous and Varied Biological Activities. *Pharmaceutical Biology.* 2004;42:149-158.
42. Arteaga S, Andrade-Cetto A, Cárdenas R. Larrea tridentata (Creosote bush), an abundant plant of Mexican and US-American deserts and its metabolite nordihydroguaiaretic acid. *Journal of Ethnopharmacology.* 2005;98:231-239.
43. Orange Book: Approved Drug Products with Therapeutic Equivalence Evaluations. 2015; http://www.accessdata.fda.gov/scripts/cder/ob/docs/obdetail.cfm?Appl_No=019940&TABLE1=OB_Disc. Accessed July 22, 2015.
44. Lambert JD, Zhao D, Meyers RO, Kuester RK, Timmermann BN, Dorr RT. Nordihydroguaiaretic acid: hepatotoxicity and detoxification in the mouse. *Toxicon.* 2002;40:1701-1708.
45. McGillis ST, Fein H. Topical treatment strategies for non-melanoma skin cancer and precursor lesions. *Seminars in Cutaneous Medicine Surgery.* 2004;23:174-183.
46. Sheikh NM, Philen RM, Love LA. Chaparral-associated hepatotoxicity. *Archives of Internal Medicine.* 1997;157:913-919.
47. Grant KL, Boyer LV, Erdman BE. Chaparral-Induced Hepatotoxicity. *Integrative Medicine.* 1998;1:83-87.
48. Sahu SC, Ruggles DI, O'Donnell MW. Prooxidant activity and toxicity of notdihydroguaiaretic acid in clone-9 rat hepatocyte cultures. *Food and Chemical Toxicology.* 2006;44:1751-1757.
49. Gordon DW, Rosenthal G, Hart J, Sirota R, Baker AL. Chaparral ingestion. The broadening spectrum of liver injury caused by herbal medications. *Journal of the American Medical Association.* 1995;273:489-490.

50. Batchelor WB, Heathcote J, Wanless IR. Chaparral-induced hepatic injury. *American Journal Gastroenterology.* 1995;90:831-833.
51. Goodman T, Grice HC, Becking GC, Salem FA. A cystic nephropathy induced by nordihydroguaiaretic acid in the rat. Light and electron microscopic investigations. *Laboratory Investigation.* 1970;23:93-107.
52. Dunn SP, Jr. DRH, Moliterno DJ. Drug-Drug interactions in cardiovascular catheterizations and interventions. *Journal of the Americal College of Cardiology: Cardiovascular Interventions.* 2012;5:1195-1208.
53. Qato DM, Alexander G, Conti RM, Johnson M, Schumm P, Lindau S. USe of prescription and over-the-counter medications and dietary supplements among older adults in the united states. *Journal of the American Medical Association.* 2008;300:2867-2878.
54. Zhang L, Zhang YD, Strong JM, Reynolds KS, Huang SM. A regulatory viewpoint on transporter-based drug interactions. *Xenobiotica.* 2008;38:709-724.
55. Zhao P, Zhang L, Huang S-M. Complex Drug Interactions: Significance and Evaluation. In: Pang KS, Rodrigues AD, Peter RM, eds. *Enzyme- and Transporter-Based Drug-Drug Interactions*: Springer New York; 2010:667-692.
56. Zhang L, Zhang YD, Zhao P, Huang SM. Predicting drug-drug interactions: an FDA perspective. *AAPS Journal.* 2009;11:300-306.
57. Zhang L, Zhang Y, Huang SM. Scientific and regulatory perspectives on metabolizing enzyme-transporter interplay and its role in drug interactions: challenges in predicting drug interactions. *Molecular Pharmaceutics.* 2009;6:1766-1774.
58. Josephy PD, Mannervik B. *Molecular Toxicology.* Second Edition ed. 198 Madison Avenue, New York, New York 10016: Oxford University Press; 2006.
59. Cuzzolin L, Benoni G. Attitudes and Knowledge toward Natural Products Safety in the Pharmacy Setting: an Italian Study. *Phytotherapy Research.* 2009;23:1018-1023.
60. Adverse Reaction Information. 2012. Accessed July 30, 2015.
61. Pan Q, Lu Q, Zhang K, Hu X. Dibenzocyclooctadiene lignans: a class of novel inhibitors of P-glycoprotein. *Cancer Chemotherapy Pharmacoogyl.* 2006;58:99-106.
62. Uetrecht J, Naisbitt DJ. Idiosyncratic adverse drug reactions: current concepts. *Pharmacology Reviews.* 2013;65:779-808.
63. Attia SM. Deleterious effects of reactive metabolites. *Oxidative Medicine and Cellular Longevity.* 2010;3:238-253.
64. Ioannides C, Lewis DFV. Cytochromes P450 in the Bioactivation of Chemicals. *Current Topics in Medicinal Chemistry.* 2004;4:1767-1788.
65. Ma S, Zhu M. Recent advances in applications of liquid chromatography-tandem mass spectrometry to the analysis of reactive drug metabolites. *Chemico-Biological Interactions.* 2009;179:25-37.
66. Valavanidis A, Vlachogianni T, Fiotakis K, Loridas S. Pulmonary Oxidative Stress, Inflammation and Cancer: Respirable Particulate Matter, Fibrous Dusts and Ozone as Major Causes of Lung Carcinogenesis through Reactive Oxygen Species Mechanisms. *International Journal of Environmental Research and Public Health.* 2013;10:3886-3907.
67. Sies H. Oxidative stress: oxidants and antioxidants. *Experimental Physiology.* 1997;82:291-295.

68. Xu C, Yong-Tao C, Kong A-NT. Induction of Phase I, II and III Drug Metabolism/Transport by Xenobiotics. *Archives of Pharmacal Research.* 2005;28:249-268.
69. Nakata K, Tanaka Y, Nakano T, et al. Nuclear receptor-mediated transcriptional regulation in phase I, II, and III xenobiotic metabolizing systems *Drug Metabolism and Pharmacokinetics.* 2006;21:437-457.
70. Flanagan RJ, Taylor A, Watson ID, Whelpton R. *Fundamentals of Analytical Toxicology.* The Atrium Sothern Gate, Chichester, West Sussex PO19 8SQ, England: John Wiley & Sons Ltd.; 2007.
71. Sigma-Aldrich. Microsomes from Liver, Pooled from mouse (CD-1), male. In: Sigma-Aldrich, ed. 3050 Spruce Street, St. Louis, MO 63103 USA: Sigma-Aldrich; 2013.
72. Sim SC, Ingelman-Sundberg M. The Human Cytochrome P450 (CYP) Allele Nomenclature website: a peer-reviewed database of CYP variants and their associated effects. *Human Genomics.* 2010;4:278-281.
73. Lim EL, Seah TC, Koe XF, et al. In vitro evaluation of cytochrome P450 induction and the inhibition potential of mitragyne, a stumlent alkaloid. *Toxicology in Vitro.* 2013;27:812-824.
74. Yoshitomi S, Ikemoto K, Takahashi J, Miki H, Namba M, Asahi S. Establishment of the transformants expressing human cytochrome P450 subtypes in HepG2 and their application on drug metabolism and toxicology. *Toxicology in Vitro.* 2001;15:245-256.
75. Zhou SF, Liu JP, Chowbay B. Polymorphism of human cytochrome P450 enzymes and its clinical impact. *Drug Metabolism Reviews.* 2009;41:89-295.
76. Dean L. Warfarin Therapy and the Genotypes CYP2C9 and VKORC1. *Medical Genetics Summaries*. Bethesda, MD: National Center for Biotechnology Information; 2012.
77. Wang X, Thomas B, Sachdeva R, et al. Mechanism of arylating quinone toxicity involving Michael adduct formation and induction of endoplasmic reticulum stress. *Proceedings of the National Academy of Sciences of the United States of America.* 2006;103:3604-3609.
78. Bolton JL, Acay NM, Vukomanovic V. Evidence That 4-Allyl-o-quinones Spontaneously Rearrange to Their More Electrophilic Quinone Methides: Potential Bioactivation Mechanism for the Hepatocarcinogen Safrole. *Chemical Research in Toxicology.* 1994;7:443-450.
79. Thompson DC, Thompson JA, Sugumaran M, Moldéus P. Biological and toxicological consequences of quinone methide formation. *Chemico-Biological Interactions.* 1993;86:129-162.
80. Yu L, Liu H, Li W, et al. Oxidation of Raloxifene to Quinoids: Potential Toxic Pathways via a Diquinone Methide and o-Quinones. *Chemical Research in Toxicology.* 2004;17:879-888.
81. Krol ES, Bolton JL. Oxidation of 4-alkylphenols and catechols by tyrosinase: ortho-substituents alter the mechanism of quinoid formation. *Chemico-Biological Interactions.* 1997;104:11-27.
82. Sigma-Aldrich. Tyrosinase from mushroom. In: Sigma-Aldrich, ed. 3050 Spruce Street, Saint Louis, Missouri 63103 USA2012.
83. Iverson SL, Hu LQ, Vukomanovic V, Bolton JL. The Influence of the p-Alkyl Substituent on the Isomerization of o-Quinones to p-QuinoneMethides- Potential

Bioactivation Mechanism for Catechols. *Chemical Research in Toxicology.* 1995;8:537-544.
84. Jacobs E, Metzler M. Oxidative metabolism of the mammalian lignans enterolactone and enterodiol by rat, pig, and human liver microsomes. *Journal of Agriculture and Food Chemistry.* 1999;47:1071-1077.
85. Schweigert N, Zehnder AJB, Eggen RIL. Chemical properties of catechols and their molecular modes of toxic action in cells, from microorganisms to mammals. *Environmental Microbiology.* 2001;3(2):81-91.
86. Yuan R, Madani S, Wei X-X, Reynolds K, Huang S-M. Evaluation of Cytochrome P450 Probe Substrates Commonly Used by the Pharmaceutical Industry to Study in Vitro Drug Interactions. *Drug Metabolism and Disposition.* 2002;30:1311-1319.
87. Kenworthy, Bloomer, Clarke, Houston. CYP3A4 drug interactions: correlation of 10 in vitro probe substrates. *British Journal of Clinical Pharmacology.* 1999;48:716-727.
88. Olson ER, Melton T, Dong Z, Bowden GT. Stabilization of Quercetin Paradoxically Reduces Its Proapoptotic Effect on UVB-Irradiated Human Keratinocytes. *Cancer Prevention Research.* 2008;1:362-368.
89. Maini S, Hodgson HL, Krol ES. The UVA and Aqueous Stability of Flavonoids Is Dependent on B-Ring Substitution. *Journal of Agricultural and Food Chemistry.* 2012;60:6966-6976.
90. Enache TA, Oliveira-Brett AM. Phenol and para-substituted phenols electrochemical oxidation pathways. *Journal of Electroanalytical Chemistry.* 2011;655:9-16.
91. Iverson SL, Hu LQ, Vukomanovic V, Bolton JL. The Influence of the p-Alkyl Substituent on the Isomerization of o-Quinones to p-Quinone Methides: Potential Bioactivation Mechanism for Catechols. *Chemical Research in Toxicology.* 1995;8:537-544.
92. Bolton JL, Wu HM, Hu LQ. Mechanism of isomerization of 4-propyl-o-quinone to its tautomeric p-quinone methide. *Chemical Research in Toxicology.* 1996;9:109-113.
93. Thompson D, Constantin-Teodosiu D, Egestad B, Mickos H, Moldéus P. Formation of glutathione conjugates during oxidation of eugenol by microsomal fractions of rat liver and lung. *Biochemical Pharmacology.* 1990;39:1587-1595.
94. Fenoll LG, Rodríguez-López JN, Varón R, García-Ruiz PA, García-Cánovas F, Tudela J. Kinetic characterisation of the reaction mechanism of mushroom tyrosinase on tyramine/dopamine and l-tyrosine methyl esther/l-dopa methyl esther. *The International Journal of Biochemistry & Cell Biology.* 2002;34:1594-1607.
95. Espín JC, Varón R, Fenoll LG, et al. Kinetic characterization of the substrate specificity and mechanism of mushroom tyrosinase. *European Journal Of Biochemistry.* 2000;267:1270-1279.
96. Yada RY, Jackman RL. *Protein Structure-Function Relationships in Foods.* Springer US; 2012.
97. Bolton JL, Acay NM, Vukomanovic V. Evidence that 4-allyl-o-quinones spontaneously rearrange to their more electrophilic quinone methides: potential bioactivation mechanism for the hepatocarcinogen safrole. *Chemical Research in Toxicology.* 1994;7:443-450.
98. Billinsky JL, Marcoux MR, Krol ES. Oxidation of the Lignan Nordihydroguaiaretic Acid. *Chemical Research in Toxicology.* 2007;20:1352-1358.

99. Sasame HA, Gillette JR. The inhibitory effects of endogenous NADPH-pyrophosphatase on the reduction of cytochrome c and the oxidation of drugs by liver microsomes. *Archives of Biochemistry and Biophysics.* 1970;140:113-121.
100. Witham AA, Beach DG, Gabryelski W, Manderville RA. Hydroxyl Radical-Induced Oxidation of a Phenolic C-Linked 2′ -Deoxyguanosine Adduct Yields a Reactive Catechol. *Chemical Research in Toxicology.* 2012;25:315-325.
101. Bonnet U. Moclobemide: therapeutic use and clinical studies. *CNS drug reviews.* 2003;9:97-140.
102. Gram LF, Guentert TW, Grange S, Vistisen K, Brøsen K. Moclobemide, a substrate of CYP2C19 and an inhibitor of CYP2C19, CYP2D6, and CYP1A2: A panel study. *Clinical Pharmacology & Therapeutics.* 1995;57:670-677.
103. Desta Z, Zhao X, Shin JG, Flockhart DA. Clinical significance of the cytochrome P450 2C19 genetic polymorphism. *Clinical Pharmacokinetics.* 2002;41:913-958.
104. Presson A, Ingelman-Sundberg M. Pharmacogenomics of Cytochrome P450 Dependent Metabolism of Endogenous Compounds: Implications for Behavior, Psychopathology and Treatment. *Journal of Pharmacogenomics & Pharmacoproteomics.* 2014;5:127.
105. Ishii G, Suzuki A, Oshino S, Shiraishi H, Otani K. CYP2C19 polymorphism affects personality traits of Japanese females. *Neuroscience letters.* 2007;411:77-80.
106. Yasui-Furukori N, Kaneda A, Iwashima K, et al. Association between cytochrome P450 (CYP) 2C19 polymorphisms and harm avoidance in Japanese. *American Journal of medical genetics. Part B, Neuropsychiatric Genetics.* 2007;144b:724-727.
107. Sim SC, Nordin L, Andersson TM, et al. Association between CYP2C19 polymorphism and depressive symptoms. *American Journal of Medical Genetics. Part B, Neuropsychiatric Genetics.* 2010;153b:1160-1166.
108. Farmer RF, Seeley JR. Temperament and character predictors of depressed mood over a 4-year interval. *Depression and Anxiety.* 2009;26:371-381.

9.0 Appendix A

Analogues that were determined to be unstable, SECO-1, -3 and -4 at pH 7.4 were also analyzed using a non-linear regression analysis fitted to a phase 1 decay model prior to the linear transformation. Individual trials fit the model well with R^2 values > 0.97. Figure 29 shows a representative graph of a SECO-4 trial at pH 7.4.

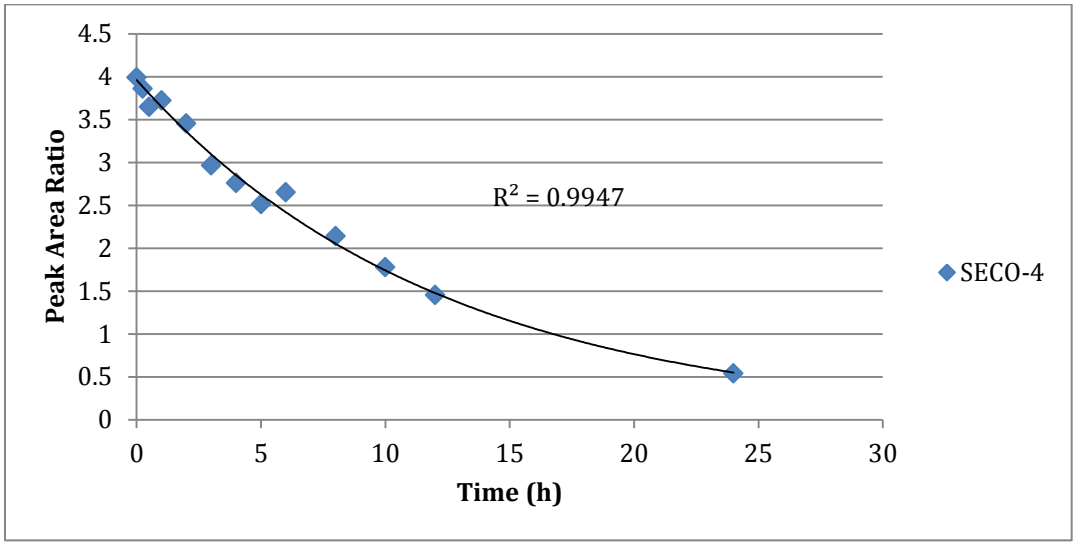

Figure 9.1 Chemical degradation profile of SECO-4, in 50 mM Na_2HPO_4 pH 7.4 at 37°C over time (h). Change in concentration was determined from the peak area under the curve, normalized to the internal standard (KA-1-09-2) and plotted as a function of time (h). Data was fitted to a phase 1 decay model, $R^2 = 0.99$.

All four trial replicates were considered for statistical analysis using a non-linear regression fit to a phase 1 decay model (Figure 30).

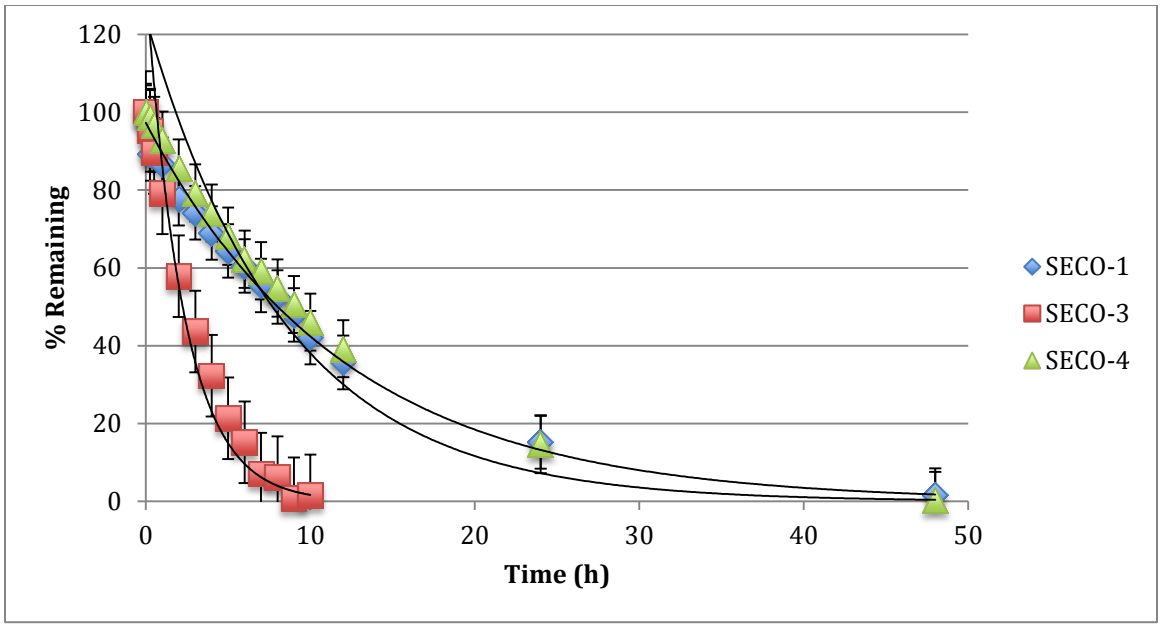

Figure 9.2 Chemical degradation profile of SECO-1, -2, -3 and -4, in 50 mM Na_2HPO_4 pH 7.4 at 37°C over time (h). Change in concentration was determined from the peak area under the curve, normalized to the internal standard (KA-1-09-2) and plotted as a function of time (h). Curves plotted using data from 4 trials. Error bars represent +/- Standard Error (SE).

Table 5 depicts a summary of the kinetic parameters of the unstable SECO analogues (1, 3 and 4) calculated using a non-linear regression fit to a phase 1 decay model.

Table 9.1 Summary of kinetic data for SECO analogue autoxidation at pH 7.4 using a normalized data fit to a phase 1 decay model.

	SECO-1	SECO-3	SECO-4
k (h^{-1})	0.08	0.25	0.07
$t_{1/2}$ (h)	8.30	2.74	9.49
R^2	0.88	0.99	0.833